mechanisms and regulation of iron transport

By

Sachie Yamaji

A thesis submitted in partial fulfilment of the requirements for the degree of

PhD Biochemistry

University College, London

2005

ProQuest LLC
789 East Eisenhower Parkway
P.O. Box 1346
Ann Arbor, MI 48106-1346

Abstract

Iron is an essential micronutrient for almost all the organisms, yet toxic in excess. Because there is no physiological mechanism to excrete iron, absorption is tightly regulated. In mammals, absorption takes place mainly in upper part of duodenum, and exact mechanisms are still unclear. In the past 5 years, a number of proteins involved in iron absorption has been identified and characterised. Divalent metal transporter 1 (DMT1, also known as Nramp2, DCT1, and SLC11A2) is the only known importer of inorganic iron into the body, and iron regulated transporter 1 (IREG1, also known as ferroportin, and MTP1) has been characterised as the iron exporter out of the enterocytes. The regulatory mechanisms of iron absorption are still unknown, though it is influenced by dietary iron, body iron store, and erythropoiesis. The level of other metals, such as zinc and copper, is also known to influence iron absorption. In thesis Caco-2 TC7 cells were used as a model of human intestine to investigating the possible regulatory mechanism of iron uptake by dietary metals (iron, copper, and zinc), and humoral signal from body store.

Cells were cultured in plates for 21 days. For the final 24 h of the culture period, metals (iron, copper, and zinc) or human synthetic hepcidin (humoral signal) was added to the basolateral medium. At

the end of the incubation period cells were used for analysis of changes in transporter gene expression. Caco-2 cells were also cultured in transwell, and used to measure ^{55}Fe transport across the cell monolayers.

Following exposure to iron, apical transporter, DMT1, was down regulated, whereas basolateral iron transporter IREG1 expression was unaffected. Interestingly gene expression of Hephaestin, which co-work with IREG1 at basolateral surface of the cell, was also down regulated. Copper, and zinc also down regulated DMT1 and hephaestin expression, as well as apical zinc transporter Zip1 in Caco-2 TC7 cells. Interestingly, exposure to copper and zinc significantly up regulated the expression of IREG1. Iron uptake across the apical membrane of Caco-2 cells was significantly decreased by exposure to hepcidin, whereas efflux across the basolateral membrane was unaffected by hepcidin treatment. In agreement with the transport data, the gene expression of DMT1 was decreased by hepcidin treatment and expression of IREG1 was unaffected. Additionally, the effect of iron (hemin) in macrophages was also investigated and found that their responses do not correspond to intestine.

Table of Contents

List of Figures

List of Tables

Acknowledgments

The experiments in this thesis were carried out in the Wolfson's laboratory of Department of Biochemistry and Molecular Biology, Royal Free Campus, University College London. The work was funded by BBSRC.

I wish to thank supervisors Professor Kaila Srai and Dr. Paul Sharp for their guidance and support. I also would like to express appreciation to Dr. Tony Michel as my mentor.

I am very grateful to members of Wolfson's laboratory Dr. Bala Ramesh, Dr. Henry Bayele, Dr. Clare Turner and Nita Solanky for discussions and support.

Thank you to Dr. Ted Debnam and Dr. Jo Marks for the important advice and support.

I am grateful to Dr. Serah Tandy and Dr. Jason Tennant for their help in the early years.

Experimental work shown in this thesis contributed to following publications.

Journals Publications

Yamaji, S. Tennant, J. Tandy, S. Williams, M. Srai S. S. K. and Sharp, P. *Zinc regulates the function and expression of the iron transporters DMT1 and IREG1 in human intestinal Caco-2 cells.* **FEBS Lett**, 2001. 507(2): p. 137-41.

Sharp, P. Tandy, S. **Yamaji, S.** Tennant, J. Williams, M. and Srai S. S. K. *Rapid regulation of divalent metal transporter (DMT1) protein but not mRNA expression by non-haem iron in human intestinal Caco-2 cells.* **FEBS Lett**, 2002. 510(1-2): p. 71-6.

Tennant J, Stansfield M, **Yamaji S**, Srai SK, Sharp P *Effects of copper on the expression of metal transporters in human intestinal Caco-2 cells.* **FEBS Lett**, 2002. 527(1-3) p. 239-44.

Yamaji, S. Sharp, P. Ramesh, B. and Srai S. S. K. *Inhibition of iron transport across human intestinal epithelial cells by hepcidin.* **Blood**, 2004. 104 (7), p2178-2180

Johnson DM, **Yamaji S**, Tennant J, Srai SK, Sharp PA. *Regulation of divalent metal transporter expression in human intestinal epithelial cells following exposure to non-haem iron.* **FEBS Lett.** 2005 579(9):1923-9.

Poster Publications

Yamaji, S. Tennant, J. Sharp, P. and Singh Srai, S. K.*Differential regulation of intestinal iron transpoter (DMT1) expression by non-haem iron in human intestinal Caco-2 cells.* 675th Biochemical Society Meeting joint with the physiological society. December 2001 University of York.

Yamaji, S. Ramesh, B. Sharp, P. and Singh Srai, S. K. *The antimicrobial peptide hepcidin decreases iron uptake by human intestinal Caco-2 cells.* Physiology Society Meeting April 2003, University of Newcastle upon Tyne.

Yamaji, S. Ramesh, B. Sharp, P. and Singh Srai, S. K. *The antimicrobial peptide hepcidin decreases iron uptake by human intestinal Caco-2 cells.* BioIron 2003 meeting, Washington, U.S.A.

Abbreviations

ANOVA. Analysis of Variance

bp. Base pair

cDNA. Complementary DNA

DMT1. Divalent metal transporter 1

Dcytb. Duodenal cytochrome b

DFO. Desferrioxamine

DMEM. Dulbecco's modified Eagle's medium

DNA. Deoxyribonucleic acid

EDTA. Ethylenediamine tetraacetic acid

EtBr. Ethidium bromide

FAC. Ferric ammonium citrate

Fe-S cluster. Iron-Sulphur cluster

GAPDH. Glyceraldehyde-3-phosphate dehydrogenase

Hepes. N-(2-hydroxyethyl)-piperazine-N'-2-ethanesulfonic acid

HEMOX. Haemoxygenase

IRE. Iron responsive element

IREG1. Iron regulated protein 1

IRP. Iron regulatory protein

kb. Kilobase

kDa. Kilodalton

MES. 2-(N-morpholino)ethano-sulphonic acid

NADH. Nicotinamide-adenine dinucleotide (reduced)

NADPH. Nicotinamide-adenine dinucleotide phosphate (reduced)

Nramp1. Natural resistance associated macrophage protein 1

Nramp2. Natural resistance associated macrophage protein 2

Oligo. Oligodeoxynucleotide

ORF. Open reading frame

PBS. Phosphate buffered saline

PCR. Polymerase chain reaction

RNA. Ribonucleic acid

rpm. Revolution per minute

RT-PCR. Reverse transcription-polymerase chain reaction

sla. Sex linked anaemia

S.E.M. Standard error mean

TAE. Tris acetic acid EDTA

Tf. Transferrin

TfR. Transferrin receptor

TNFα. Tumour necrosis factor α

μM. micromolar

UTR. Untranslated region

Nucleotide addreviation

A. Adenine

C. Cytosine

G. Guanine

T. Thymine

U. Uracil

All amino acids were abbreviated using standard abbreviations.

S.I. units and chemical formulae were used according to convention.

Chapter 1 : General introduction

1.1 Iron and biological systems

Iron is an essential micronutrient. It exists in two forms in aqueous solution, soluble ferrous (Fe^{2+}) and insoluble ferric (Fe^{3+}) irons. The importance of iron in life is unquestionable and necessary to many organisms, yet toxic in excess and there is no physiological mechanism to excrete iron in mammals.

Higher organisms use iron in many ways. Since iron readily undergoes oxidation and reduction, it is ideally suited to evolution of enzymes of electron transport. For example, enzymes that contain iron include cytochromes, cytochrome oxidase, succinate dehydrogenase and xanthine oxidase. Furthermore, the capacity of iron to decompose hydrogen peroxide has been utilised by the enzymes catalase and peroxidase. Certain porphyrin-iron-protein complexes have the capacity to bind large amounts of oxygen in a readily reversible manner, and have been used by higher organisms as a means for reversibly binding oxygen for storage and transport purposes. For example, haemoglobin, which normally contains the highest amount of iron, distributes oxygen in the body, transports carbon dioxide and is an efficient biological buffer system.

The redox reaction of iron known as the Fenton reaction can also be toxic because of the formation of highly reactive oxygen species, hydroxyl (OH•) and superoxide radicals ($•O_2^-$).

Iron-Catalysed Haber-Weiss reaction;

$$O_2 + Fe^{2+} \rightarrow •O_2^- + Fe^{3+}$$

$$2•O_2^- + 2H^- \rightarrow O_2 + H_2O_2$$

$$Fe^{2+} + H_2O_2 \rightarrow Fe^{3+} + •OH + OH^-$$

Those oxygen species causes DNA damage, impaired synthesis of protein, membrane lipid, and carbohydrates. To minimise free radical damage, organisms have evolved highly sophisticated mechanisms for acquisition, transport, and storage of iron in the body.

1.2 Iron homeostasis

1.2.1 Balance of iron in the body

Because iron is not actively excreted from the body, the adult preserves a constant level of body iron by efficient conservation of this element, maintaining rigid control over absorption to balance losses (Fig. 1.1).

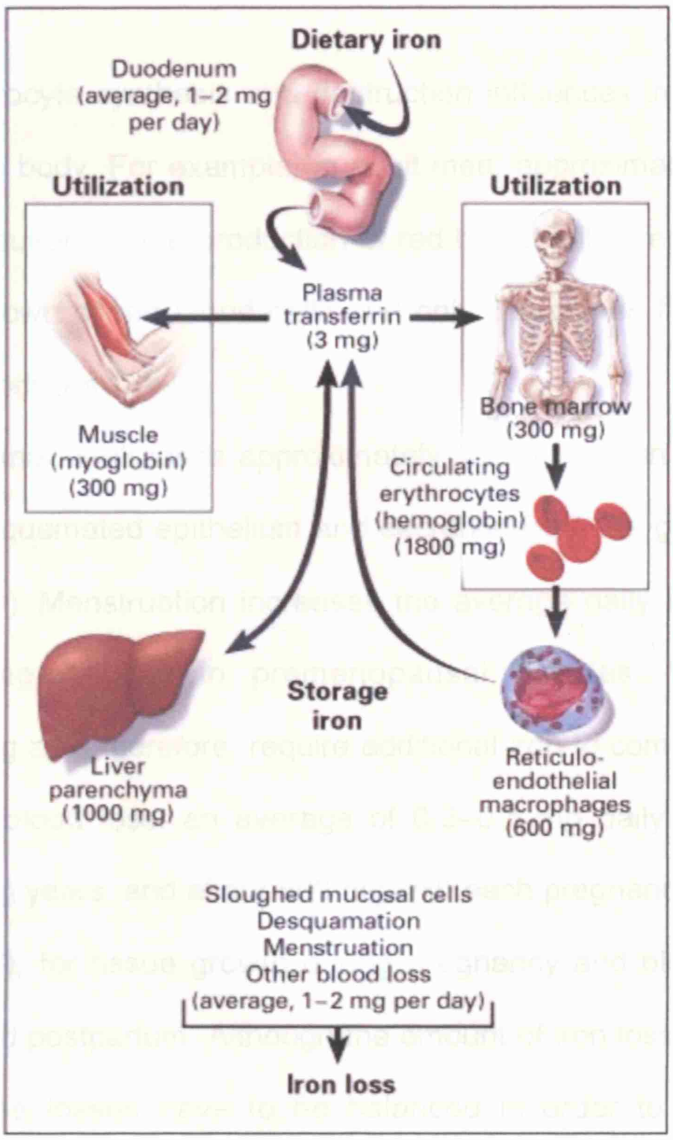

Figure 1.1 Distribution of iron in adults. In the balanced state, 1 to 2 mg of iron enters and leaves the body each day. Dietary iron is absorbed by duodenal enterocytes. It circulates in plasma bound to transferrin. Most of the iron in the body is incorporated into haemoglobin in erythroid precursors and mature red cells. Approximately 10 to 15 % is present in muscle fibres (in myoglobin) and other tissues (in enzymes and cytochromes). Iron is stored in parenchymal cells of the liver and reticuloendothelial macrophages. These macrophages provide most of the usable iron by degrading haemoglobin in senescent erythrocytes and reloading ferric iron onto transferrin for delivery to cells. From (Andrews 1999).

Erythrocyte synthesis and destruction influences iron turnover most in the body. For example, in adult men, approximately 95% of the iron required for the production of red blood cell is recycled from the breakdown of red blood cells and only 5% comes from dietary sources (Andrews 1999).

A normal adult loses approximately 1-2 mg of iron every day, mostly desquamated epithelium and secretion from the gut and skin (FAO/WHO). Menstruation increases the average daily iron loss to about 2 mg per day in premenopausal females. Women of childbearing age, therefore, require additional iron to compensate for menstrual blood loss, an average of 0.3–0.5 mg daily during the childbearing years, and about 800 mg with each pregnancy (Hallberg et al. 1970), for tissue growth during pregnancy and blood loss at delivery and postpartum. Although the amount of iron loss may seem small, these losses have to be balanced in order to avoid iron deficiency.

In adults, iron is lost daily through faeces and desquamated mucosal and skin cells, providing a limited but selective loss of body iron (Hallberg *et al.* 1970). There is a normal daily faecal loss of about 0.3 mg of iron, and usually little iron is excreted in the urine (0.1

mg/day), unless a patient develops sustained intravascular haemolysis, which can cause urinary iron losses severe enough to produce iron deficiency (10-20 mg/day) (Hallberg *et al.* 1970). The absorption of iron also has to be balanced as excessive amounts without compensatory excretion of iron is toxic and can cause siderosis and tissue damage.

1.2.1 Iron deficiency

Iron deficiency is one of the most common nutritional deficiencies, particularly in children and women of childbearing age. It is due to insufficient body iron arising from excessive loss and utilisation, e.g. caused by bleeding, pregnancy, and rapid growth. It is a leading cause of anaemia, affecting over half a billion people worldwide and has several causes (Table 1.1). Iron deficiency represents a spectrum (Table 1.1) ranging from iron depletion, which causes no obvious physiological impairments, to iron-deficiency anaemia, which affects the functioning of several organ systems.

A body that is depleting iron may retain the functional iron by utilising the storage iron. Further shortage of iron depletes the stored form, resulting in reduction of transport iron and limits red blood cell production. In iron-deficiency anaemia, the most severe form of iron

deficiency, the shortage of iron leads to underproduction of iron-containing functional compounds, including haemoglobin.

TABLE 1.1 CAUSES OF IRON DEFICIENCY.

Increased iron requirements	Inadequate iron absorption
Blood loss	Diet low in bioavailable iron
Menstruation	Impaired absorption
Gastrointestinal tract	Intestinal malabsorption
Food sensitivity	Gastric surgery
Hookworms	Hypochlorhydria
Genitourinary tract	
Respiratory tract	
Blood donation	
Growth	
Pregnancy	

The iron deficiency incidence varies widely with age, sex, race, and economic status. In the adult male, iron deficiency is a relatively uncommon disease. On the other hand, the low-income female of childbearing age is at highest risk of iron deficiency, due to, for example, multiple pregnancies, poor absorption of iron, inadequate intake and parasitic infection, such as malaria. Therefore it is not surprising to find that iron deficiency is widespread and serious problem in developing countries, and less so in developed country (FAO/WHO 2002).

The symptom of iron deficiency is severe fatigue, headache, dizziness, gastrointestinal disturbance, and paresthaesias. Nail changes, atrophy of the tongue, splenomegaly and achlorhydria are

other findings that are associated with iron deficiency. Depletion of iron stores precedes impaired production of iron-containing proteins, most importantly haemoglobin.

Severe iron deficiency is usually easy to diagnose. On the other hand, mild iron deficiency is often more difficult to diagnose because the plasma iron may be normal, as may be the iron-binding capacity (Beutler et al. 1963). Therefore it is often more difficult treat deficiency of iron in early stages.

1.2.2 Iron overload

Total body iron overload occurs most often due either to repeated transfusions in patients with severe anaemia or to hereditary hemochromatosis.

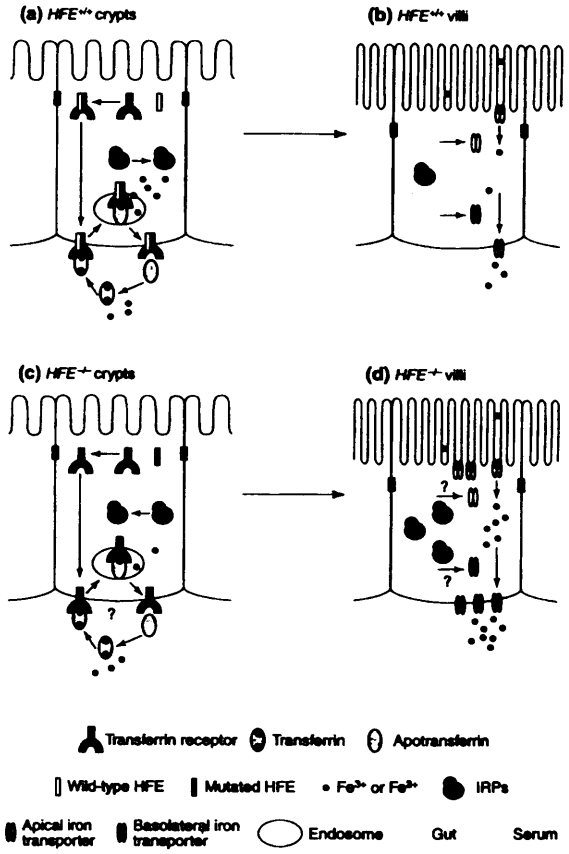

Figure. 1.2 A model for the regulation of intestinal iron absorption. (a) Crypts of normal (HFE+/+) individuals. (b) Villi of normal individuals. (c) Crypts of haemochromatosis patients (HFE-/-) (d) Villi of haemochromatosis patients. It was postulated that, in crypt cells, HFE assists uptake of iron from serum by transferrin receptor. The availability of iron from transferrin influences iron-regulatory protein (IRP) activity and ferritin levels. Crypt cells differentiate to form villus cells and adjust the rate of iron absorption from the intestinal lumen with respect to the availability of serum iron that was sensed initially. When HFE is mutated or missing, an unknown step in transferrin-iron uptake is perturbed, crypt cells become iron deprived and, once differentiated, increase iron absorption accordingly. From (Kuhn 1999).

The gene responsible for iron-overload disorder, hereditary or type 1 hemochromatosis is HFE, the defective allele of which is carried by more than 5% of Caucasians, and one in 300 individuals has both

alleles mutated (Kuhn 1999). A model for the regulation of intestinal iron absorption is illustrated on Figure 1.2. Iron homeostasis is defective in hemochromatosis and increases dietary iron absorption 2 to 3 fold. This excess iron is accumulated in the liver, the pancreas and heart muscle (Kuhn 1999), and reaches dangerously high levels after 30 to 40 years. The disorder is found mainly in men over 40 years old, who develop complications such as liver cirrhosis, diabetes and/or heart failure. Other types of hemochromatosis are recently found. Type 2 is juvenile hereditary hemochromatosis, type 2B associated to mutations in hepcidin, type 3 associated to mutations in the transferrin receptor 2 gene, and type4 associated to mutations in the IREG1 gene (Frazer and Anderson. 2003).

The only way of survival for severe anaemia patients is regular blood transfusions. Early detection and treatment of anaemia may avoid the need of blood transfusion, which carry the risk of transmitting HIV and other viruses. As a consequence of repeated transfusion, the patient often develops iron overload due to accumulation of transfused red blood cells. Iron accumulation with repeated transfusion reflects the retention of the haem iron from the transfused red cells after they become senescent and are destroyed. Because visible signs of iron overload, such as bronze or slate grey

skin pigmentation, don't usually appear until sufficient iron has accumulated to cause tissue damage, the treatments often begin after organ damage has occurred. Each unit of transfused red cells contains 200-250 mg of iron. Thus, a patient who receives 2 units of blood each month would accumulate approximately 5-6 g of extra iron in one year. Treatment to remove this excess iron is time consuming and inconvenient.

1.3 Acquisition of Iron

1.3.1 Dietary iron supply

Under physiological conditions, the body lacks excretory mechanism for iron removed and the supply of the body's iron requirement is controlled by entry into the gastrointestinal tract. The recommended daily intake of iron for adults is 12 mg in the UK and 14 mg in the EU per day, and a slightly higher intake recommended for women. The desirable iron content of premenopausal women, whose iron requirement is higher than that of other persons, is an additional 10 mg per 1000 Kcal (Hallberg *et al.* 1970).

The iron in different food sources is often chelated and its content varies enormously. Examples of foods that are low in iron are sugar, soft drinks and malt liquors, butter, margarine, and milk and milk products with an iron content varying between 0 and 1.6

mg/1000Kcal (Hallberg *et al.* 1970). Among foods more rich in iron are bread and other grain products, meat and meat products, root vegetables and other vegetables with an iron content varying between 10 and 134 mg/1000 Kcal (Hallberg *et al.* 1970). Therefore, extreme dietary habits, such as vegetarian or junk food diet, may influence body iron contents.

1.3.2 Absorption of Iron

Although excretion of iron is quantitatively as important as absorption in the maintenance of normal iron balance, absorption is the main regulatory system of body iron balance, since no physiological mechanism regulates iron excretion. The dietary intake of iron is normally greatly in excess of the body's needs. A typical human diet contains approximately 15 mg iron per day with a daily requirement for an adult male of about 10 mg in most of countries (Hallberg *et al.* 1970). The physiological situation is that man must be able to prevent the absorption of about 95 % in order to prevent iron overload.

Iron absorption occurs mainly in the duodenum, and the physical state of iron entering the duodenum greatly influences its absorption. At physiological pH, ferrous iron (Fe^{2+}) is rapidly oxidised to the

insoluble ferric (Fe^{3+}) form. Gastric acid lowers the pH in the proximal duodenum, enhancing the solubility and uptake of ferric iron.

Haem iron is absorbed by a different mechanism to that of inorganic (chelated) iron. The process is more efficient than free iron and is independent of duodenal pH. Consequently, meats are excellent nutrient sources of iron. Iron absorption is influenced predominantly by the amount of stored iron, but a number of dietary factors also play some part (see Table 1.2).

TABLE 1.2 FACTORS INFLUENCE DIETARY NON-HAEM IRON ABSORPTION.
From (FAO/WHO).

Enhancing factors	• Ascorbic acid • Meat and fish • Fermented vegetable	e.g. Fruits, potatoes e.g. sauerkraut
Inhibiting factors	• Phytates and other inositol phosphates • Iron-binding phenolic compounds • Calcium • Soy proteins	e.g. bran products, oats, rice e.g. tea, coffee, red wine e.g. milk, cheese

1.3.3 Mechanisms of inorganic iron absorption

The absorption of iron takes place mainly at upper villus of duodenum, and iron move through the apical and basolateral membranes of the enterocyte to the plasma (Fig. 1.3). Most dietary iron is in the form of insoluble ferric iron. Therefore, soluble ferrous iron is reduced from ferric iron by membrane bound ferrireductase, Dcytb, at external surface (McKie et al. 2001), as most of dietary iron

is in insoluble ferrous form at physiological pH. The apical surface of enterocyte villus lacks transferrin receptor. Instead, a proton coupled metal transporter protein, divalent metal transporter (DMT1), serves as the apical gateway of ferrous iron, in pH dependent manner (Gunshin et al. 1997). The mutation of DMT1 at G185R (Lee et al. 1998) seen in microcytic anaemia (mk) mice (Fleming et al. 1997) and Belgrade (b) rats (Fleming et al. 1998) result in severe iron deficiency anaemia, indicating the importance of DMT1 in iron homeostasis.

Iron taken up by DMT1 may bind to ferritin, which has high binding affinity to iron, reducing the risk of free radical formation by chelating iron. The iron incorporated in ferritin within the enterocytes is lost, as the cell completes its limited life cycle, with exfoliation of the senescent intestinal epithelium (Andrews 1999; Roy and Enns 2000; Roy and Enns 2000), and this is an important means of iron loss. Alternatively, iron exits the cell to the plasma via the basolateral iron transporter, iron regulated transporter (IREG1) (Donovan et al. 2000; McKie et al. 2000), working together with a multicopper ferroxidase protein, hephaestin (Vulpe et al. 1999). This exit mechanism is disrupted in sex-linked anaemia (sla) mice by mutation of hephaestin, failing to incorporate iron into the circulation, and develop microcytic hypochromic anaemia (Vulpe *et al.* 1999). A soluble ferroxidase,

ceruloplasmin, loads iron onto transferrin in other cell types, such as reticuloendothelial and parenchymal cells.

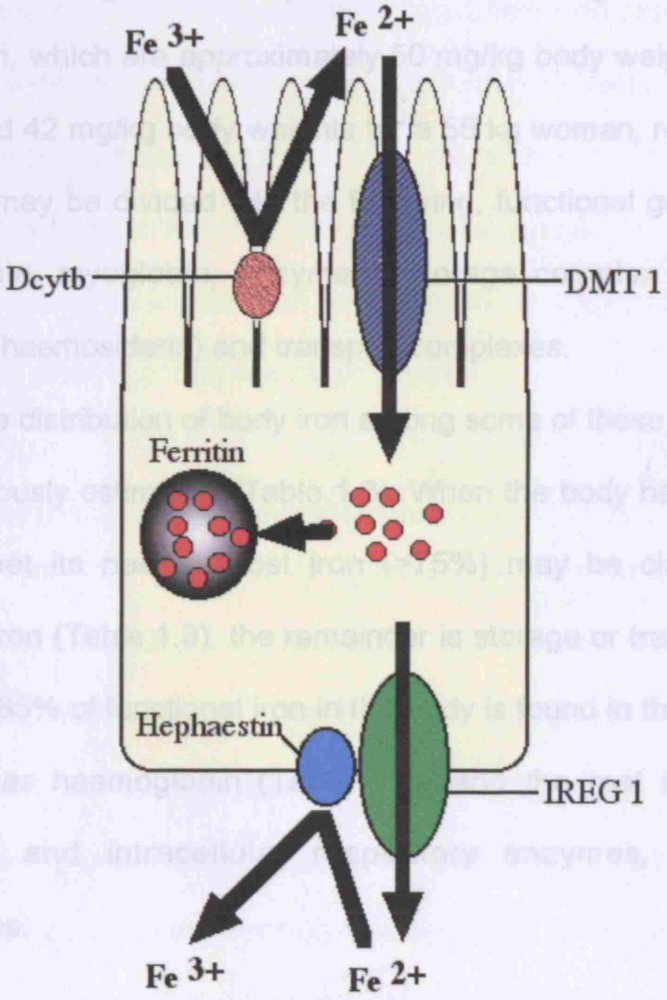

Figure 1.3 Iron transport across duodenal enterocytes. Duodenal enterocytes absorb iron from the diet. Ferrous iron is reduced by a ferric reductase in the brush border and is transported into the cell through the transmembrane iron transporter DMT1. Some iron pass through the basolateral membrane to reach the plasma, remainder is stored within the cell in ferritin. An iron exporter, IREG1, carries out basolateral iron transfer in cooperation with hephaestin, a possible ferroxidase. Iron exits the cell and loaded onto transferrin for circulation.

1.4 Iron in the body

1.4.1 Distribution of iron in the body

The averages total body iron is between 3-4 g in men and 2-3 g in women, which are approximately 50 mg/kg body weight for a 75 kg man and 42 mg/kg body weights for a 55 kg woman, respectively. Body iron may be divided into the following, functional groups, (e.g. haemoglobin, myoglobin, enzymes), storage complex group (i.e. ferritin and haemosiderin) and transport complexes.

The distribution of body iron among some of these groups has been previously estimated (Table 1.3). When the body has sufficient iron to meet its needs, most iron (>75%) may be classified as functional iron (Table 1.3), the remainder is storage or transport iron. More than 85% of functional iron in the body is found in the red blood cell mass as haemoglobin (Table 1.3), and the rest is found in myoglobin and intracellular respiratory enzymes, such as cytochromes.

TABLE 1.3 DISTRIBUTION OF IRON IN THE BODY (70 KG MAN).
From (Worwood 1999).

Protein	Location	Iron content (mg)
Haemoglobin	Erythrocytes	3000
Myoglobin	Muscle	400
Haem enzymes	All tissues	50
Transferrin	Plasma and extravascular fluid	5
Ferritin and Haemosiderin	Liver, Spleen and bone marrow	0-1000

The amount of iron in each category varies widely, especially in disease, but also in health, and the storage complexes probably show the greatest fluctuation according to the body's needs. The stores are usually lower in women than in men as women's demand of iron is normally greater by menstruation or pregnancy. Storage iron can be increased in disease due to inflammation or treatment of disease such as anaemia, because of blood transfusions or high iron administration. The amount of haemoglobin iron depends on the haemoglobin level and with the blood volume.

1.4.2 Transport iron and iron uptake from serum

Ionic iron can be toxic to tissues. Its transport, therefore, requires it to be bound with reversible protein complexes. Serum transferrin is the principal iron transport protein in vertebrates, carrying up to two iron atoms from sites of absorption, storage and haemoglobin degradation to the cells of the body requiring iron. Transferrin binds iron very strongly but reversibly, protecting the body against the free radical damage associated with free iron. Normally, only 30% of transferrin is saturated with iron in the blood, so serum transferrin has a high capacity to bind and transport iron (Enns 2001).

Cells in the body acquire iron from the plasma transferrin through specific transferrin receptors and receptor-mediated

endocytosis. Cells that require iron express the transferrin receptor and iron-laden transferrin binds to it at the surface of the cell. These complexes are internalised through clathrin-coated pits and form specialised endosomes. A proton pump decreases the pH within endosomes which result in dissociation of iron from transferrin due to its conformational changes. DMT1 present in the endosome transports iron to the cytoplasm, and the receptor-transferrin complex returns to the cell surface. The neutral pH enables the release of apo-Tf (transferrin without binding of iron) and completes the cycle of endocytosis. Although transferrin receptor is absent in fully differentiated enterocytes, crypt cells of the duodenum express transferrin receptor and acquire iron via receptor-mediated endocytosis (Fig.1.4).

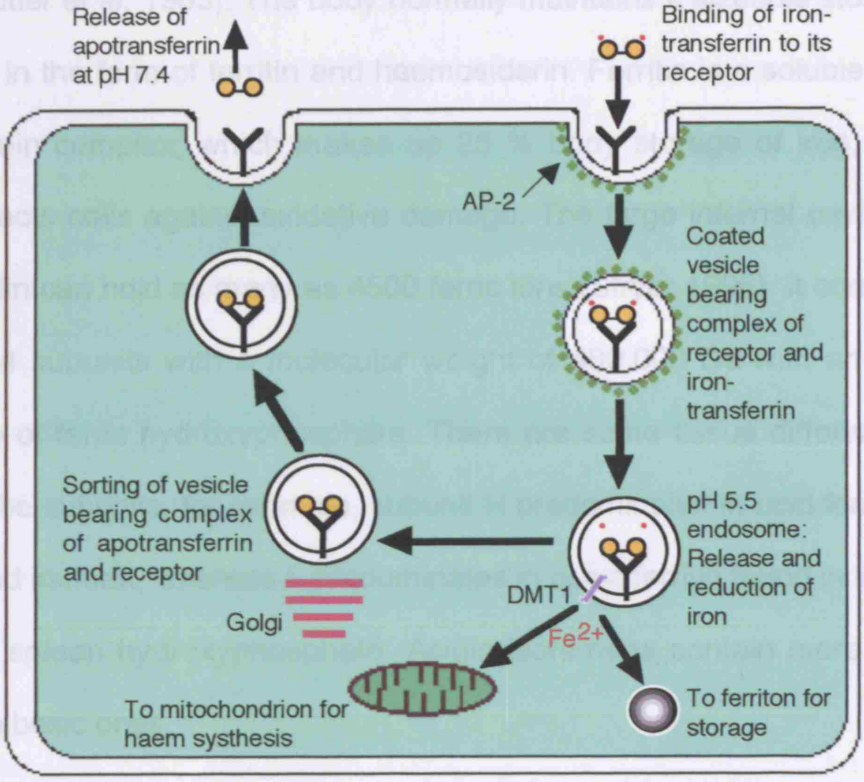

Figure 1.4 The receptor-mediated transferrin cycle. Iron loaded transferrin binds to transferrin receptors on the cell surface. Endocytosis is initiated by formation of clathrin-coated pit. Endosome is formed, in which iron-transferrin complex is internalised. Endosome becomes acidified through the action of a proton pump. Acidification leads to protein conformational changes that release iron from transferrin. Acidification also enables proton-coupled iron transport out of the endosomes through DMT1. Transferrin and the transferrin receptor both return to the cell surface, where they dissociate at neutral pH.

1.4.3 Storage Iron

Every tissue in the body contains some iron. Stores of iron are present mainly in the liver, bone marrow, skeletal muscles and spleen, but they are also found in many other organs including brain

(Beutler *et al.* 1963). The body normally maintains a sizeable store of iron in the form of ferritin and haemosiderin. Ferritin is a soluble iron protein complex, which makes up 25 % body storage of iron, and protects cells against oxidative damage. The large internal cavity of ferritin can hold as many as 4500 ferric ions (Stryer 1996). It consists of 24 subunits with a molecular weight of 480,000 Da with an iron core of ferric hydroxyphosphate. There are some tissue differences for the subunits, for example, subunit H predominates in acid ferritins found in heart, whereas L predominates in basic ferritin found in livers and spleen hydroxyphosphate. Acidic isoferritins contain more iron than basic ones.

Haemosiderin is a complex, variable, and insoluble mixture of peptides, carbohydrates, lipid and iron, which contains large amounts of iron hydroxyphosphate. In healthy persons, iron is stored primarily as ferritin and smaller amounts are stored as haemosiderin. In long-term negative iron balance, iron stores are depleted before iron becomes deficient.

1.5 Proteins involved in iron uptake

1.5.1 Divalent metal transporter 1 (DMT1)

Divalent metal transporter 1 (DMT1), also known as natural resistance associated macrophage protein 2 (Nramp2), and divalent

cation transpoter 1 (DCT1), is an apical iron transporter protein that was identified by two groups independently (Fleming *et al.* 1997; Gunshin *et al.* 1997). The SLC11A2 gene, which encodes DMT1, is more than 36 kb, consists of 17 exons and is located in chromosome 12 (12q13) in humans (Lee *et al.* 1998). It contains open reading frame of 561 amino acids (Garrick et al. 2003) with predicted molecular weight of 90-116 KDa (Tabuchi et al. 2000). The protein is predicted to have twelve transmembrane domains with a functional iron responsive element (IRE) in its 3' UTR (Gunshin *et al.* 1997; Fleming *et al.* 1998; Lee *et al.* 1998) (Fig. 1.5.A).

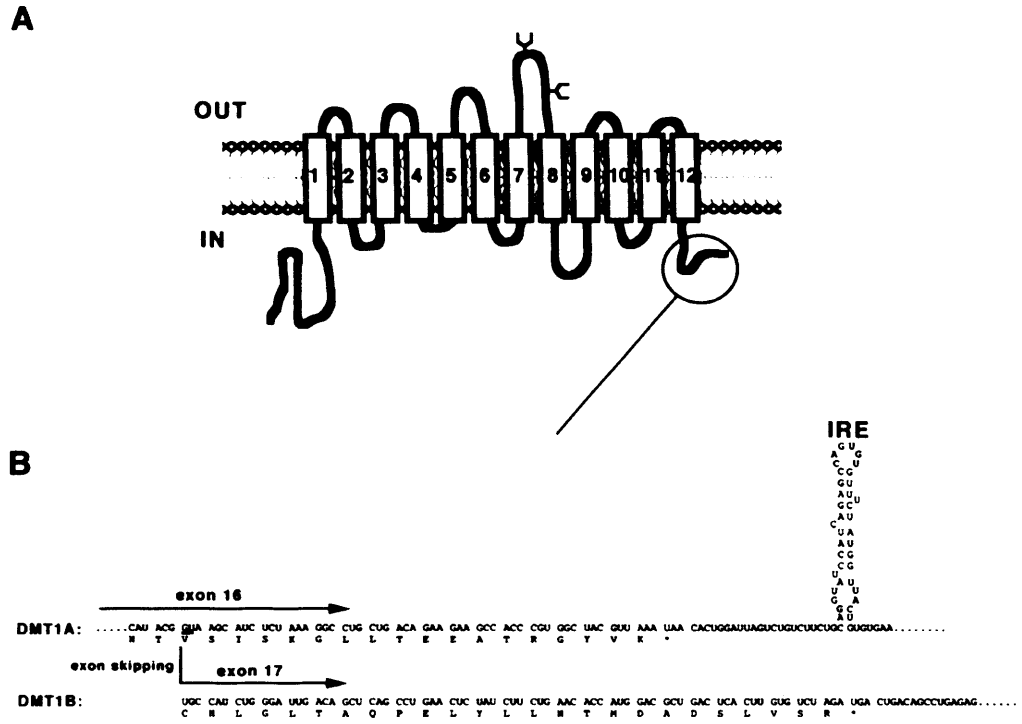

Fig.1.5 Predicted secondary structure of human DMT1 and 3' UTR alternative splicing of DMT1 mRNA. Transmembrane domains 1 to 12 are indicated, and possible glycosylation site are shown in the fourth extracellular loop (A). IRE containing form and non-IRE containing form are generated by alternative splicing of 3' end exon (B). From (Tabuchi et al. 2002).

There are at least four different splice isoforms of DMT1. Splicing in exon 16 give rise to two 3' untranslated region (UTR), one contains an iron regulatory element (IRE) (DMT1+IRE) (Fleming *et al.* 1997; Gunshin *et al.* 1997; Lee *et al.* 1998) and one without the IRE (DMT1-IRE) (Lee *et al.* 1998) (Fig. 1.5.B). The presence of the IRE in 3' UTR suggests post-transcriptional regulation by intracellular iron concentration. Two further isoforms were found at the 5'UTR end of

the gene, tissue specific upstream exon 1A and ubiquitously expressed exon 1B (Hubert and Hentze 2002) (Fig. 1.6). Exon 1A, specific to duodenum and kidney, is highly regulated by iron but not 1B (Hubert and Hentze 2002). In fact all isoforms of DMT1 mRNA except exon 1B non IRE form are regulated by intracellular iron (Hubert and Hentze 2002).

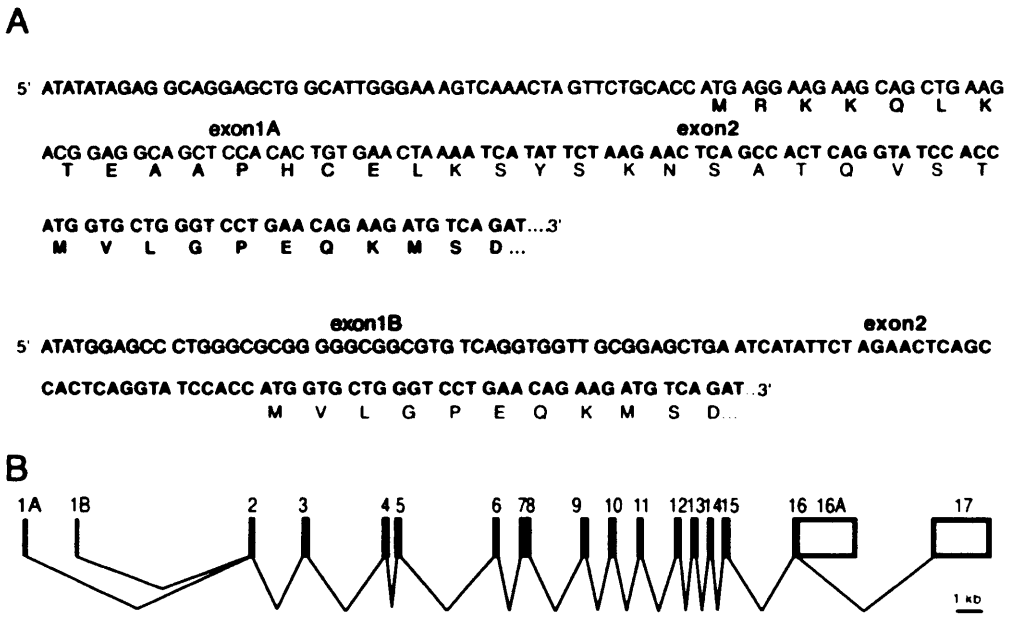

Fig.1.6. Comparison of DMT1 exon1A and exon 1B isoforms. (A) Sequence of the alternative 5′ regions of the human DMT1 mRNA. The sequences of the two DMT1 variants are identical after reaching the sequence corresponding to exon 2. The specific sequences of each isoform are boxed in blue for the newly identified exon 1A and in green for the previously described exon 1B. (B) Revised genomic organization of the human DMT1 gene. The sequence of the exon 1A has been mapped 1.9 kb upstream of exon 1B in the human genomic sequence (NT-009782). The two 59DMT1variants are generated by alternative promoter usage followed by splicing to exon 2. From (Hubert and Hentze 2002).

DMT1+IRE is abundant in proximal intestine, kidney, thymus and brain, and expressed in testis, liver, colon, heart, spleen, skeletal muscle, lung, bone marrow and stomach (Gunshin *et al.* 1997; Hubert and Hentze 2002). It is highly expressed in the apical membrane of duodenal enterocytes and kidney epithelial cells (Gunshin *et al.* 1997; Burdo *et al.* 2001; Ferguson *et al.* 2001; Tallkvist *et al.* 2001). DMT1-IRE is abundantly expressed in kidney, lung, spleen, and thymus, and less in heart, stomach, duodenum, jejunum and ileum (Hubert and Hentze 2002). It is also expressed in non-epithelial cells such as neuronal cells (Roth et al. 2000) and particularly in erythroid cells (Canonne-Hergaux et al. 2001). Both isoforms are present at the plasma membrane surface, but in cytosolic vesicles, DMT1+IRE is localised in late endosome/lysosomes, whereas DMT1-IRE found in early endosome (Tabuchi *et al.* 2002). Additionally, nuclear localisation was also demonstrated by DMT1-IRE (Roth *et al.* 2000; Garrick *et al.* 2003).

The function of DMT1 was determined through mutations in Microcytic anaemia (*mk*) mice (Fleming *et al.* 1997) and Belgrade (*b*) rats (Fleming *et al.* 1998). The two animals have the same missense mutation (G185R) in the predicted transmembrane 4 (Fleming *et al.* 1997; Fleming *et al.* 1998), that results in microcytic, hypochromic

anaemia due to severe impairment of iron transport in intestine and erythroid iron utilisation (Su et al. 1998). Gunshin *et al* first demonstrated the function of DMT1 as a pH dependant, proton coupled iron transporter using Xenopopus oocytes in 1997 (Gunshin *et al.* 1997). Gunshin *et al* also showed conductivity by a range of divalent cations including Zn^{2+}, Cd^{2+}, Mn^{2+}, Cu^{2+}, Fe^{2+}, Co^{2+}, Ni^{2+}, and Pb^{2+}, listed in descending order of magnitude, suggesting a broad substrate range of DMT1. Ubiquitous expression suggests multiple functions of DMT1: apical iron uptake by enterocytes (Gunshin *et al.* 1997; Canonne-Hergaux *et al.* 1999; Trinder *et al.* 2000), trafficking iron into cells via the transferrin cycle (Tabuchi *et al.* 2000; Touret *et al.* 2003), and non-transferrin bound iron uptake into cells (Garrick et al. 1999). Of the four isoforms, exon1A DMT1+IRE is thought to be the main apical iron transporter in the intestine (Hubert and Hentze 2002), however, functions of other isoforms in various tissues and cell types are not as transparent.

1.5.2 Iron Regulated Transporter 1 (IREG1)

Iron regulated transporter 1 (IREG1), also known as ferroportin 1 and metal transport protein 1 (MTP1), is an iron exporter protein that has been isolated by three groups independently (Abboud and Haile 2000; Donovan *et al.* 2000; McKie *et al.* 2000). The sequence is

encoded in the 20 kb gene SLC11A3, located in chromosome 2 (2q32) in humans, and consist of 8 exons (Njajou et al. 2001), and contains open reading frame of 571 amino acids (Donovan *et al.* 2000) with predicted molecular weight of 62 KDa.(McKie *et al.* 2000). The protein is predicted to have a multi-transmembrane structure, with possibly nine (Devalia et al. 2002) or ten transmembrane domains (Abboud and Haile 2000; Donovan *et al.* 2000; McKie *et al.* 2000). The mRNA was a functional iron responsive element (IRE) in its 5' UTR (Abboud and Haile 2000; Donovan *et al.* 2000; McKie *et al.* 2000).

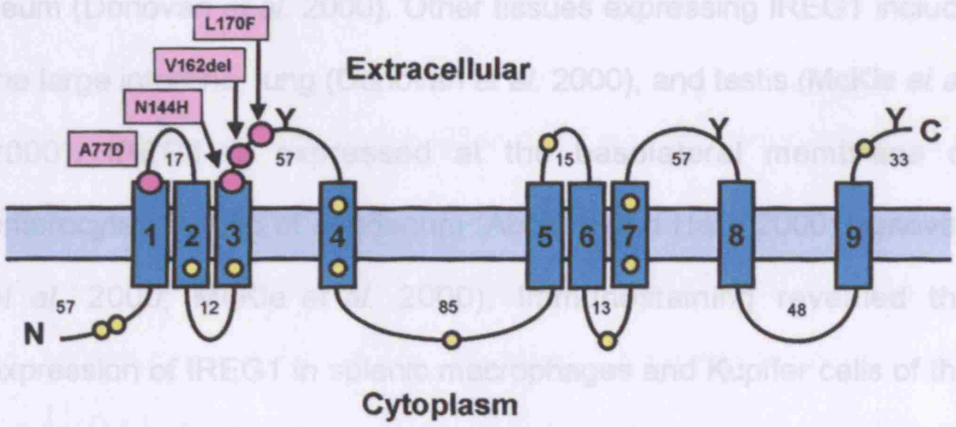

Fig. 1.7 Predicted secondary structure of human IREG1. Transmembrane domains 1 to 9 and position of four mutation sites (red circles) and 12 Cys residues (yellow circles) are indicated (Devalia *et al.* 2002).

Further sequence analysis by McKie et al (2000) showed that it contains a putative NADP/ adenine-binding site (IFVCGP), also found in NADH and NADPH reductase families, and a PDZ target motif ((T/S-X-V/L), recognised by PDZ domains for sorting of membrane proteins to the basolateral membrane, in its C-terminus. Those findings indicate a possible reductase activity and basolateral membrane localisation of IREG1 protein.

IREG1 is strongly expressed in tissues involved in iron metabolism such as, liver, spleen, kidney, and placenta, and is also abundant in heart, skeletal muscle, and duodenum of small intestine (Abboud and Haile 2000; Donovan *et al.* 2000) but not jejunum or ileum (Donovan *et al.* 2000). Other tissues expressing IREG1 include the large intestine, lung (Donovan *et al.* 2000), and testis (McKie *et al.* 2000). IREG1 is expressed at the basolateral membrane of enterocyte villus tip of duodenum (Abboud and Haile 2000; Donovan *et al.* 2000; McKie *et al.* 2000). Immunostaining revealed the expression of IREG1 in splenic macrophages and Kupffer cells of the liver (Abboud and Haile 2000; Donovan *et al.* 2000). In Kupffer cells, IREG1 has predominantly a cytoplasmic/intercellular localisation, and not at the surface membrane (Abboud and Haile 2000).

The function of IREG1 as an iron exporter was demonstrated using *Xenopopus* oocytes (Donovan *et al.* 2000; McKie *et al.* 2000). Cytosolic iron and ferritin depletion by overexpression of IREG in HEK293 cells (Abboud and Haile 2000) further support its exporter function. IREG1 is regulated by LPS (Yang et al. 2002), cellular iron level (Abboud and Haile 2000; McKie *et al.* 2000) and hypoxia (McKie *et al.* 2000) in duodenum. IREG1 in macrophage, liver, spleen and marrow are also regulated by LPS (Yang *et al.* 2002), and mutation is associated with autosomal dominant hemochromatosis (Montosi *et al.* 2001; Njajou *et al.* 2001; Devalia *et al.* 2002) characterised by reticuloendothelial iron overload (Devalia *et al.* 2002).

1.5.3 Dcytb

Duodenal cytochrome b (Dcytb) is a ferric reductase that is responsible for reduction of insoluble ferric to soluble ferrous iron before it is taken up by DMT1 (McKie et al. 2001). Dcytb is a homolog of cytochrome b561 with six predicted transmembrane domains. Unlike ferric reductases in plants (Robinson et al. 1999), Dcytb lacks NADH, NADPH, or flavin binding motifs that makes them electron donors. Instead Dcytb was suggested to receive an electron from ascorbate, as does its homologue cytochrome b561 (McKie *et al.*

2001). Unlike some other proteins of iron metabolism, Dcytb also lacks an iron responsive element in its mRNA (McKie *et al.* 2001).

Dcytb is highly expressed in the brush-border membrane of duodenal enterocytes (McKie *et al.* 2001; Latunde-Dada *et al.* 2002). Dcytb is also found in the surface of other tissues and in the cytoplasmic vesicles (Latunde-Dada *et al.* 2002). The function of Dcytb as ferric reductase was demonstrated using *Xenopopus* oocytes (McKie *et al.* 2001). The up regulation of Dcytb expression was demonstrated by iron deficiency and hypoxia (McKie *et al.* 2001; Frazer *et al.* 2002) suggesting regulation by iron status via an unknown mechanism that is separate from the IRE/IRP system.

1.5.4 Hephaestin

Hephaestin is a membrane bound multicopper ferroxidase homologue to a serum ferroxidase, ceruloplasmin. Its sequence is encoded in a ~100kb kb gene DXS1194, located on chromosome X (Xq11-12) in human, consisting of 20 exons (Vulpe et al. 1999; Syed et al. 2002). The predicted molecular weight of human hephaestin with its signal peptide is 130.4 KDa and 127.8 KDa without putative signal peptide (Syed *et al.* 2002). The protein contains type I, II, and

III copper-binding sites and one predicted transmembrane domain at the C terminus (Fig. 1.8).

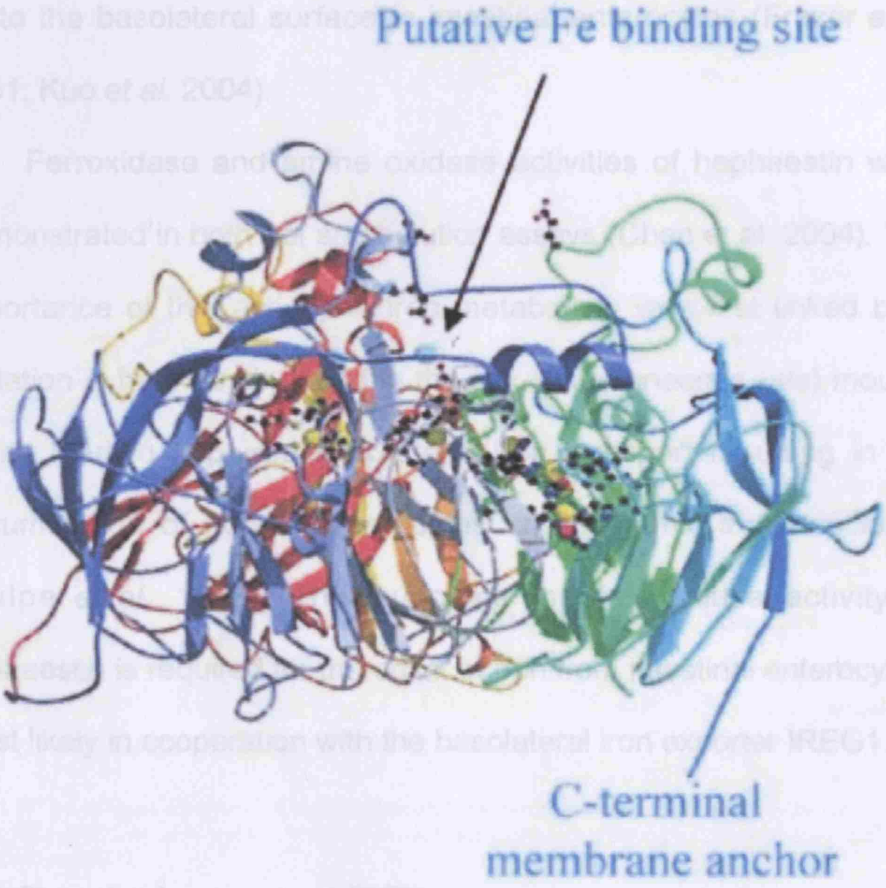

Fig. 1.8 The ribbon diagram of human hephaestin. Side view of hephaestin molecule showing the putative iron binding site. The sequence is shaded in blue for domain 1, green for domain 2, yellow for domain 3, red for domain 4, purple for domain 5, and grey for domain 6. From (Syed *et al.* 2002).

Hephaestin is highly expressed in duodenum and to a lesser extent in the colon (Frazer et al. 2001). Low level of expression is also detected in other tissues such as spleen and lung (Frazer *et al.* 2001).

Hephaestin is predominantly expressed in the cells of the mid to upper villus, but not in the crypt, of the small intestine (Vulpe *et al.* 1999). It is primarily localised to a supranuclear compartment as well as to the basolateral surface in intestinal enterocytes (Frazer *et al.* 2001; Kuo *et al.* 2004).

Ferroxidase and amine oxidase activities of hephaestin were demonstrated in both gel and solution assays (Chen et al. 2004). The importance of this activity in iron metabolism was first linked by a mutation in hephaestin found in the sex-linked anaemia (*sla*) mouse, which lead to impaired basolateral iron transport resulting in the accumulation of iron in enterocytes and systemic iron deficiency (Vulpe *et al.* 1999). This suggests the ferroxidase activity of hephaestin is required for the efflux of iron from intestinal enterocytes, most likely in cooperation with the basolateral iron exporter IREG1.

1.5.5 Transferrin receptor 1 (TfR)

Human transferrin receptor 1 (TfR) is a transmembrane glycoprotein dimer with two transferrin binding sites. The sequence is encoded in chromosome 3 (3q29) with molecular weight of 185 KDa (Brittenham et al. 2000). Two identical polypeptide chains, weighing 95 KDa, contain three regions within each 760-residue subunit; a

globular extracellular portion where transferrin binds, a hydrophobic intramembranous region and the remaining region lying within the cytoplasm (Aisen 2004) (Fig. 1.9.).

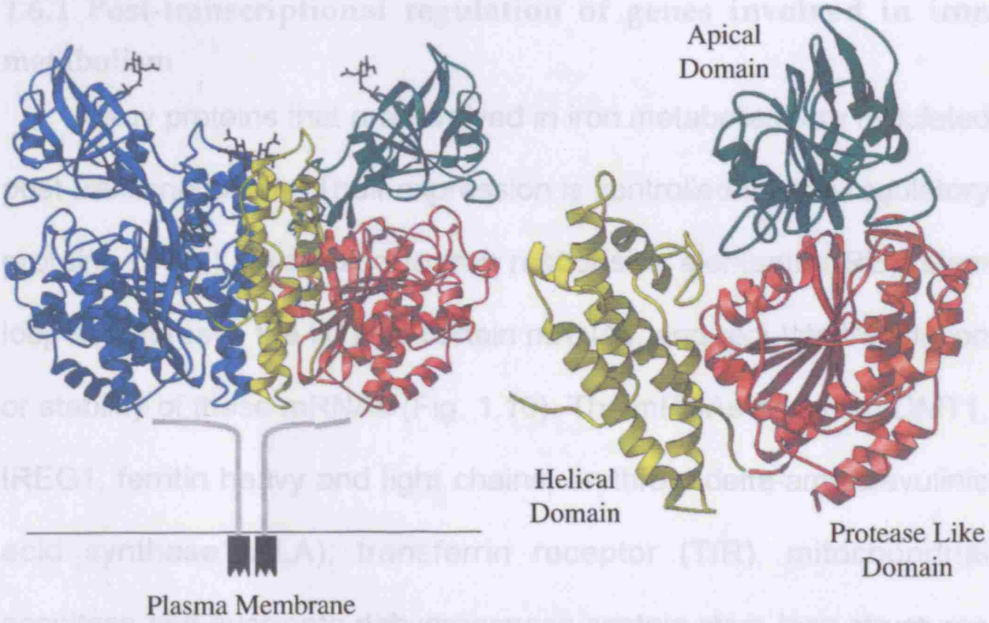

Fig. 1.9 The ribbon diagram of human transferrin receptor. One monomer is shown on the right. The protease-like, apical, and helical domains are red, green, and yellow, respectively. From (Aisen 2004)

Transferrin receptors are ubiquitously expressed on the surface membrane of all nucleated cells except the differentiated enterocytes of duodenum. The expression is highest in cells with high iron demand such as erythroid marrow, liver and placenta (Ponka et al. 1998; Aisen 2004). Transferrin receptor is required for iron delivery

from transferrin to cells. Transferrin receptor binds to its ligand transferrin at the cell surface and is internalised by receptor-mediated endocytosis (see Fig. 1.4).

1.6 Regulation of iron metabolisms

1.6.1 Post-transcriptional regulation of genes involved in iron metabolism

Many proteins that are involved in iron metabolism are regulated post-transcriptionally. Their expression is controlled by iron regulatory proteins (IRPs) which bind to iron responsive elements (IRE), stem loop structures in the UTR of certain mRNAs, and regulate translation or stability of these mRNAs (Fig. 1.10). The mRNAs encoding DMT1, IREG1, ferritin heavy and light chains, erythroid delta-aminolevulinic acid synthase (ALA), transferrin receptor (TfR), mitochondrial aconitase and succinate dehydrogenase contain stem-loop structures which function as iron responsive elements (IRE) and to which an iron regulatory protein (IRP) binds when cells are depleted of iron.

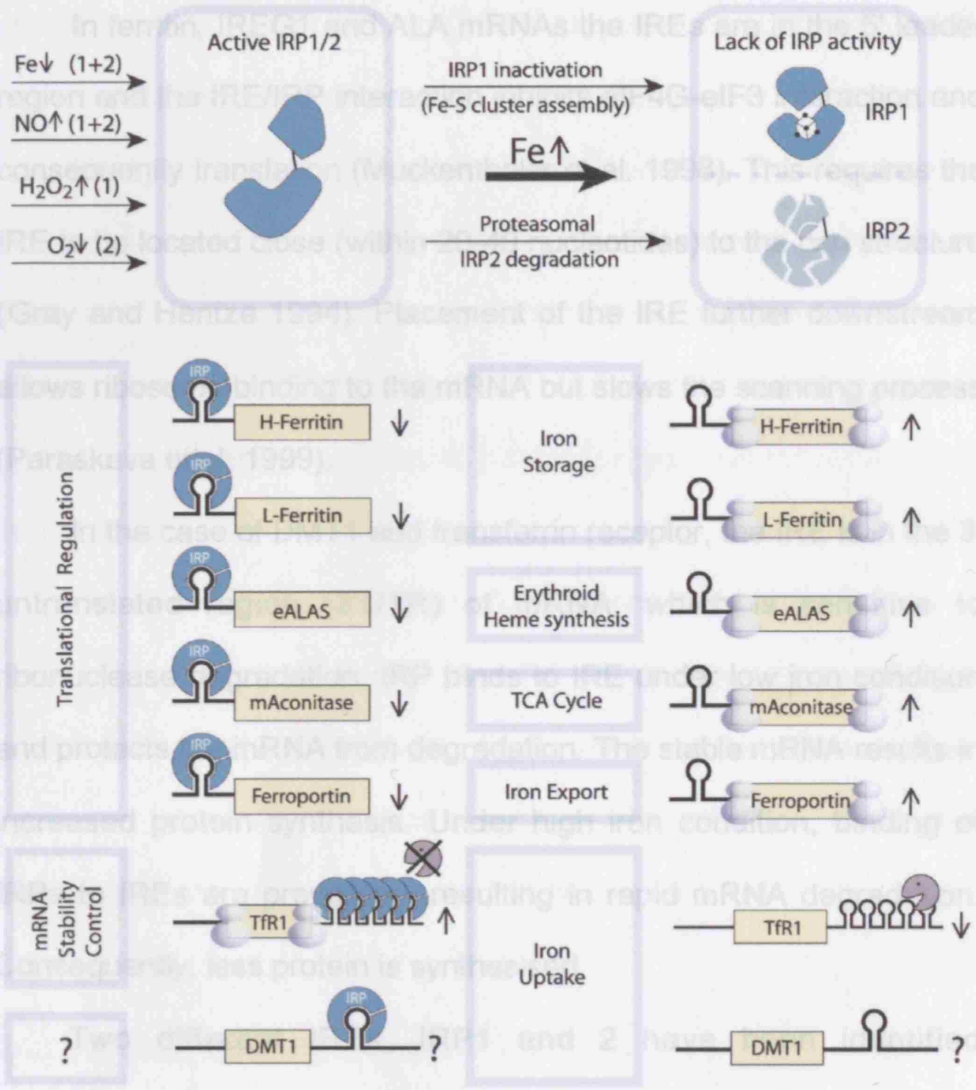

Figure 1.10 The IRE/IRP regulatory system. Proteins involved in iron storage, erythroid haem synthesis, the TCA cycle, iron export, and iron uptake are co-ordinately regulated by the interaction of the iron regulatory proteins (IRPs) with conserved RNA secondary structures, the iron-responsive elements (IREs). The binding of IRPs to single IREs in the 5′-untranslated regions (UTRs) of mRNAs blocks their translation, while IRP binding to multiple IREs in the 3′ UTR stabilizes the TfR-1 mRNA. IRPs exist in two isoforms, IRP1 and IRP2. Increased iron levels favour the conversion of IRP1 from its active RNA binding form into an Fe-S cluster containing cytoplasmic aconitase that lacks IRE binding activity as well as the proteasomal degradation of IRP2. Low iron levels or the action of NO promote accumulation of the active apoprotein form of IRP1 and stabilize IRP2. In contrast, H2O2 only activates IRP1, while hypoxia interferes with IRP2 degradation. From (Hentze et al. 2004)

In ferritin, IREG1 and ALA mRNAs the IREs are in the 5' leader region and the IRE/IRP interaction inhibits eIF4G-eIF3 interaction and consequently translation (Muckenthaler et al. 1998). This requires the IRE to be located close (within 20-40 nucleotides) to the cap structure (Gray and Hentze 1994). Placement of the IRE further downstream allows ribosome binding to the mRNA but slows the scanning process (Paraskeva et al. 1999).

In the case of DMT1 and transferrin receptor, the IRE is in the 3' untranslated region (3'UTR) of mRNA, which is sensitive to ribonuclease degradation. IRP binds to IRE under low iron condition and protects the mRNA from degradation. The stable mRNA results in increased protein synthesis. Under high iron condition, binding of IRPs to IREs are prevented, resulting in rapid mRNA degradation. Consequently, less protein is synthesised.

Two different IRPs, IRP1 and 2 have been identified (Samaniego et al. 1994). They have molecular weights of 98 KDa (IRP1) and 105 KDa (IRP2) and are 57% identical. Both have similar but not the same affinity and specificity with regard to IRE binding in ferritin mRNAs and they show tissue-specific expression (Schalinske et al. 1997). IRP1 was cloned from several species. It is identical to cytoplasmic aconitase and contains an iron-sulphur (4S-4Fe) cluster,

which prevents it from binding IRE. This cluster is located in a cleft, which separates two domains of the protein and contains the active site. The fourth iron of this cluster is labile and is lost when cellular iron levels drop. Loss of iron results in the disassembly of the (4S-4Fe) cluster, loss of aconitase activity and gain of RNA binding activity (Haile et al. 1992). Unlike IRP1, IRP2 is oxidised, ubiquitinated and rapidly degraded by proteasomes under high iron conditions (Iwai et al. 1998).

Consequently, under iron replete conditions, iron uptake is reduced through degradation of the TfR mRNA whereas iron storage and utilization are activated through enhanced ferritin and haem synthesis. Under iron depletion conditions iron utilisation and storage are reduced and iron uptake is stimulated.

1.6.2 Pre-programming of enterocytes

The epithelial cell layers of duodenum respond to body iron demand and absorb iron accordingly. The epithelial cells originate in the intestinal crypts and migrate toward the tip of the villus as they differentiate (maturation axis) (Fig. 1.11) (Andrews 1999). The expression of protein related to iron uptake and transport in crypt cells differ from those in differentiated enterocytes (Roy and Enns 2000).

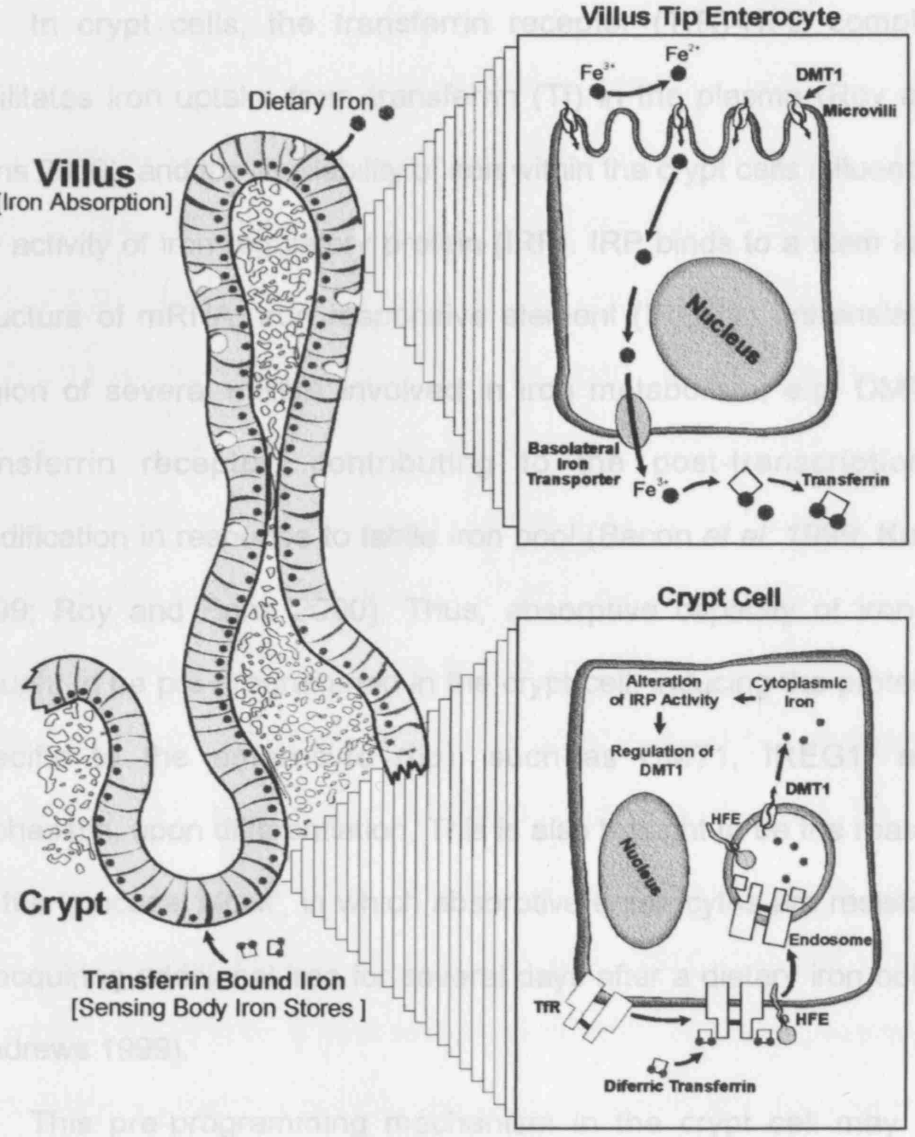

Figure 1.11 Hypothesis of regulation of iron absorption. An intestinal villus is shown with insert enlargements of an enterocyte on the villus tip (where iron is absorbed from the intestine) and a deep crypt cell (where the body iron stores are sensed via transferrin-mediated and HFE-modulated iron transport). Ferric iron is reduced in the intestine to ferrous iron and absorbed via the divalent metal transporter (DMT-1) into the enterocyte on the villus tip. In the enterocyte, iron is oxidized to ferric and transported via basolateral iron transporter, IREG1, into the circulation. In deep crypt, HFE bound to the TfR modulates the uptake of diferric-transferrin. The level of cytoplasmic iron then acts through the binding of IRPs to IREs on the production of DMT-1 transporter mRNA. Mutations in HFE cause lack of cell surface expression of HFE and dysregulation of TfR-mediated iron uptake and consequent alterations in DMT-1 production. From (Bacon et al. 1999).

In crypt cells, the transferrin receptor (TfR)-HFE complex facilitates iron uptake from transferrin (Tf) in the plasma (Roy and Enns 2000), and the availability of iron within the crypt cells influences the activity of iron regulatory protein (IRP). IRP binds to a stem loop structure of mRNA, iron responsive element (IRE), in untranslated region of several mRNA involved in iron metabolism, e.g. DMT1, transferrin receptor, contributing to the post-transcriptional modification in response to labile iron pool (Bacon *et al.* 1999; Kuhn 1999; Roy and Enns 2000). Thus, absorptive capacity of iron is thought to be pre-programmed in the crypt cell, inducing the proteins specific to the enterocyte (tip), such as DMT1, IREG1, and hephaestin, upon differentiation. This is also thought to be the reason for the 'mucosal block', in which absorptive enterocytes are resistant to acquiring additional iron for several days after a dietary iron bolus (Andrews 1999).

This pre-programming mechanism in the crypt cell may be disrupted in hereditary hemochromatosis by mutation of the HFE gene, as demonstrated in HFE knock-out mice, since DMT1 is up-regulated despite the saturation of transferrin and liver iron (Fleming et al. 1999).

1.6.3 Stores regulator

The humoral factors must also exist to regulate iron homeostasis. Iron uptake changes in response to body iron stores such as liver, skeletal muscle, and blood (Andrews 1999; Roy and Enns 2000). The stores regulator facilitates uptake, to a limited extent, in decreased iron stores, and reduces upon repletion, preventing overload. Recently a candidate peptide that might explain the link between body iron level and the regulation of intestinal iron absorption has been identified (Nicolas et al. 2001). An antimicrobial peptide called hepcidin is predominantly expressed in the liver, and dramatically up regulated when liver iron is elevated and down regulated when the stores are depleted (Pigeon et al. 2001). Further evidence of the link between hepcidin and iron homeostasis comes from the death of transgenic mice overexpressing hepcidin shortly after birth due to severe anaemia (Nicolas et al. 2002a). Subsequent studies shown that hepcidin expression is dramatically decreased in iron deficient and anaemic mice (Nicolas et al. 2002b). This evidence strongly suggests that hepcidin is secreted in response to liver iron levels and has an inhibitory effect on iron absorption (Fig. 1.12).

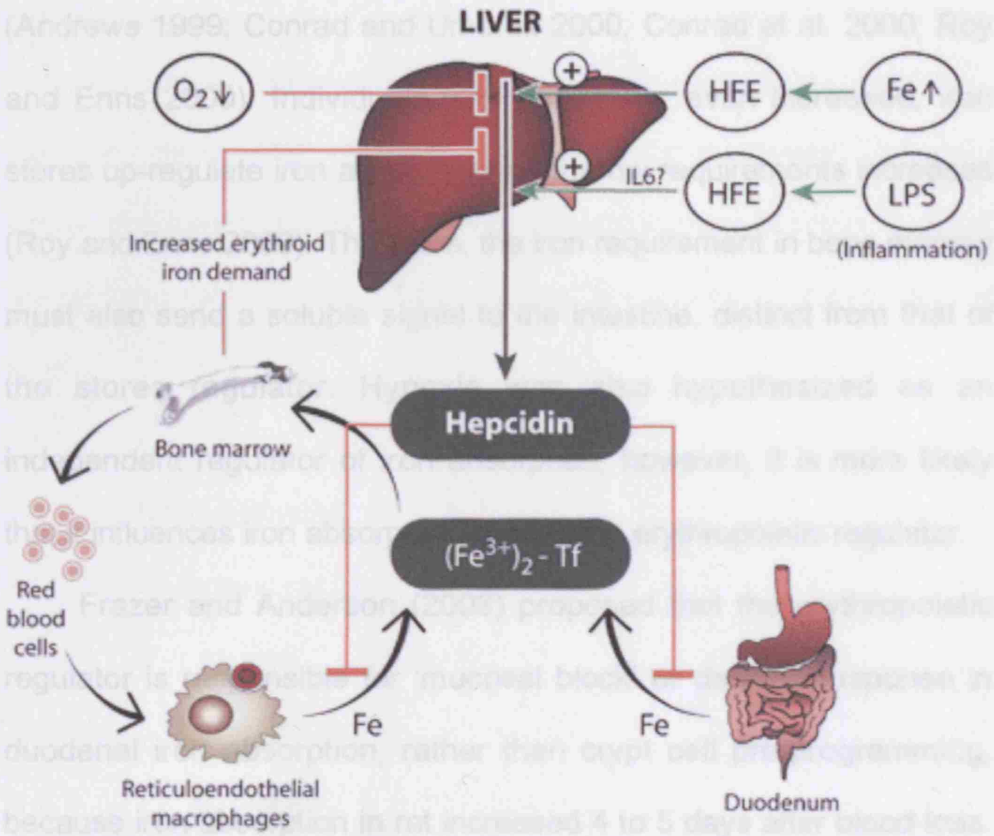

Figure 1.12 Role of hepcidin, HFE, and other molecules in the regulation of systemic iron homeostasis. Hepcidin is an antimicrobial, ß defensin-like peptide secreted by the liver. It diminishes iron release from reticuloendothelial macrophages and duodenal enterocytes. As a consequence, serum iron levels decrease. Hepcidin expression is regulated by iron levels, inflammatory stimuli, the erythroid iron demand, and hypoxia. Recent data indicate that the former two responses require HFE function. From (Hentze *et al.* 2004).

1.6.4 Erythroid regulator

The iron demand for erythropoiesis also modifies uptake by duodenal enterocytes. This is known as the erythropoietic regulator, which alters iron absorption in response to the requirement of erythropoiesis, and acts independently from the stores regulators

(Andrews 1999; Conrad and Umbreit 2000; Conrad et al. 2000; Roy and Enns 2000). Individuals with normal, or even increased, iron stores up-regulate iron absorption as marrow requirements increases (Roy and Enns 2000). Therefore, the iron requirement in bone marrow must also send a soluble signal to the intestine, distinct from that of the stores regulator. Hypoxia was also hypothesized as an independent regulator of iron absorption; however, it is more likely that it influences iron absorption through the erythropoietic regulator.

Frazer and Anderson (2003) proposed that the erythropoietic regulator is responsible for 'mucosal block' or delayed response in duodenal iron absorption, rather than crypt cell pre-programming, because iron absorption in rat increased 4 to 5 days after blood loss. This increase in absorption was in conjunction with a decrease in plasma iron level, plasma iron clearance, and intestinal iron content. It is more likely that any delay in response to iron absorption regulator represents the time taken for the body to recognise its iron needs rather than the time taken for a maturation of crypt cells (Frazer and Anderson 2003).

1.7 Aim of Study

The exact mechanism by which intestinal enterocytes respond to the many factors that influence iron absorption is unclear. The main aim of this thesis is to obtain better understandings of the role of the following in the regulation of intestinal iron uptake at the molecular level:

1. Differentiation
2. Inorganic metals
    a. Iron
    b. Copper
    c. Zinc
3. Hepcidin – the stores regulator

In addition, molecular mechanisms of macrophage iron metabolism were also studied in comparison to that of intestine.

Chapter 2 : Methods

2.1 Standard buffers and solutions

Hepes buffer pH 7.5

NaCl	140 mM
KCl	5 mM
$NaHPO_4$	1 mM
$CaCl_2$	1 mM
$MgCl_2$	0.5 mM
Glucose	5 mM
Hepes	10 mM
Bovine Serum Albumin	0.2 %

MES buffer pH 6.5

NaCl	140 mM
KCl	5 mM
$NaHPO_4$	1 mM
$CaCl_2$	1 mM
$MgCl_2$	0.5 mM
Glucose	5 mM
MES	10 mM
Bovine Serum Albumin	0.2 %

Phosphate buffered saline (PBS) pH 7.5

Na_2HPO_4	11.5 g
NaH_2PO_4	2.96 g
NaCl	5.84 g

Dilute to 1 L with distilled water. Adjust pH if necessary.

50 x TAE buffer

Tris base	242 g
0.5 M EDTA pH 8.0	100 ml
Glacial acetic acid	57.1 ml
dH_2O	to 1l

0.5 M EDTA pH. 8.0

EDTA	18.6 g
dH_2O	to 100 ml

1% TAE agarose gel with ethidium bromide

Agarose	1.5 g
1 x TAE	150 ml
Ethidium bromide	0.5 g/ml

50 x TAE buffer

Tris base	242 g
0.5 M EDTA pH 8.0	100 ml
Glacial acetic acid	57.1 ml
dH_2O	to 1L

10 x loading buffer for agarose gel electrophoresis

Bromophenol blue	0.4 %
Glycerol	67 %
in 10 x TAE buffer	

DNA marker for agarose gel electrophoresis

Hyper ladder IV (100 – 1000 Kb) BioLine, London UK

2.2 Methods

2.2.1 Culture of cells

2.2.1.1 Caco-2 TC7 cells

Caco-2 cells were derived from a human colorectal adenocarcinoma cell. In culture, they differentiate spontaneously into polarised intestinal cells with an apical brush border and tight

junctions between adjacent cells, and they express microvillar transporters, typical of small intestine.

TC7 cells are a sub-clone of Caco-2 cells that were produced by dilution cloning, and express more small intestine-like characteristics compared with the parent Caco-2 cells.

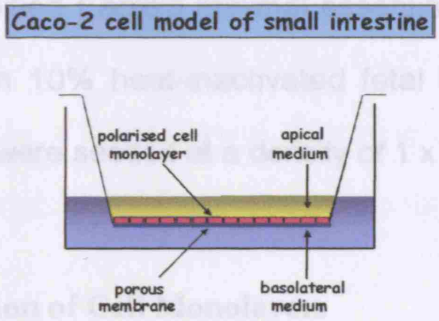

Figure 2.1 Caco-2 cell model of small intestine using Transwell. Apical medium represents intestinal lumen and basolateral medium represents plasma. Transepithelial electrical resistance were used to measure the formation of monolayer.

Caco-2 TC7 cells grow as a monolayer and differentiate on a semi-permeable membrane for transport studies. The monolayer separates the apical medium from the basolateral medium, which correspond to the intestinal lumen and the plasma, respectively (Figure 2.1). Transepithelial electrical resistance was measured to monitor the health and formation of Caco-2 TC7 cell monolayer. Cells were seeded onto 6 well/75 cm^2 tissue culture flasks for isolation of

total RNA. Caco-2 TC7 cells require 21 days to complete morphological and functional differentiation in the following conditions (Sharp *et al.* 2002).

Stock culture of Caco-2 TC7 cells were obtained from Drs Monique Rousset and Edith Brot-Laroche, INSERM U505, Paris, France. Cells were cultured in a 95% air 5% CO_2 atmosphere at 37°C in Dulbecco's modified Eagle's minimal essential medium (DMEM), supplemented with 10% heat-inactivated fetal bovine serum. For experiments, cells were seeded at a density of 1 x 10^4 cells/cm^2.

2.2.1.2 Trypsinisation of Cell Monolayers

The monolayer was washed with PBS, and Trypsin-EDTA solution was added to the cells and left for one minute at room temperature. The excess trypsin solution was removed, and incubated at 37°C until cells were detached from the culture vessel. Cells were then resuspended in the growth medium and cell aggregates dispersed by pipetting the cell suspension up and down vigorously several times. The appropriate number of cells was added to the fresh culture vessel containing growth medium.

2.2.1.3 Preservation of living cells

90% confluent flask of growing cells was trypsinised, and resuspended in medium at a concentration of 3-4 x10^6 cells per ml. The cell suspension was cooled on an ice-water bath, and dimethylsulphoxide (DMSO) was added to give a final concentration of 10% (v/v). A 1 ml aliquot of the suspension was transferred to a sterile vial. The vial was placed in a polystyrene box, and allowed to freeze deep in a –70°C for minimum of two hours, providing a cooling rate of approximately 1°C per minute. The vials of aliquot were then stored in the vapour phase of liquid nitrogen container.

2.2.1.4 Recovery of frozen cells

A vial of aliquot cells was removed from the liquid nitrogen freezer, and thawed in a water bath at 37 °C. The outside of the vial was washed with 70% ethanol and allowed to dry at room temperature. The contents of vial were transferred to a growth flask, adding sufficient growth medium to dilute the DMSO at least ten fold. Cells were incubated as in 2.2.1, and the medium was replaced with fresh growth medium after 24 hours.

2.2.1.5 Experiment using cultured cells

All experiments were carried out on cells between passage numbers 32-40.

2.2.1.6 Materials used in cell culture

Cell culture medium, serum and plasticware were purchased from Invitrogen (Paisley, UK) unless stated. All other chemicals were of highest grade available and bought from Sigma-Aldrich UK (Dorset, UK).

2.2.2 Gene expression using thermal cycler

2.2.2.1 Total RNA isolation using TRIzol

Caco-2 TC7 cells monolayer in a 3.5 cm diameter dish were incubated in 1 ml TRIzol reagent (Gibco BRL life technologies, Paisley, U.K.) for five minutes at room temperature to allow complete dissociation. 200 µl of chloroform were added and the samples were mixed thoroughly, incubated for 3 minutes. The mixture were centrifuged at 12000 x g for 15 minutes at 4°C. The colourless upper aqueous phase containing the RNA was transferred to a fresh tube and the lower red phenol-chloroform phase was discarded. RNA was precipitated from the aqueous phase by addition of 500µl of isopropyl alcohol (Sigma-Aldrich Co., Ltd., Poole, UK), incubated at room

temperature for 10 minutes and then centrifuged at 12000 x g for 10 minutes at 4°C. The RNA was precipitated and formed a gel like pellet on the side and bottom of the tube. The RNA pellet was washed with 75% ethanol and centrifuged at 7500 x g for 5 minutes at 4°C. The final pellet was air dried and resuspended in 20 µl of RNAse free distilled water (Promega UK Ltd., Southampton, UK). Quantitation and quality of total RNA were determined by measuring the absorbance at 260 nm using a spectrophotometer (Beckman DU 650 Spectrophotometer, High Wickam, Bucks. UK). RNA concentration was calculated using the formula shown below.

$$A_{260} = 1 = 40\ \mu g/ml\ (in\ water)$$

i.e. An absorbance of 1 unit at 260 nm corresponds to 40 µg of RNA per ml

An estimate of purity of RNA was provided by the ratio between the reading at 260 nm and 280 nm (A_{260}/ A_{280}). In distilled water, a ratio of 1.6 – 1.9 indicates RNA free of protein contamination. Quality of RNA was further assessed by running on a 1 % agarose gel with ethidium bromide. Gels were visualised under UV light so that DNA contamination and RNA degradation can be detected. RNA samples were resuspended in RNase free water to a concentration of 1 mg/ml and stored at -80°C until further use.

2.2.2 2 Semi quantitative gene expression

The reverse-transcription (RT) polymerase chain reaction (PCR) is a sensitive method to analyse mRNA expression in cells. Reverse transcription polymerase chain reaction (RT-PCR) was performed in a single step reaction, using Ready-to-go RTPCR Beads (Amersham Pharmacia Biotech) on total RNA samples (1 µg per tube) using the specific primer sequences.

TABLE 2.2 PRIMERS USED FOR SEMI-QUANTITATIVE GENE EXPRESSION.
Annealing temperatures (Tm) are shown in °C. Amplification cycle number and product size in base pair (bp) are also listed.

Gene	Primer sequence (5' to 3')	Tm	Cycle	Size (bp)
GAPDH	For. GCC ATC AAT GAC CCC TTC AT Rev. GAG GGG GCA GAG ATG ATG AC	59	28	280
DMT1	For. GGT GTT GTG CTT GGA TGT TA Rev. AGT ACA TGT TGA TGG AGC AG	57	28	385
DMT1-IRE	For. GGA CCT AGG GCA TGT GGC AT Rev. ACA CAA GTG AGT CAG CGT GG	64	28	180
DMT1+IRE	For. AGT GGT TTA TGT CCG GGA CC Rev. TTT AAC GTA GCC ACG GGT GG	64	28	179
IREG1	For. ATT GGT GCT AGA ATC GGT CT Rev. AGA CTG AAA TCA ATA CGA GC	50	28	198

The cDNA transcript was produced by incubation at 42°C for 30 min. PCR was performed for 28 cycles of 95°C for 30 s, Tm °C for 30 s, 72°C for 1 min, followed by a final single extension at 72°C for 10 min in a PTC-100 thermal cycler (MJ Research, NV, USA). PCR products were stained with ethidium bromide on a 2 % agarose gel and visualised using a Fluor-S MultiImager (Bio-Rad Laboratories,

Hertfordshire, UK), and bands were analysed using MultiAnalyst (Bio-Rad) image analysis software. mRNA levels were normalised to GAPDH expression.

2.2.3 Gene expression using real time PCR

2.2.3.1 Total RNA isolation QIAamp RNA Blood Mini Kit

Total RNA from Caco-2 TC7cells was isolated using a QIAamp RNA Blood Mini Kit (Qiagen). All steps were performed at room temperature (15-25 °C). Caco-2 TC7 cells monolayer in a 3.5 cm diameter dish was lysed by addition of 600 µl buffer RLT with ß-ME. Lysate was loaded into a QIAshedder column and centrifuged at 13000g for 2 minutes at room temperature to homogenise. An equal volume of 70 % ethanol was added to homogenised lysate in a colletion tube and mixed well by pipetting. The sample was transferred into a new QIAamp spin column and centrifuged at 6000g for 1 minute at room temperature. The flow-through and collection tube were discarded, and a QIAamp spin column was transferred into a new collecting tube. 700 µl buffer RW1 was added to the column and centrifuged for 1 minute at 6000g to wash. Flow-through and collection tube were discarded, and the QIAamp spin column was transferred into a new collecting tube again. 500 µl buffer RPE was added to the column and centrifuged for 1 minute at 6000g to wash.

500 µl buffer RPE was added again to the column and centrifuged for 3 minute at 13000g. The QIAamp spin column was transferred into a 1.5 ml collection tube and 20 µl of RNase-free water was pipetted directly onto the QIAamp membrane. The sample was centrifuged for 2 minutes at 6000g to elute, and quantitation and quality of total RNA were determined as in 2.2.2.1.

2.2.3.2 cDNA synthesis

1µg of total RNA was reverse transcribed with 1.6µg oligo-$p(dT)_{15}$ primer using a 1st strand cDNA synthesis kit for RT-PCR (AMV) (Roche diagnostics, Penzberg, Germany). RNA mixed with reagents was incubated at 25 °C for 10 minutes and then at 42 °C for 60 minutes. AMV reverse transcriptase was denatured by incubating the reaction at 99 °C for 5 minutes and then cooled to 4 °C for 5 minutes. Quantitation and quality of total cDNA were determined by measuring the absorbance at 260 nm using a spectrophotometer (Beckman DU 650 Spectrophotometer, High Wickam, Bucks. UK). cDNA concentration was calculated using the formula shown below.

$$A_{260} = 1 = 50\ \mu g/ml\ (in\ water)$$

i.e. An absorbance of 1 unit at 260 nm corresponds to 50 µg of cDNA per ml

An estimate of purity of the cDNA was provided by the ratio between the reading at 260 nm and 280 nm (A_{260}/ A_{280}). In distilled water, a ratio of 1.6 – 1.9 indicates cDNA free of protein contamination. Quality of cDNA was further assessed by running on a 1 % agarose gel with ethidium bromide. cDNA samples were resuspended to a concentration of 1 mg/ml and stored at -80°C until further use.

2.2.3.3 Real time PCR amplification

The resulting cDNA transcripts of Caco2-TC7 mRNA were used for PCR amplification using the Roche Lightcycler (Roche diagnostics, Penzberg, Germany) and FastStart DNA Master SYBR Green 1 kit (Roche diagnostics, Penzberg, Germany).

FastStart DNA Master SYBR Green 1 contains FastStart Taq Polymerase, reaction buffer, a dNTP mix (with dUTP instead of dTTP), SYBR Green I dye, and 10 mM $MgCl_2$. Each PCR reaction mix contained 1 µg cDNA template, 0.5 µM forward and 0.5 µM reverse primers, 2 µl FastStart DNA Master SYBR Green 1, 4mM $MgCl_2$ and distilled water to a final volume of 20µl. SYBR green I, present in the PCR mix, only emits light when bound to double-stranded DNA, once bound it is excited at 494 nm and emits light at 521nm. The lightcycler

fluorimeter monitors emissions at 521nm, and values are recorded by a computer (Dell Computers, Bracknell, UK). For primer sequences see Table 2.3.

TABLE 2.3 PRIMERS USED FOR REAL TIME PCR.
Annealing temperatures (Tm) are shown in °C. Amplification cycle number and product size in base pair (bp) are also listed.

Gene	Primer sequence (5' to 3')	Size (bp)
HPRT	For. TTG TAG CCC TCT GTG TGC TCA AG Rev. GCC TGA CCA AGG AAA GCA AAG TC	269
DMT1	For. GTC ATT GGC TCA GCC ATT GC Rev. ATG CCC TTG AGT ACC TGG CT	225
DMT1-IRE	For. GGA CCT AGG GCA TGT GGC AT Rev. ACA CAA GTG AGT CAG CGT GG	180
DMT1+IRE	For. AGT GGT TTA TGT CCG GGA CC Rev. TTT AAC GTA GCC ACG GGT GG	179
IREG1	For. CGT CAT TGC TGC TAG AAT CG Rev. AGA CTG AAA TCA ATA CGA GC	202
DcytB	For. ACA GTG ATT GCA ACA GCA CTT Rev. TGA CGT TAT ATG GCT CTA TCT	387
Hephaestin	For. GCA GAT GTG GTG GAT CTG TT Rev. TCA ATG TCT CTG GGG GGC AC	197
Transferrin Receptor 1	For. TGAACAAAGTGCCACGAGCA Rev. CTGAATAGTCCAAGTAGCTAG	460
Haem Oxygenase 1	For. CCT AAA CTT CAG AGG GGG CG Rev. AGT TAG ACC AAG GCC ACA GTG	350
Nramp1	For. GGC GCA ATC TTA ACT CA Rev. CAC GCC TGT AAT TCC CA	195

2.2.3.4 Real-time PCR cycling parameters

The FastStart Taq polymerase present in the SYBR Green I reaction mix significantly reduces non-specific priming and the formation of primer dimers. The PCR cycling conditions were initial denaturation of 95°C for 10 minutes, followed by 30 cycle of

denaturation at 95°C for 10 seconds, annealing at 60°C for 5 seconds, and extension at 72°C for 10 seconds. The temperature of fluorescence acquisition was set at 78°C for 5 seconds, 20°C below the product melting temperature. The product melting temperature was determined in a test run by examining the melting curve (described in section 2.2.3.7). All experiments were performed in triplicate and the gene of interest and the control gene were run in parallel for each sample. A ratio of relative abundance of the gene of interest to the constitutively expressed gene hypoxanthine phosphoribosyl transferase (HPRT) was calculated by the second derivative maximal method (described in section 2.2.3.5), using the Lightcycler Relative Quantification software version 1.0 (RelQuant) (Roche Diagnostics, Penzberg, Germany). HPRT was chosen as a control gene because its expression level is not affected by metal treatments.

2.2.3.5 The second derivative maximal method

The lightcycler software version 3.5 (Roche diagnostics, Penzberg, Germany) calculates the PCR cycle at which the maximal increase in fluorescence occurs in the log/linear phase of cycling. This is known as the second derivative maximum method, and the

cycle at which this occurs is usually different for each sample. The cycle number at which maximal increase in fluorescence occurs is compared to that of standards with known concentration of PCR product using RelQuant software (Roche Diagnostics, Penzberg, Germany).

2.2.3.6 Preparation of standard curves

PCR products (dsDNA) for each gene were separated on a 2% agarose-TAE gel and purified using a GENECLEAN SPIN kit (Bio 101, CA, USA). 300mg of gel containing the PCR band of interest was excised from the agarose gel and placed in 400 µl glassmilk (silica beads in high salt solution). The glassmilk-DNA solution was heated at 55°C for 5 minutes to melt the agarose gel. After cooling, the mixture was placed in a GENECLEAN spin filter column and centrifuged at 13000g for 1 minute. DNA was retained by the membrane-filter and the supernatant was discarded. The membrane-filter was washed twice with 500 µl GENECLEAN SPIN new wash and dried by centrifuging for a further 2 minutes. DNA was eluted with 10-25µl distilled water and centrifuged at 13,000 x g for 1 minute. The concentration of each PCR product DNA was determined using a

spectrophotometer (Beckman DU 650 Spectrophotometer, High Wickam, Bucks. UK), and calculated using the formula;.

$$A_{260} = 1 = 50\ \mu g/ml\ (in\ water)$$

i.e. An absorbance of 1 unit at 260 nm corresponds to 50 µg of cDNA per ml

Purified DNA was serially diluted 10- fold covering a dynamic range of 7 logarithmic orders. 1.0 µl of each standard dilution was amplified by PCR using the lightcycler and specific primers. One set of gene of interest standards was run in triplicate with the duplicate HPRT house keeping standards to generate two linear standard curves of log concentration against cycle number (Fig 2.2).

A

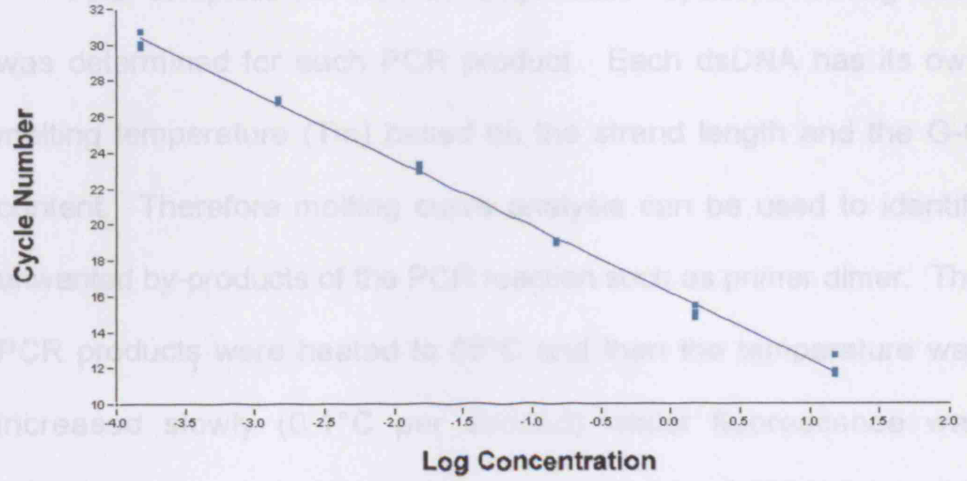

B

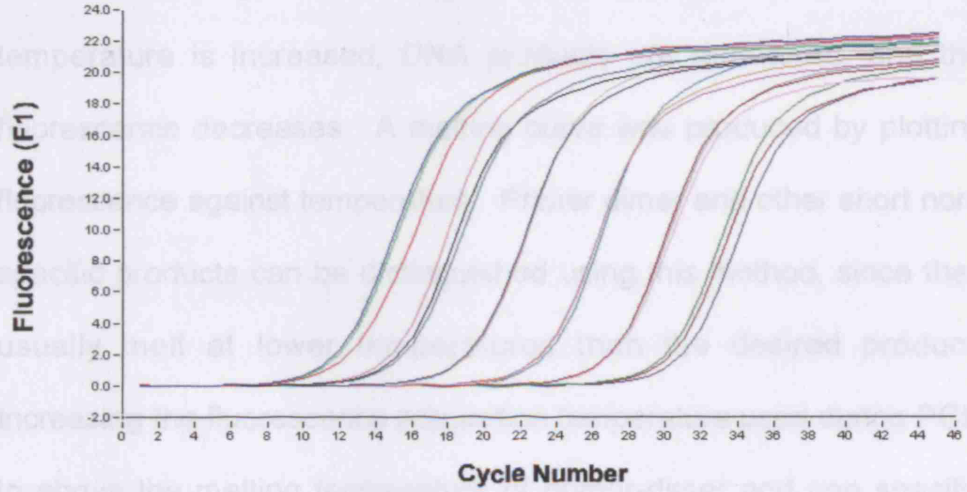

Figure 2.2 Representative graphs showing light cycler fluorescence emission data for a standard curve. A liner regression line (A) were drown by plotting known log concentration of purified DNA against the cycle against the cycle number at which the initial increase in fluorescence was detected (Baseline line) (B).

2.2.3.7 Analysis of the melting curve

After completion of the PCR amplification cycles, a melting curve was determined for each PCR product. Each dsDNA has its own melting temperature (Tm) based on the strand length and the G-C content. Therefore melting curve analysis can be used to identify unwanted by-products of the PCR reaction such as primer dimer. The PCR products were heated to 65°C and then the temperature was increased slowly (0.1°C per second) whilst fluorescence was continually monitored. At low temperatures all DNA is double stranded, SYBR green 1 binding and fluorescence is maximal. As the temperature is increased, DNA products are denatured, and the fluorescence decreases. A melting curve was produced by plotting fluorescence against temperature. Primer dimer and other short non-specific products can be distinguished using this method, since they usually melt at lower temperatures than the desired product. Increasing the fluorescence acquisition temperature used during PCR to above the melting temperature of primer-dimer and non specific products eliminates any fluorescence due to the presence of these products. PCR products were also analyzed by 2 % agarose gel electrophoresis with ethidium bromide and visualized using a Bio-Rad multi-imager (Bio-Rad, Hemel Hempstead, Herts, UK).

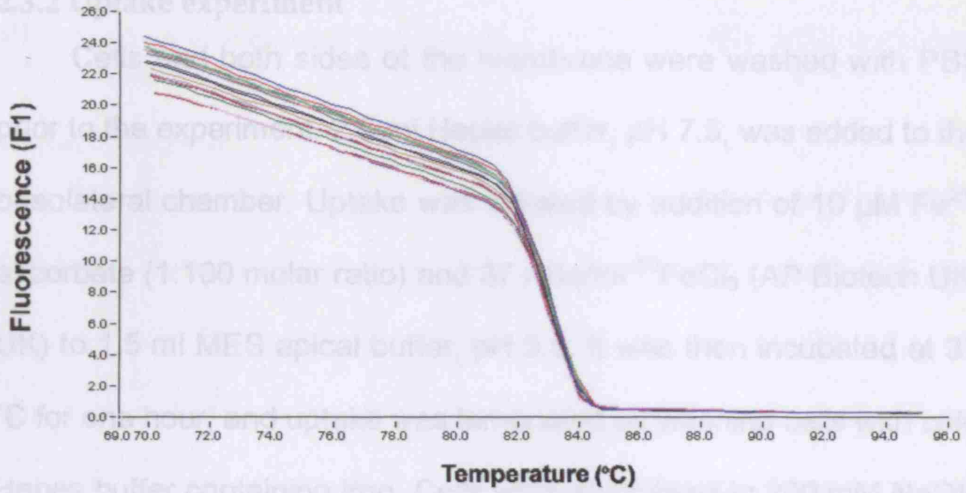

Figure 2.3 Represenative graphs showing light cycler fluorescence emission data for a melting curve. PCR product melting curves (B) were generated by gradual heating from 65 °C to 95°C with continued monitoring of fluorescence. At the melting temperature of the PCR product, there is a steep decrease in fluorescence emission where the dsDNA is denatured.

2.3 Iron uptake

2.3.1 Transepithelial pH gradient

An apical to basolateral transepithelial pH gradient was generated as described in Tandy *et al* (2000), with Hepes buffer (140 mM NaCl, 5 mM KCl, 1mM Na_2HPO_4, 1 mM $CaCl_2$, 0.5 mM $MgCl_2$, 5 mM glucose, 10 mM Hepes, 0.2 % Bovine Serum Albumin (BSA), pH 7.5) in the basolateral chamber and MES buffer (the same ionic composition but with 10 mM MES instead of Hepes, pH 5.5) added to the apical chamber of the transwell.

2.3.2 Uptake experiment

Cells and both sides of the membrane were washed with PBS prior to the experiment. 2.5 ml Hepes buffer, pH 7.5, was added to the basolateral chamber. Uptake was initiated by addition of 10 μM Fe^{2+}: ascorbate (1:100 molar ratio) and 37 KBq/ml $^{55}FeCl_3$ (AP Biotech UK, UK) to 1.5 ml MES apical buffer, pH 5.5. It was then incubated at 37 °C for one hour, and uptake was terminated by washing cells with cold Hepes buffer containing iron. Cells were solubilised in 200 mM NaOH overnight, and 50 μl solubilised sample was subject to scintillation counting in 4ml scintillation fluid (Aquasol-2 Universal LSC-cocktail, PerkinElmer Life and Analytical Sciences, Bucks, UK) on a Tri-Carb 2900TR liquid scintillation analyzer (Packard Bioscience Co, USA) to determine cell iron uptake. An aliquot of the basolateral buffer was also counted to determine transepithelial iron movement.

2.4 Data analysis

Data are presented as the mean ± S.E.M. Statistical analysis was carried out using the SPSS statistical package, or Excel, and utilised one-way ANOVA followed by Scheffe's post-hoc test, or Student's unpaired t-test where appropriate. Differences were considered significant at $p<0.05$.

Chapter 3 : Gene expression during Caco-2 TC7 cells differentiation

3.1 Introduction

The enterocytes in the duodenum are produced as a result of stem cell division and proliferation in the crypts of Lieberkuhn, and migrate onto the villus where they differentiate, taking on their absorptive function in the upper villus regions before finally undergoing cell death at the villus tip. The expressions of iron transport proteins in crypt cells differ that of fully differentiated enterocytes (Bacon *et al.* 1999).

The characteristics of Caco-2 TC7 cells at various stages during the culture period, from day 7 through to day 21 after seeding, were previously analysed by protein expression of villin and TfR as a reference (Sharp *et al.* 2002). It is associated with increase in the expression of the brush border membrane structural protein villin and a decrease in the proliferative cell marker TfR (Sharp *et al.* 2002). Human intestinal epithelial cells take about three days to differentiate from the proliferative stage, and this takes three weeks in Caco-2 TC7 cells (Fig. 3.1). At day 7, Caco cells are still essentially proliferative, and start differentiating at day 10 (initial stage), undergoing differentiation at day 14 (intermediate stage), and Caco-2 cells are

fully differentiated and exhibit a small intestinal enterocyte-like phenotype at day 21 (terminal stage).

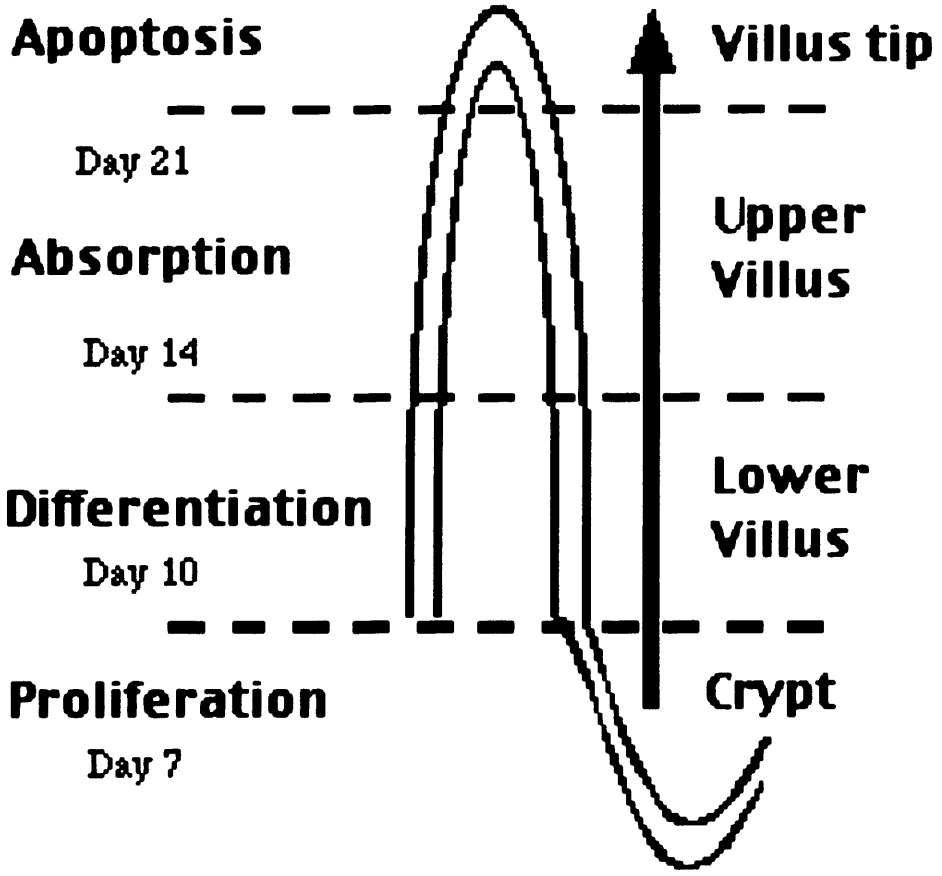

Figure 3.1 The Differential stages of Caco-2 TC7 cells as a life cycle of duodenal enterocyte. Cell lines are representing enterocytes that are produced in the crypts and undergo differentiation along the villus axis before exfoliation at the villus tip.

The advantage of the cell culture approach is that we can measure changes in iron transporter mRNA and protein expression as

well as associated regulation of transport function in defined populations of cells during the differentiation process. Scanning gene expression during cell differentiation in Caco-2 TC7 cells give us an estimate of changes that occur during differentiation in human enterocytes. However, when interpreting these data, it is important to remember that Caco-2 cells are derived from an adenocarcinoma of the colon and as such are not identical to normal duodenal enterocytes.

3.2 Methods

3.2.1 Cell culture

Caco-2 TC7 cells were cultured as described in chapter 2.2.1. Experiments were carried out on either day 7, 10, 14 or 21 following seeding. In some experiments, cells were incubated with 100 μM $FeCl_3$ for the final 24 h of the culture period to determine the effects of increased iron on DMT1 mRNA expression.

3.2.2 Gene expression using thermal cycler

RT-PCR was carried out as described in chapter 2.2.2.

3.2.3 Data analysis

Data are presented as the mean ± S.E.M. and were analysed as described in chapter 2.4.

3.3 Results

3.3.1 Gene expression of DMT1 in Caco-2 TC7 cell during cell differentiation

DMT1 mRNA (normalised to GAPDH expression) was expressed in Caco-2 TC7 cells at all stages of differentiation, increased with cell differentiation reaching the maximal level at day 21 (Fig. 3.2.). The expression was lowest at day 7, increased significantly at day 10 and 14, and it further increased significantly to its highest level at day 21. The apical iron transporter DMT1 mRNA expression was greatest at day 21 of cell culture which represent an enterocytes that are fully differentiated.

These expressions pattern of DMT1 mRNA correlate with protein expression and iron uptake findings in our lab (Sharp *et al.* 2002). Both DMT1 protein and pH-dependent iron transport showed lowest activity in the proliferating cells (day 7) and highest activity in the differentiated cells (day 14 and 21) (Sharp *et al.* 2002).

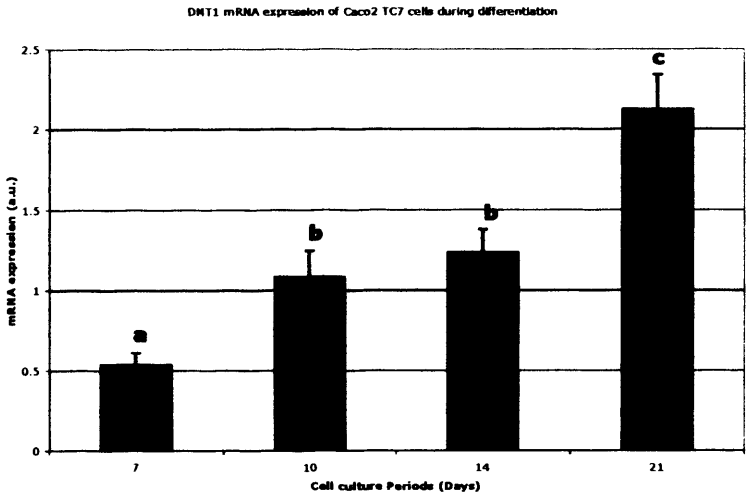

Figure 3.2 Differentiation-dependent regulation of DMT1 mRNA expression in Caco-2 TC7 cells. Cells at days 7(proliferative), 10 (at start of differentiation), 14 and 21 (fully differentiated) were used to draw a maturation axis, and mRNA levels increased during differentiation. Gene expression was normalised to GAPDH using MultiAnalyst image analysis software (Bio-Rad) and presented in arbitrary units. Data are presented as mean ±S.E.M. of six separate samples in each group. Different letters above data bars indicate the statistically significant difference in each group ($p<0.05$).

There are two splice variants of DMT1 at the 3'UTR, one contains a single iron responsive element (IRE) and the other lacks this 3'-IRE (Lee *et al.* 1998). To investigate the expression of these two isoforms of DMT1 during differentiation, PCR was performed using the isoform specific primers. It is clear that the expression pattern of the two isoforms differ from each other during Caco-2 TC7 cell differentiation (Fig. 3.3). At day 7 of the proliferating cells, DMT1+IRE was barely expressed, and DMT1 mRNA was predominantly the DMT1-IRE form. DMT1+IRE form starts to appear

from day 10 and gradually increased its expression to its maximal at day 21. The expression level of DMT1–IRE form remained at the level of proliferating cells at day 10 and 14, and elevated at day 21 by about 10 fold. It is apparent that expression pattern of the two isoforms are different along the maturation axis of Caco-2 TC7 cells. The expression of DMT1+IRE isoform increased with cell differentiation, whereas DMT1-IRE form only amplified when cells are fully differentiated (day 21).

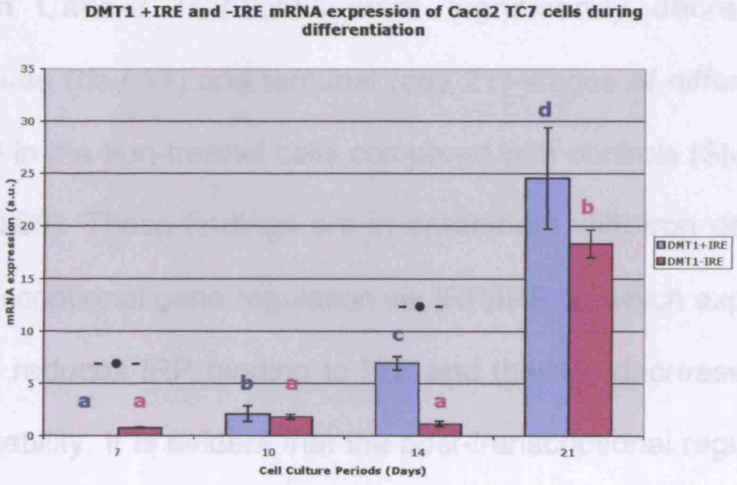

Figure 3.3 Differentiation-dependent regulation of DMT1 mRNA isoforms expression in Caco-2 TC7 cells. Cells at days 7(proliferative), 10 (at start of differentiation), 14 and 21 (fully differentiated) were used to draw a maturation axis, and mRNA levels increased during differentiation. Gene expression was normalised to GAPDH using MultiAnalyst image analysis software (Bio-Rad) and presented in arbitrary units. Data are presented as mean ±S.E.M. of six separate samples in each group. •P< 0.05 (Student's unpaired t-test). Different letters above data bars indicate that these groups are statistically different from each other ($p<0.05$).

3.3.2 Effect of high iron in DMT1 mRNA isoforms in Caco-2 TC7 cells during cell differentiation

To investigate the relationship between non-haem iron and the functional expression of the two DMT1 mRNA isoforms, Caco-2 TC7 cells at various stages of differentiation were exposed to high iron (100 μM) for final 24 hours of the culture period (Fig 3.4 and 3.5). Proliferative cells (day 7) and cells in the initial stage of differentiation (day 10) were found to be unaffected by exposure to high iron for 24 hours. This is most likely due to the low level of DMT1+IRE mRNA expression (Fig. 3.3) such that the level of gene expression is not sufficient to show any difference at this stage. DMT1+IRE mRNA levels in Caco-2 TC7 cells were significantly decreased at intermediate (day 14) and terminal (day 21) stages of differentiation (Fig. 3.4) in the iron-treated cells compared with controls (Student's t-test, $P<0.05$). These findings are in agreement with iron dependent post-transcriptional gene regulation via IRP/IRE, in which exposure to high iron reduces IRP binding to IRE and thereby decreases DMT1 mRNA stability. It is evident that the post-transcriptional regulation of DMT1+IRE by the IRE/IRP system is functional in differentiated Caco-2TC7 cells.

The findings that incubating cells with 100 μM iron for 24 hours did not significantly alter DMT1-IRE mRNA at any stage during the

differentiation process (Fig. 3.5) further supports post-transcriptional regulation of DMT1 mRNA via IRP/IRE. As IRP are unable to bind to the mRNA due to lack of an IRE in the 3'UTR of DMT1-IRE forms, its regulation remained independent of changes in cellular iron status throughout cell maturation. Taken together, these data suggest that only differentiated absorptive cells along crypt-villus have the capacity to respond to changes in the local dietary environment at post-transcriptional level via IRP/IRE system.

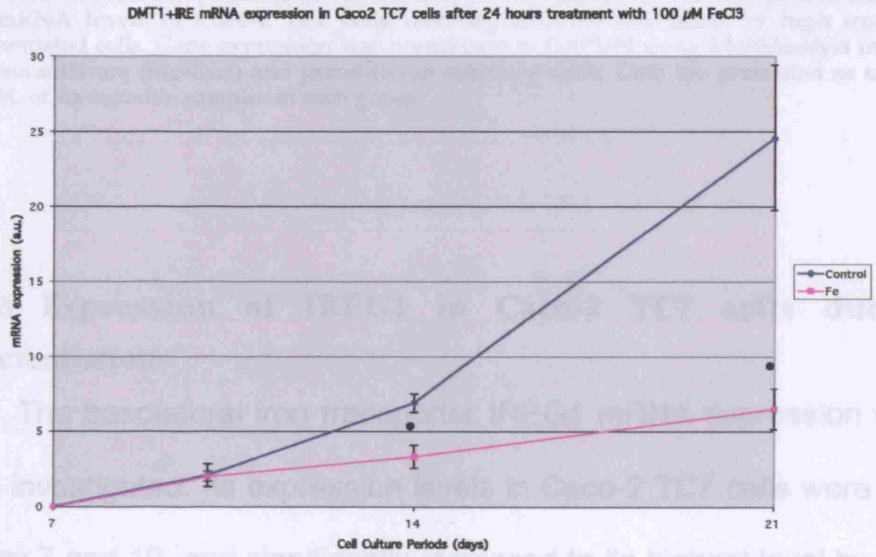

Figure 3.4 Effect of exposure to high iron on DMT1+IRE mRNA expression. Caco-2 TC7 cells were incubated in presence of 100 μM iron for the final 24 h of culture period. DMT1+IRE mRNA levels of Caco-2 TC7 cells were significantly decreased by high iron in differentiated cells. Gene expression was normalised to GAPDH using MultiAnalyst image analysis software (Bio-Rad) and presented in arbitrary units. Data are presented as mean ±S.E.M. of six separate samples in each group. •$P < 0.05$ (Student's unpaired t-test).

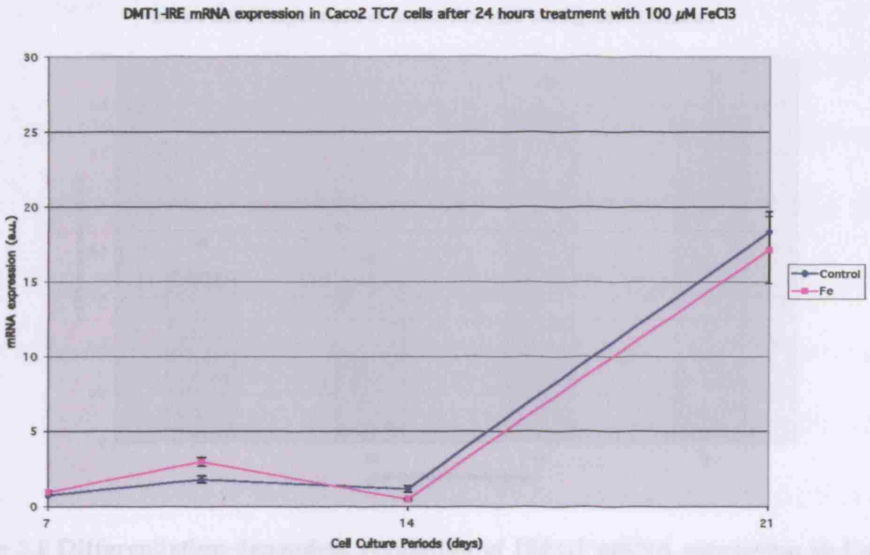

Figure 3.5 Effect of exposure to high iron on DMT1-IRE mRNA expression. Caco-2 TC7 cells were incubated in presence of 100 μM iron for the final 24 h of culture period. DMT1-IRE mRNA levels of Caco-2 TC7 cells were significantly decreased by high iron in differentiated cells. Gene expression was normalised to GAPDH using MultiAnalyst image analysis software (Bio-Rad) and presented in arbitrary units. Data are presented as mean ±S.E.M. of six separate samples in each group.

3.2.3 Expression of IREG1 in Caco-2 TC7 cells during differentiation

The basolateral iron transporter IREG1 mRNA expression was also investigated. Its expression levels in Caco-2 TC7 cells were low at day 7 and 10, and significantly increased to its highest level by day 14 and remained at that level to day 21 (Fig. 3.6).

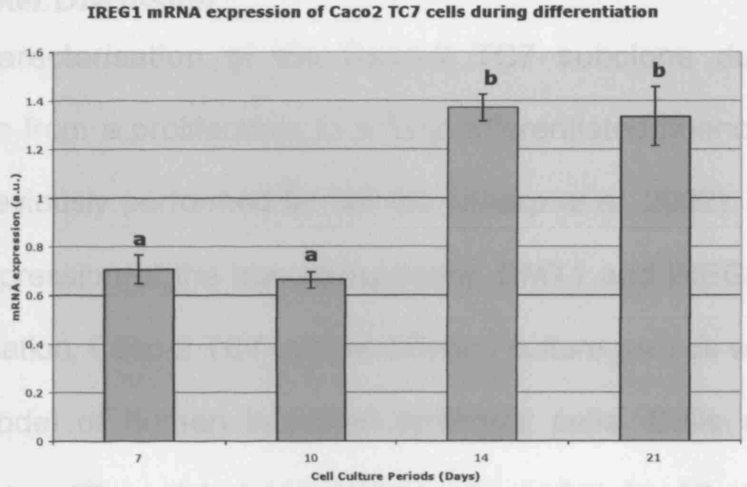

Figure 3.6 Differentiation-dependent regulation of IREG1 mRNA expression in Caco-2 TC7 cells. Cells at days 7(proliferative), 10 (at start of differentiation), 14 and 21 (fully differentiated) were used to draw maturation axis, and mRNA levels increased during differentiation. Gene expression was normalised to GAPDH using MultiAnalyst image analysis software (Bio-Rad) and presented in arbitrary units. Data are presented as mean ±S.E.M. of six separate samples in each group. Different letters above data bars indicate that these groups are statistically different from each other ($p<0.05$).

3.3 Chapter Discussion

Characterisation of the Caco-2 TC7 subclone during the transition from a proliferative to a fully differentiated phenotype has been previously performed by our lab (Sharp *et al.* 2002). To study gene expression of the iron transporters, DMT1 and IREG1, during differentiation, Caco-2 TC7 cells at different culture periods were used as a model of human intestinal epithelial cells. Cells at day 7 represent undifferentiated proliferative cells, and at day 10 cells are in the initial, at day 14 in intermediate, and day 21 at terminal stages of differentiation.

Gene expression of both iron transporters, DMT1 and IREG1, in Caco-2 TC7 cells was observed at all stages of differentiation and increased markedly with time in culture (Fig. 3.2 and 3.6). A similar increase in DMT1 mRNA with time has been noted previously in post confluent Caco-2 cells (Han et al. 1999), and this work also found DMT1 mRNA in pre-confluent undifferentiated proliferating cells (day 7). Crypt cells depend on receiving iron from transferrin and not from dietary sources, just like other cell types in the body. Only the fully differentiated enterocyte obtains iron from diet. This is evident from the decrease in transferrin receptor expression along the differentiation axis, with expression highest in 7 day old cells (Sharp *et al.* 2002). The findings in this chapter are consistent with the

requirement for DMT1 in the cellular accumulation of iron from transferrin via the endosomal pathway (Canonne-Hergaux *et al.* 1999; Tabuchi *et al.* 2000). The increase of DMT1 mRNA with time in culture was reflected in marked increase in expression of DMT1 protein and pH-dependent iron transport observed in our lab (Sharp *et al.* 2002).

The relative amounts of DMT1+IRE form to non IRE form varies in different tissues, and intestine is known to have high ratios of the IRE to the non IRE form (Lee *et al.* 1998). This is may be the case in differentiated cells, however, results described in this chapter revealed that it is not the case in proliferating cells. Pre-confluent undifferentiated proliferating cells were found to have a much lower ratio of the IRE to the non IRE form, as found in cells of the spleen and pancreas. This ratio was created due to difference in differentiation-dependent expression of the two isoforms. DMT1+IRE form expression is almost negligible in proliferative cells and gradually increased to its maximal level at day 21, whereas the expression level of DMT1–IRE form remained at low level from proliferating cells to intermediate stage of differentiation, and sharply elevated at day 21 by about 10 fold (Fig. 3.6). Therefore, as Caco-2 TC7 cells differentiate and develop enterocyte like characteristics, the

DMT1+IRE form dominates the expression, whereas increased expression of both isoforms are responsible for the maximal DMT1 expression at the terminal stages of differentiation.

This ratio of the IRE form to non-IRE form of DMT1 becomes an important factor determining the modulation of total DMT1 mRNA levels by iron, since only the IRE form was found to respond to iron (Fig. 3.4 and 3.5). The IRE form of DMT1 mRNA includes one IRE element in the 3'UTR, which is sensitive to ribonuclease degradation. Under high iron conditions, binding of IRPs to IREs is prevented, resulting in rapid mRNA degradation (Muckenthaler *et al.* 1998). Unlike the IRE form, the non-IRE form of DMT1 mRNA was found to be not sensitive to iron treatment (Fig. 3.5). The regulation of the non-IRE form is independent of cellular iron levels, and must be regulated by some other cellular signals.

It is possible to assume that increases in DMT1 and IREG1 gene expression during differentiation are due to an increase in demand for iron associated with cell growth. However, cells in early stages of differentiation are unable to respond to high iron, whereas the DMT1+IRE mRNA in differentiated cells responds to high iron significantly. Although TfR protein was employed as the proliferative cell marker and decreased with differentiation, its mRNA contains five

IREs in 3'UTR and should respond in the same way as DMT1 mRNA in response to changes to cellular iron status. A similar conclusion was made by others from the findings that while TfR protein was decreased, the cellular ferritin content was not altered by differentiation of Caco-2 cells (Han *et al.* 1999). The cellular signals that regulate DMT1 and IREG1 gene expression during differentiation are unknown, but are likely to be independent of iron status to which the two isoforms of DMT1 respond differently.

Chapter 4 : The effect of metals on iron absorption by Caco-2 TC7 cells

4.1 Introduction

Iron, copper and zinc are essential trace elements that exhibit important interactions however there are possibilties that those minerals inhibit each other's transport and bioavailability (Barone et al. 1998). Excessive intake of one of these elements, for example in high dose supplements, may result in deficiency of another element.

Such information is important as well as useful, for example the antagonism between zinc and copper has been known for long time, and zinc salts are beneficially exploited for the treatment of Wilson's disease as a preventive measure to Cu accumulation (Barone *et al.* 1998; Wapnir 1998). Iron is known to decrease zinc absorption (Sandstrom 2001) and copper deficiency causes anaemia due to decrease in copper-requiring proteins including the multicopper oxidase, hephaestin, required for efficient export of iron from the intestine .

The apical iron transporter DMT1 is thought to have a wide substrate range on the basis of ion conductances that were elicited by other metals in a similar manner to iron (Gunshin *et al.* 1997). These include Fe^{2+}, Mn^{2+}, Ni^{2+}, Cu^{2+}, Co^{2+} (Conrad *et al.* 2000) and possibly

other cations, such as Zn^{2+}, are thought to inhibit iron uptake (Tandy et al. 2000; Sacher et al. 2001; Yamaji et al. 2001). Garrick *et al* (2003) summarised current information on which metals are potentially transported by DMT1 and is presented in Table 4.1.

TABLE 4.1 DMT1 INTERACTIONS WITH INORGANIC METALS.
(modified from Garrick et al. 2003).

Metal	Conduction	Uptake	Competition
Fe^{2+}	Yes	Yes	Yes
$Fe^{3}+$	No	No	No
Zn^{2+}	Yes	No	No
Mn^{2+}	Yes	Yes	Yes
Ni^{2+}	Yes	Yes	Yes
Co^{2+}	Yes	Yes	Yes
Cu^{2+}	Yes	Untested	Yes
Cd^{2+}	Yes	Untested	Yes
Pb^{2+}	Yes	Untested	Yes

The purpose of the study in this chapter is to gain better understanding of the interaction between zinc, copper and iron at molecular level in the intestine, using Caco-2 TC7 cells as a model of human intestinal enterocytes.

4.2 Methods

4.2.1 Cell culture

Caco-2 TC7 cells were cultured as described in chapter 2.2.1. Experiments were carried out on day 21 following seeding. Prior to all experiments, cells were incubated with 100 μM $FeCl_3$, $CuCl_2$, $ZnSO_4$ or Desferrioxamine (DFO) for the final 24 h or 48 h of the culture period.

4.2.2 Gene expression using thermal cycler

PCR was carried out as described in chapter 2.2.2.

5.2.5 Data analysis

Data are presented as the mean ± S.E.M. and were analysed as described in chapter 2.4.

4.3 Results

4.3.1 Effect of high iron on gene expression of proteins that are involved in iron uptake in Caco-2 TC7 cells

After 24 hours exposure to 100 μM iron, DMT1 mRNA expression in Caco-2 TC7 cells was dramatically reduced (Fig. 4.1). However, basolateral iron transporter, IREG1, was not affected by the same exposure to iron (Fig. 4.2). Interestingly, gene expression of hephaestin, the basolateral copper oxidase thought to work in conjunction with IREG1, was significantly down-regulated (Fig. 4.3).

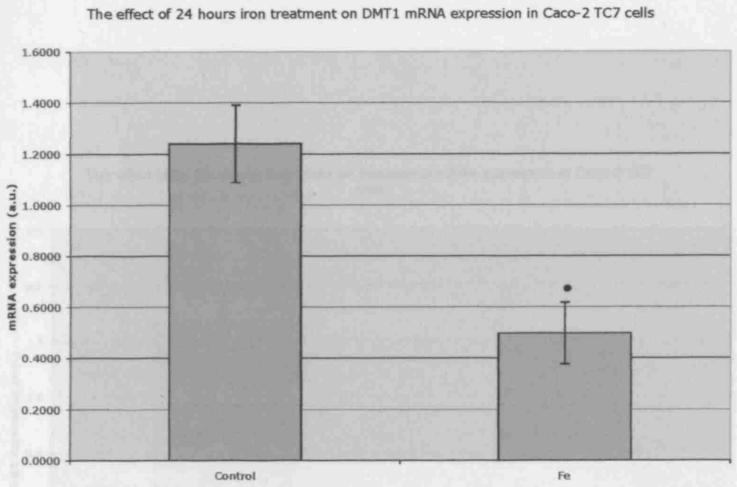

Figure 4.1 Effect of iron exposure on DMT1 mRNA in Caco-2 TC7 cells at 21 days. Cells were treated with 100μM $FeCl_3$ for final 24hours of culture period. Gene expression was quantified using Real-Time PCR (Roche) and normalised to HPRT using Relative Quantification Software (V 1.0, Roche) and presented in arbitrary units. Data are presented as mean ±S.E.M. of six separate samples in each group. •P< 0.05 (Student's unpaired t-test).

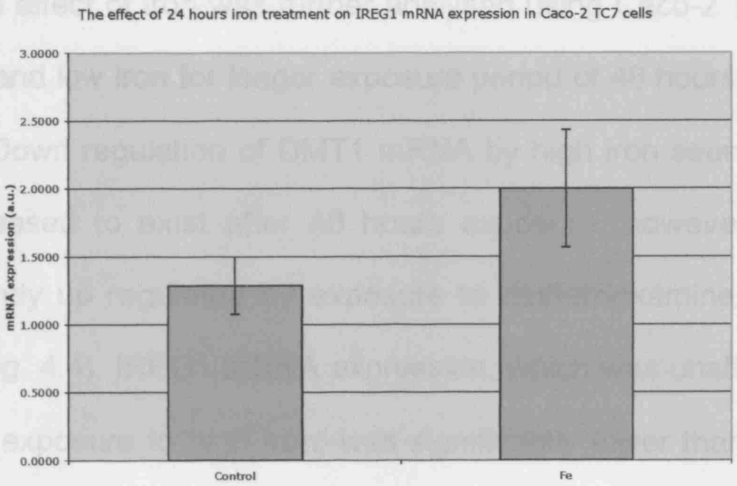

Figure 4.2 Effect of iron exposure on IREG1 mRNA in Caco-2 TC7 cells at 21 days. Cells were treated with 100μM $FeCl_3$ for final 24hours of culture period. Gene expression was quantified using Real-Time PCR (Roche) and normalised to HPRT using Relative Quantification Software (V 1.0, Roche) and presented in arbitrary units. Data are presented as mean ±S.E.M. of six separate samples in each group.

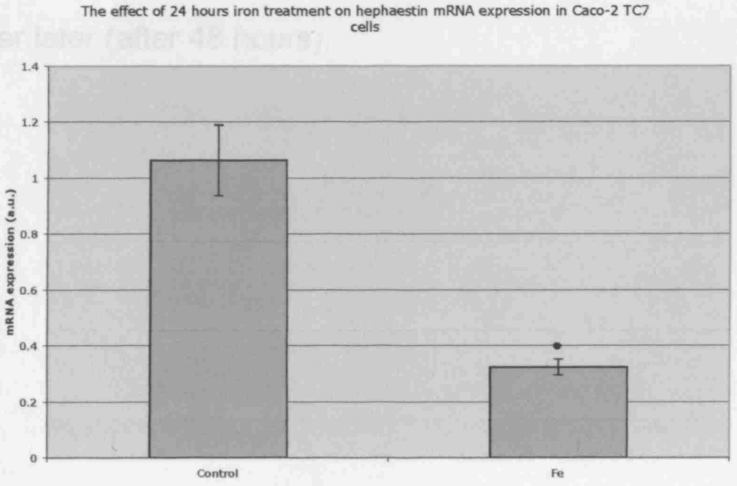

Figure 4.3 Effect of iron exposure on hephaestin mRNA in Caco-2 TC7 cells at 21 days. Cells were treated with 100μM $FeCl_3$ for final 24hours of culture period. Gene expression was quantified using Real-Time PCR (Roche) and normalised to HPRT using Relative Quantification Software (V 1.0, Roche) and presented in arbitrary units. Data are presented as mean ±S.E.M. of six separate samples in each group. •$P < 0.05$ (Student's unpaired t-test).

The effect of iron was further analysed using Caco-2 TC7 cells for high and low iron for longer exposure period of 48 hours (Fig. 4.4 to 4.6). Down regulation of DMT1 mRNA by high iron seen after 24 hours ceased to exist after 48 hours exposure, however, it was significantly up regulated by exposure to desferrioxamine after 48 hours (Fig. 4.4). IREG1 mRNA expression, which was unaffected by 24hours exposure to high iron, was significantly lower than control, and desferrioxamine significantly increased IREG1 mRNA after 48 hours exposure (Fig. 4.5). Hephaestin mRNA was unaffected by either high or low iron exposure for 48 hours (Fig. 4.6). This suggests that high dietary iron alters gene expression of iron transporters at both ends, apical transporter first after 24 hours) and then basolateral transporter later (after 48 hours).

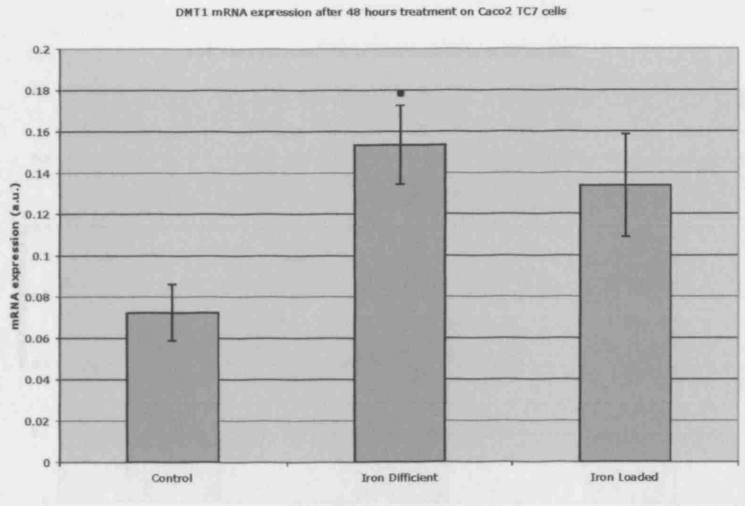

Figure 4.4 Effects of low and high iron on DMT1 mRNA in Caco-2 TC7 cells at 21 days. Cells were treated with DFO (low iron) or 100μM $FeCl_3$ (high iron) for final 48hours of culture period. Gene expression was quantified using Real-Time PCR (Roche) and normalised to HPRT using Relative Quantification Software (V 1.0, Roche) and presented in arbitrary units. Data are presented as mean ±S.E.M. of three or four separate samples in each group. •P< 0.05 (Student's unpaired t-test).

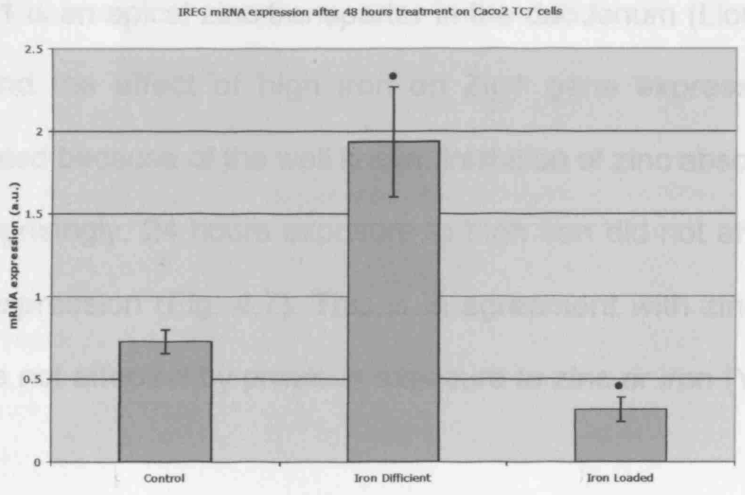

Figure 4.5 Effects of low and high iron on IREG1 mRNA in Caco-2 TC7 cells at 21 days. Cells were treated with Df (low iron) or 100μM $FeCl_3$ (high iron) for final 48 hours of culture period. Gene expression was quantified using Real-Time PCR (Roche) and normalised to HPRT using Relative Quantification Software (V 1.0, Roche) and presented in arbitrary units. Data are presented as mean ±S.E.M. of three or four separate samples in each group. •P< 0.05 (Student's unpaired t-test).

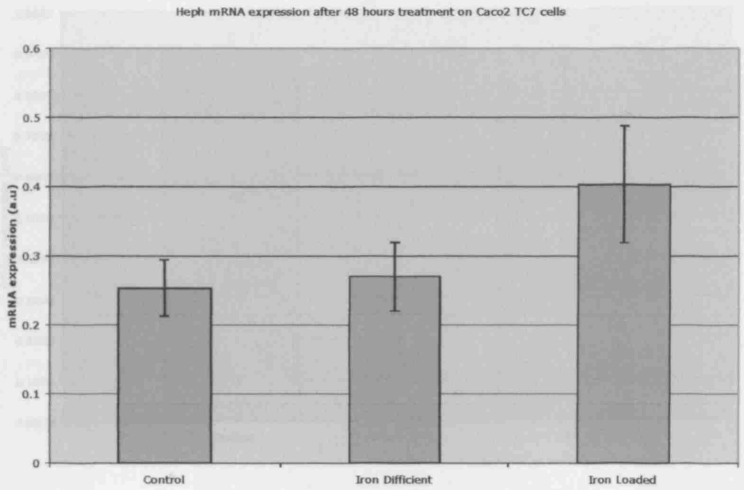

Figure 4.6 Effects of low and high iron on Hephaestin mRNA in Caco-2 TC7 cells at 21 days. Cells were treated with DFO (low iron) or 100μM $FeCl_3$, (high iron) for final 48 hours of culture period. Gene expression was quantified using Real-Time PCR (Roche) and normalised to HPRT using Relative Quantification Software (V 1.0, Roche) and presented in arbitrary units. Data are presented as mean ±S.E.M. of three or four separate samples in each group. •$P < 0.05$ (Student's unpaired t-test).

Zip1 is an apical zinc transporter in the duodenum (Lioumi *et al.* 1999) and the effect of high iron on Zip1 gene expression was investigated because of the well known inhibition of zinc absorption by iron. Surprisingly, 24 hours exposure to high iron did not affect Zip1 mRNA expression (Fig. 4.7). This is in agreement with zinc uptake that were not affected by previous exposure to zinc or iron (Yamaji *et al.* 2001).

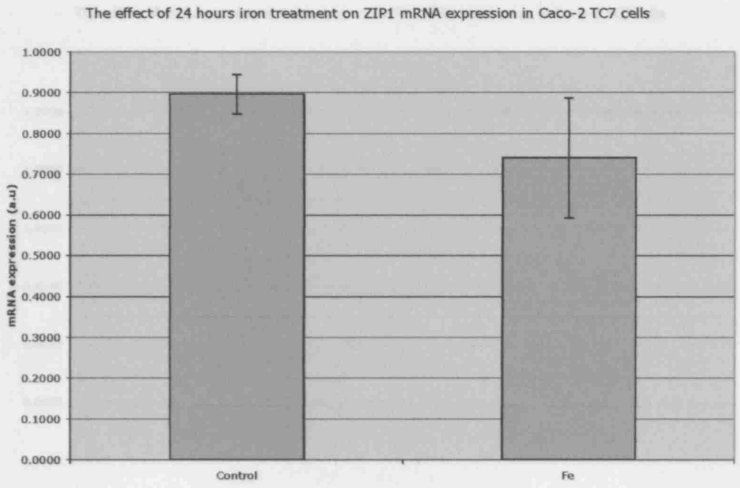

Figure 4.7 Effect of iron exposure on Zip1 mRNA in Caco-2 TC7 cells at 21 days. Cells were treated with 100μM $FeCl_3$ for final 24hours of culture period. Gene expression was quantified using Real-Time PCR (Roche) and normalised to HPRT using Relative Quantification Software (V 1.0, Roche) and presented in arbitrary units. Data are presented as mean ±S.E.M. of six separate samples in each group. •P< 0.05 (Student's unpaired t-test).

4.3.2 Effect of high copper on gene expression of proteins that are involved in iron uptake in Caco-2 TC7 cells

After 24 hours exposure to 100 μM copper, DMT1 mRNA expression in Caco-2 TC7 cells was significantly reduced (Fig. 4.8). This correlates with the finding that copper reduced iron uptake, DMT1 protein and DMT1+IRE mRNA expression in Caco-2TC7 cells (Tennant *et al.* 2002).

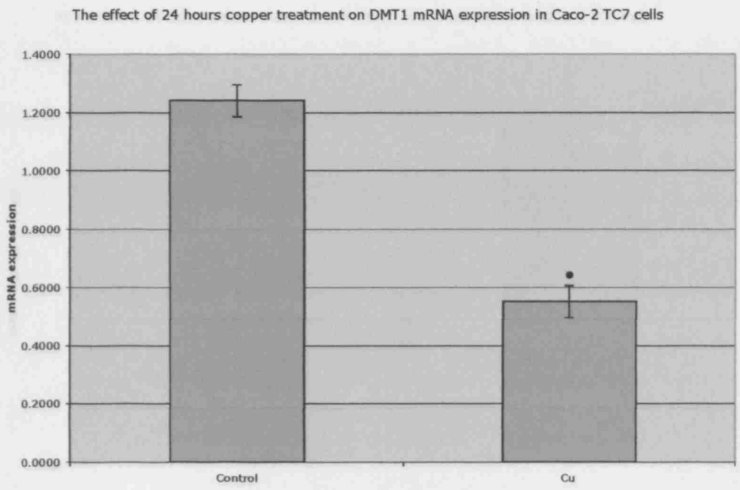

Figure 4.8 Effect of copper exposure on DMT1 mRNA in Caco-2 TC7 cells at 21 days. Cells were treated with 100μM $CuCl_2$ for final 24hours of culture period. Gene expression was quantified using Real-Time PCR (Roche) and normalised to HPRT using Relative Quantification Software (V 1.0, Roche) and presented in arbitrary units. Data are presented as mean ±S.E.M. of six separate samples in each group. •$P < 0.05$ (Student's unpaired t-test).

The basolateral iron transporter, IREG1 was significantly increased by the same exposure to copper (Fig. 4.9). This is in agreement with increased iron transport and IREG1 protein and mRNA expression shown in Tennant *et al* (2002). However, mRNA expression of a multicopper oxidase, hephaestin, thought to work in conjunction with IREG1 was significantly decreased (Fig. 4.10), suggesting this decrease does not alter efficiency of iron transport at this time scale (24 hours).

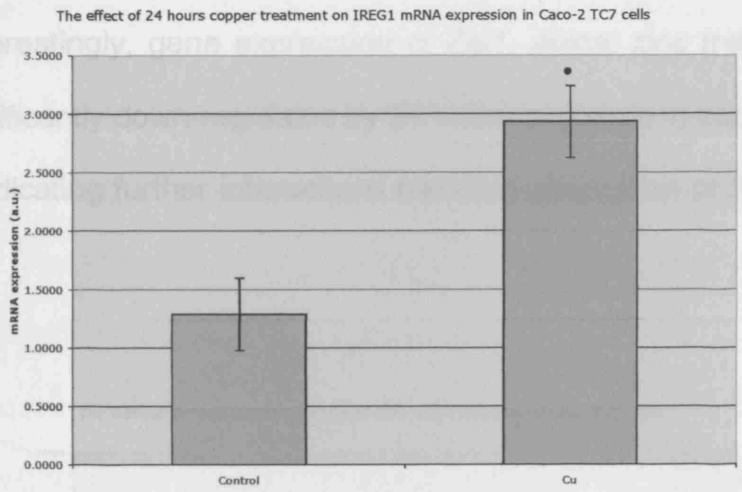

Figure 4.9 Effect of copper exposure on IREG1 mRNA in Caco-2 TC7 cells at 21 days. Cells were treated with 100μM $CuCl_2$ for final 24hours of culture period. Gene expression was quantified using Real-Time PCR (Roche) and normalised to HPRT using Relative Quantification Software (V 1.0, Roche) and presented in arbitrary units. Data are presented as mean ±S.E.M. of six separate samples in each group. •P< 0.05 (Student's unpaired t-test).

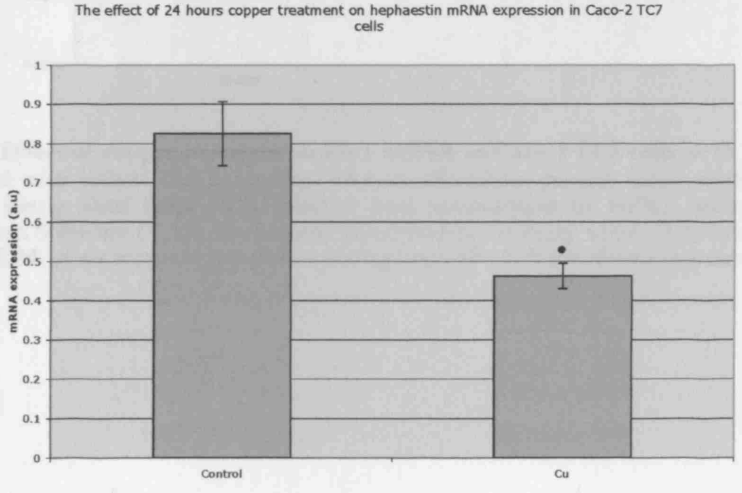

Figure 4.10 Effect of copper exposure on hephaestin mRNA in Caco-2 TC7 cells at 21 days. Cells were treated with 100μM $CuCl_2$ for final 24hours of culture period. Gene expression was quantified using Real-Time PCR (Roche) and normalised to HPRT using Relative Quantification Software (V 1.0, Roche) and presented in arbitrary units. Data are presented as mean ±S.E.M. of six separate samples in each group. •P< 0.05 (Student's unpaired t-test).

Interestingly, gene expression of Zip1, apical zinc transporter, was significantly down-regulated by 24 hours exposure to copper (Fig. 4.11), indicating further interactions between absorption of these two cations.

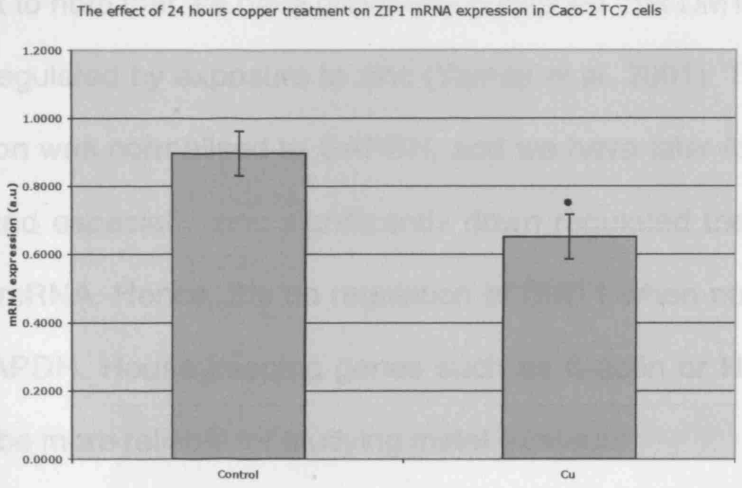

Figure 4.11 Effect of copper exposure on Zip1 mRNA in Caco-2 TC7 cells at 21 days. Cells were treated with 100μM $CuCl_2$ for final 24hours of culture period. Gene expression was quantified using Real-Time PCR (Roche) and normalised to HPRT using Relative Quantification Software (V 1.0, Roche) and presented in arbitrary units. Data are presented as mean ±S.E.M. of six separate samples in each group. •$P < 0.05$ (Student's unpaired t-test).

4.3.3 Effect of high zinc on gene expression of proteins that are involved in iron uptake in Caco-2 TC7 cells

After 24 hours exposure to 100 μM Zinc, DMT1 mRNA expression in Caco-2 TC7 cells was significantly reduced (Fig. 4.12). This is in disagreement with the finding that previous exposure to zinc increased iron uptake and DMT1 expression (Yamaji *et al.* 2001). It is important to note that we have previously published that DMT1 mRNA was up regulated by exposure to zinc (Yamaji *et al.* 2001). This gene expression was normalised to GAPDH, and we have later found that copper and especially zinc significantly down regulated the level of GAPDH mRNA. Hence, the up regulation of DMT1 when normalised using GAPDH. House keeping genes such as ß-actin or HPRT are found to be more reliable for studying metal exposure.

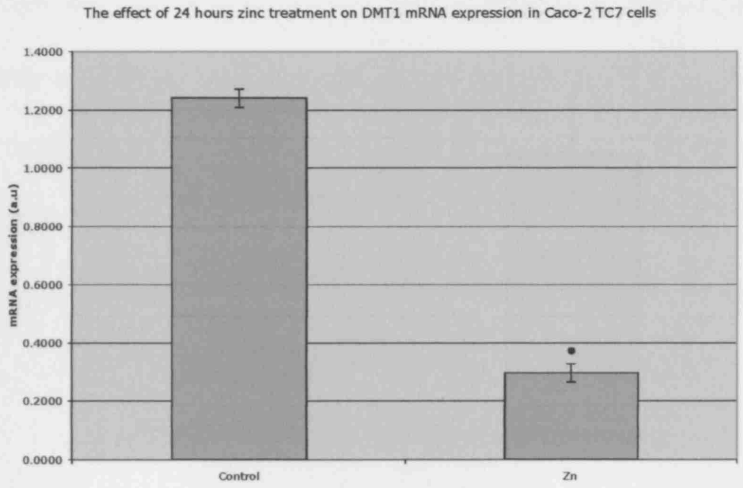

Figure 4.12 Effect of zinc exposure on DMT1 mRNA in Caco-2 TC7 cells at 21 days. Cells were treated with 100μM $ZnSO_4$ for final 24hours of culture period. Gene expression was quantified using Real-Time PCR (Roche) and normalised to HPRT using Relative Quantification Software (V 1.0, Roche) and presented in arbitrary units. Data are presented as mean ±S.E.M. of six separate samples in each group. •P< 0.05 (Student's unpaired t-test).

Basolateral iron transporter IREG1 was significantly increased by the same exposure to zinc (Fig. 4.13). This is in agreement with increased iron transport and IREG1 expression after zinc treatment shown in Yamaji *et al* (2001). However, mRNA expression of a multicopper oxidase, hephaestin, thought to work in conjunction with IREG1 was significantly decreased (Fig. 4.14), suggesting this decrease does not alter efficiency of iron transport at this time scale (24 hours).

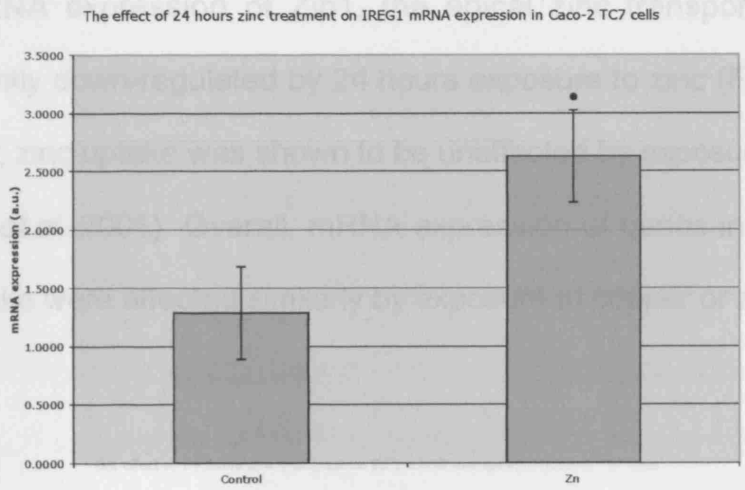

Figure 4.13 Effect of zinc exposure on IREG1 mRNA in Caco-2 TC7 cells at 21 days. Cells were treated with 100μM $ZnSO_4$ for final 24hours of culture period. Gene expression was quantified using Real-Time PCR (Roche) and normalised to HPRT using Relative Quantification Software (V 1.0, Roche) and presented in arbitrary units. Data are presented as mean ±S.E.M. of six separate samples in each group. •P< 0.05 (Student's unpaired t-test).

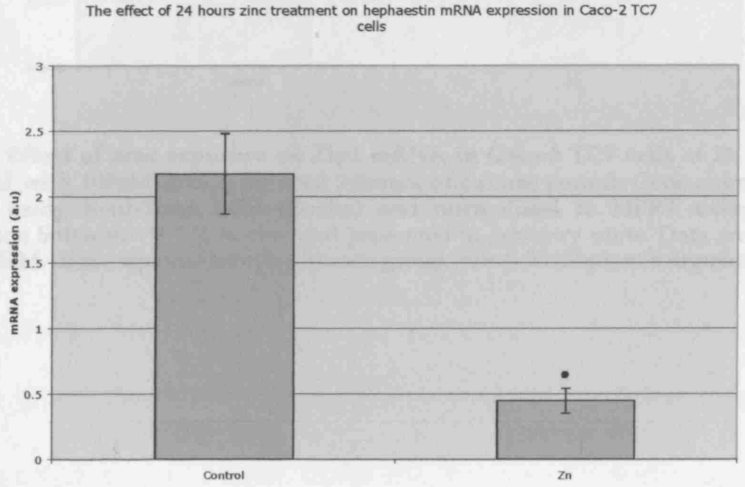

Figure 4.14 Effect of zinc exposure on hephaestin mRNA in Caco-2 TC7 cells at 21 days. Cells were treated with 100μM $ZnSO_4$ for final 24hours of culture period. Gene expression was quantified using Real-Time PCR (Roche) and normalised to HPRT using Relative Quantification Software (V 1.0, Roche) and presented in arbitrary units. Data are presented as mean ±S.E.M. of six separate samples in each group. •P< 0.05 (Student's unpaired t-test).

mRNA expression of Zip1, the apical zinc transporter, was significantly down-regulated by 24 hours exposure to zinc (Fig. 4.11), however, zinc uptake was shown to be unaffected by exposure to zinc (Yamaji *et al.* 2001). Overall, mRNA expression of genes involved in iron uptake were affected similarly by exposure to copper or zinc.

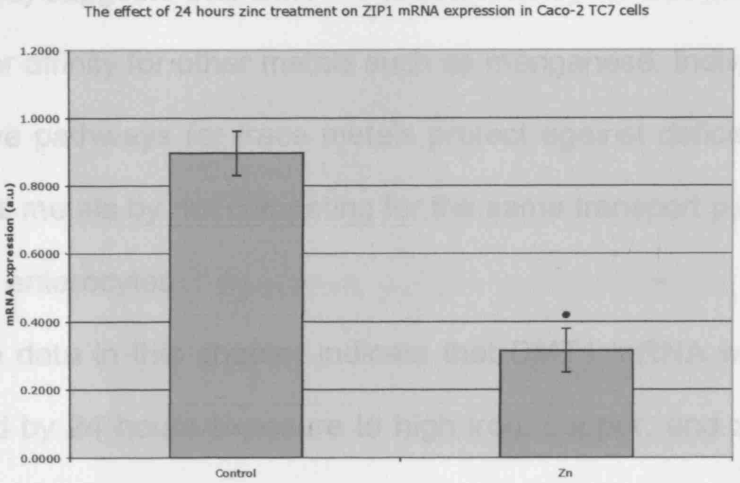

Figure 4.15 Effect of zinc exposure on Zip1 mRNA in Caco-2 TC7 cells at 21 days. Cells were treated with 100μM $ZnSO_4$ for final 24hours of culture period. Gene expression was quantified using Real-Time PCR (Roche) and normalised to HPRT using Relative Quantification Software (V 1.0, Roche) and presented in arbitrary units. Data are presented as mean ±S.E.M. of six separate samples in each group. •$P < 0.05$ (Student's unpaired t-test).

4.4 Discussion

Trace metals influence the absorption of each other from the diet, and it has been suggested that DMT1 represents a common uptake pathway for these important micronutrients (Gunshin *et al.* 1997). However, compelling evidence from our laboratory (Tandy *et al.* 2000; Yamaji *et al.* 2001) and others (Conrad *et al.* 2000; Garrick *et al.* 2003) suggests that DMT1 is predominantly an iron transporter, with lower affinity for other metals such as manganese. Individualised absorptive pathways for trace metals protect against deficiencies of other vital metals by not competing for the same transport pathway to enter the enterocytes.

The data in this chapter indicate that DMT1 mRNA was down regulated by 24 hours exposure to high iron, copper, and zinc (Fig. 4.1, 4.8, 4.12). Like iron, copper and zinc most likely regulate DMT1 mRNA via the IRE/IRP system, and data in the previous chapter has shown that exposure to iron decreases DMT1+IRE mRNA but does not change the non-IRE isoform. Further support is provided by recent data in human hepatoma cells demonstrating that non iron metals, including copper, decreases IRP1/IRE binding, possibly by replacing the labile forth position iron in the iron-sulphur cluster of IRP1, and down regulates transferrin receptor mRNA (Oshiro et al. 2002).

Up regulation of IREG mRNA by copper and zinc after 24 hours exposure (Fig. 4.9 and 4.13) is reflected in increased iron efflux following exposure to copper (Tennant *et al.* 2002) and zinc (Yamaji *et al.* 2001). In agreement with other data (Abboud and Haile 2000), IREG1 mRNA was down regulated by exposure to iron after 48 hours and induced by iron deficiency, though it was unaffected by 24 hours exposure to iron (Fig. 4.2 and 4.5). Others have shown that IREG1 mRNA is increased in response to iron deficiency (Abboud and Haile 2000; McKie *et al.* 2000).

Multi-copper ferroxidase protein hephaestin is thought to work in conjunction with IREG1 for basolateral iron transport, and its mutation results in cellular retention of iron. The reduction in hephaestin mRNA after exposure to copper and zinc (Fig. 4.10 and 4.14) is contradictory to that of IREG1, but this could also be a response to changes in body metal status or other non IRE/IRP regulation, as it does not have an IRE motif. Although Sakakibara and Aoyama (2002) demonstrated that dietary iron deficiency up regulated hephaestin mRNA level in rat small intestine, the dietary iron effect in Caco-2 TC7 cells was short lived. The down regulation of hephaestin after 24 hours exposure to high iron was not observed by 48 hours and it was unaffected by low iron after 48 hours (Fig. 4.6). The mechanisms involved in regulation

of IREG1 and hephaestin by metal ion status are unclear but may be related to regulatory elements in the promoters.

This chapter also showed that the mRNA expression of endogenous zinc transporter Zip1 is down regulated by exposure to zinc (Fig. 4.15). The Zip1 down regulation by zinc is in agreement with Costello (1999) and characteristic of zinc regulation of Zip1 and other zinc uptake transporters (Costello 1999). Interestingly mRNA of this zinc transporter was also down regulated by exposure to copper, but copper does not affect gene expression of functional copper transporter Ctr1 (Tennant *et al.* 2002). Inhibition of cellular zinc uptake has been previously demonstrated by iron (Gaither 2001; Yamaji *et al.* 2001), copper (Gaither 2001), and zinc (Conrad *et al.* 2000; Yamaji *et al.* 2001). Although Zip1 homologues in *arabidopsis* (IRT1) also serve as an iron transporter (Eide et al 1996), Zip1 is not involved in transport of iron (Gaither 2001). Rather Zip1 may transport copper as well as zinc. The characteristic of zinc regulation of Zip1 is also demonstrated by copper in this chapter, and a functional relationship of Zip1 with the S100A proteins (Lioumi *et al* 1999) which are capable of binding Zn^{2+} and Cu^{2+} (Heizmann and Cox 1998), indicate a possible pathway that is shared by zinc and copper (Conrad *et al.*

2000; Gaither 2001). Further functional studies will be needed to elucidate this hypothesis.

In summary, the molecular mechanisms involved in metal dependent regulation are elusive but metal responsive elements in the promoter regions (Lee *et al.* 1998) and modulation IRP1 by metals (Oshiro *et al.* 2002) are likely to play an important role in gene expression of key iron transport proteins.

Chapter 5 : The mechanisms involved in regulation of iron absorption in response to body iron stores

5.1 Introduction

The intestinal iron absorption is thought to be regulated by three main factors that influence iron metabolism. They are; dietary factor at the duodenum, utilisation factor mainly in the bone marrow, and the storage factor at the liver. The balances of these factors maintain the healthy iron level in the body, and there has been much speculation that communication must exist between these factors and the site of absorption by unknown signals.

Recently a candidate peptide that might explain the link between body iron levels and the regulation of intestinal iron absorption has been independently isolated in urine (Park et al. 2001) and in plasma ultrafiltrate (Krause et al. 2000). The peptide is a 20-25 amino acid, cysteine-rich antimicrobial peptide called hepcidin or Leap1 that differs in size by N-terminal truncation (Krause *et al.* 2000; Park *et al.* 2001). In solution, 25 amino acid hepcidin forms a distorted beta-sheet with an unusual disulphide bond found at the turn of the hairpin, and readily aggregates (Hunter et al. 2002) (Fig. 5.1).

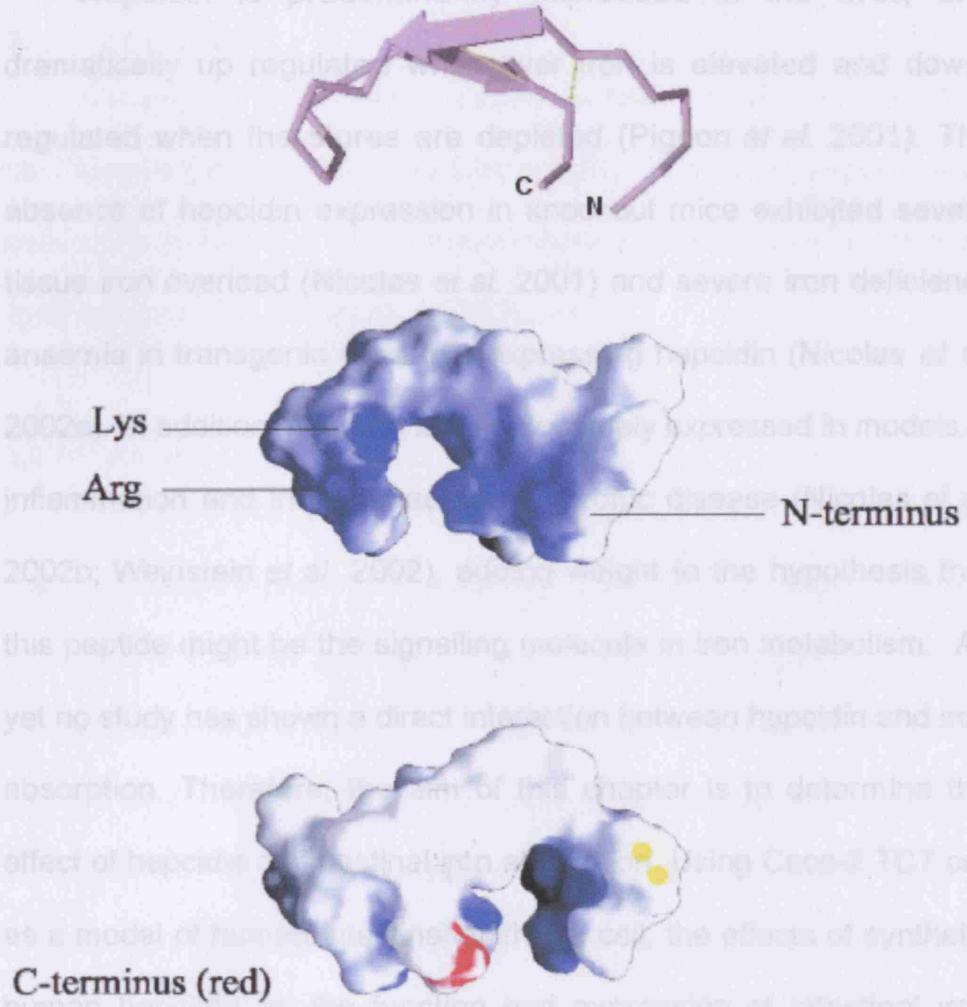

Fig. 5.1 Structure of 25 amino acid human hepcidin. Space filling diagram of hepcidin indicating cationic charges (blue) and hydrophobic (white) side with vicinal disulfide (yellow). (Generated with GRASP). Modified from Hunter et al (2002) and EBI data base (EBI; Hunter *et al.* 2002)

Hepcidin is predominantly expressed in the liver, and dramatically up regulated when liver iron is elevated and down-regulated when the stores are depleted (Pigeon *et al.* 2001). The absence of hepcidin expression in knockout mice exhibited severe tissue iron overload (Nicolas *et al.* 2001) and severe iron deficiency anaemia in transgenic mice that expressing hepcidin (Nicolas *et al.* 2002a). In addition, hepcidin is inappropriately expressed in models of inflammation and in the anaemia of chronic disease (Nicolas *et al.* 2002b; Weinstein *et al.* 2002), adding weight to the hypothesis that this peptide might be the signalling molecule in iron metabolism. As yet no study has shown a direct interaction between hepcidin and iron absorption. Therefore, the aim of this chapter is to determine the effect of hepcidin on intestinal iron absorption. Using Caco-2 TC7 cell as a model of human intestinal epithelial cell, the effects of synthetic human hepcidin on the function and expression of intestinal iron transporter proteins DMT1 and IREG1 were tested, as well as expression of other iron metabolism associated genes Dcytb and hephaestin.

5.2 Methods

5.2.1 Cell culture

Caco-2 TC7 cells were cultured as described in chapter 2.2.1. on Transwell inserts (Corning-Coster, UK). Prior to all experiments, cells were switched to serum-free medium and stimulated with human synthetic hepcidin (30µg/ml) for 24 hours.

5.2.2 Hepcidin synthesis

25 amino acid human hepcidin was synthesized by Dr. Bala Ramesh (Department of Biochemistry and Molecular Biology, Royal Free and University College London Medical School) on a Wang alcohol resin with a loading of 1.30 mmol/g on a Rainin automatic peptide synthesizer (Protein Technologies, Tuscon, AZ) using the standard Fmoc chemistry. Cysteine sulphurs were protected with trityl groups and all other side-chain functions were protected with trifluoroacetic acid (TFA)–labile groups. All the cysteines were introduced as preformed symmetrical anhydrides to prevent enantiomerization during assembly. The completed peptide was de-protected and cleaved from the resin with a mixture of TFA, ethanedithiol, and water (94:3:3). The final product was precipitated with cold diethyl ether, dried, and purified by reverse-phase high-performance liquid chromatography (HPLC) on a Vydac C18 column

(Vydac Hessperia, Anaheim, CA). The lyophilized prepurified reduced hepcidin was dissolved in neat TFA and rotary evaporated so as to give a thin film of peptide on the surface of a quick-fit flask. The peptide was further dried under vacuum for 24 hours. To this dried film, 0.1 M de-gassed ammonium bicarbonate was added and the mixture was stirred for 48 hours while open to atmosphere. The reaction was then analyzed by the Ellman reagent to ascertain complete oxidation. The mixture was lyophilized and purified by reverse-phase HPLC on a Vydac C18 column.

The mass of oxidized peptide was verified by mass spectrometry (Maldi-Tof) and was found to be 2789. The oxidized hepcidin was further analyzed by electrophoresis on a 16.5% tricine sodium dodecyl sulfate (SDS)–polyacrylamide gel. It migrated as a narrow single band with an apparent molecular weight of less than 10 000 in agreement with the apparent molecular weight of native urinary hepcidin when electrophoresed under identical conditions.

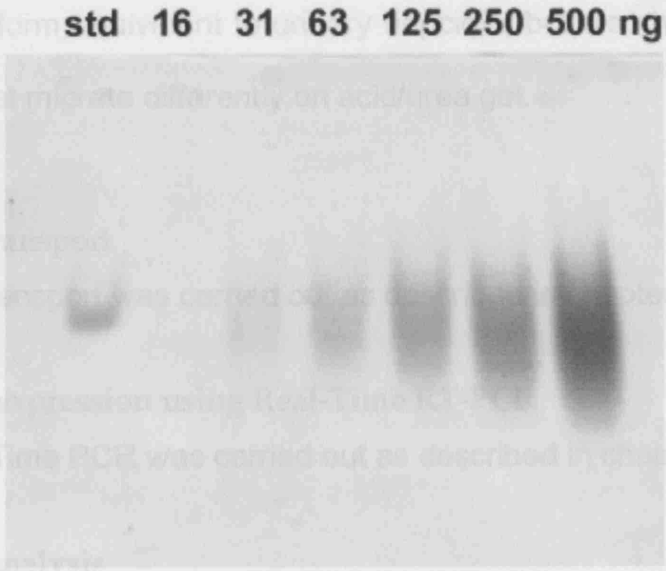

Figure 5.2 Analysis of synthetic hepcidin by 12.5% acid-urea polyacrylamide gel electrophoresis (PAGE). The gel was loaded with the indicated amounts of peptide and after electrophoresis it was stained with Coomassie blue. The standard is 1 μg hepcidin produced synthetically and validated as identical to urinary hepcidin-25 by mass spectrometry, reverse-phase high-performance liquid chromatography on a C18 column, and acid-urea PAGE (courtesy of E. Nemeth and T. Ganz, University of California, Los Angeles). (Laftah et al. 2004).

This synthetic peptide was further compared with standard hepcidin by electrophoresis on acid/urea gel (Fig. 5.2); standard hepcidin separated as a single band, whereas synthetic peptide used in this study separated as a broad band, as though it was a mixture of multiple forms. However, we found that both standard hepcidin and the synthetic hepcidin were immunoreactive with an antibody raised against urinary hepcidin. Therefore it was concluded that this synthetic peptide is the correct molecular weight for oxidized hepcidin,

contains a form equivalent to urinary hepcidin, but also has forms of hepcidin that migrate differently on acid/urea gel.

5.2.3 Iron transport

Iron transport was carried out as described in chapter 2.3

5.2.4 Gene expression using Real-Time RT-PCR

Real-Time PCR was carried out as described in chapter 2.2.3.

5.2.5 Data analysis

Data are presented as the mean ± S.E.M. and were analysed as described in chapter 2.4.

5.3 Results

5.3.1 Determination of optimal conditions in hepcidin experiment

The concentration of serum hepcidin is unclear and its estimates vary from the nanomolar range (Park *et al.* 2001) to mid- to high-micromolar range (Dallalio et al. 2003). In order to determined the optimal experimental condition for the effect of synthetic human hepcidin, the level of DMT1 mRNA expression in Caco-2 TC7 cells were tested using various concentration of hepcidin for 24 hours. Concentrations of 1 to 100 μM were hepcidin tested, to be within the two extremes of the estimated serum concentration. This concentration range gave a wide variation in response to hepcidin. The high end of the concentration range (100 μM) may have affected cell growth, and DMT1 mRNA expression was unaffected by low concentration (1 and 5 μM) of hepcidin. 10 μM treatment showed a statistically insignificant but small reduction in DMT1 mRNA expression without affecting cell growth (Fig. 5.3) after 24 hours incubation with synthetic hepcidin. For this reason, 10 μM hepcidin was considered the most suitable experimental concentration that will be apply to Caco-2 TC7 cells.

To determine the optimal duration of 10 μM hepcidin treatment, DMT1 mRNA expression was measured after 1, 24 and 48 hours time-treatments. Although statistically insignificant, out of three time-

courses tested, 24 hours treatment was found to be most effective in reducing gene expression of DMT1 (Fig. 5.4), and therefore Caco-2 TC7 cells will be treated with hepcidin for 24 hours in sabsequent experiments.

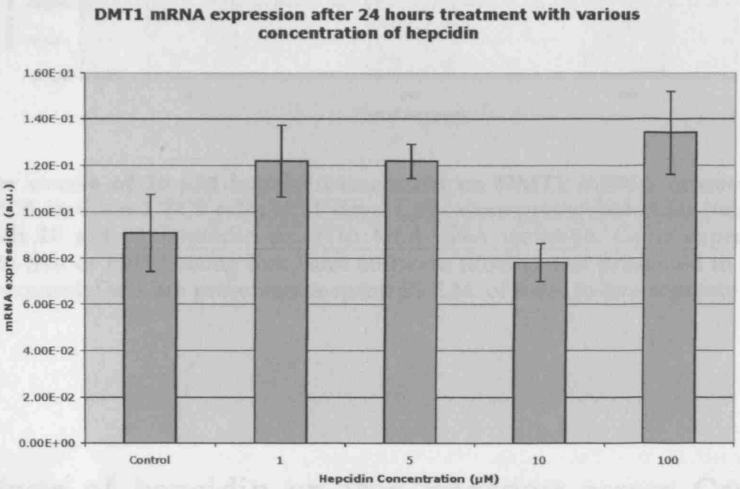

Fig. 5.3 Effect of various concentration of hepcidin on DMT1 mRNA expression using Real-Time PCR in Caco-2 TC7 cells at 21 days. Cells were preincubated for 24 hours at 37 °C with indicated concentration of hepcidin prior to total RNA isolation. Gene expression was normalised to that of HPRT using RelQuant software (Roche) and presented in arbitrary units. Data are presented as mean ±S.E.M. of at least four separate samples in each group.

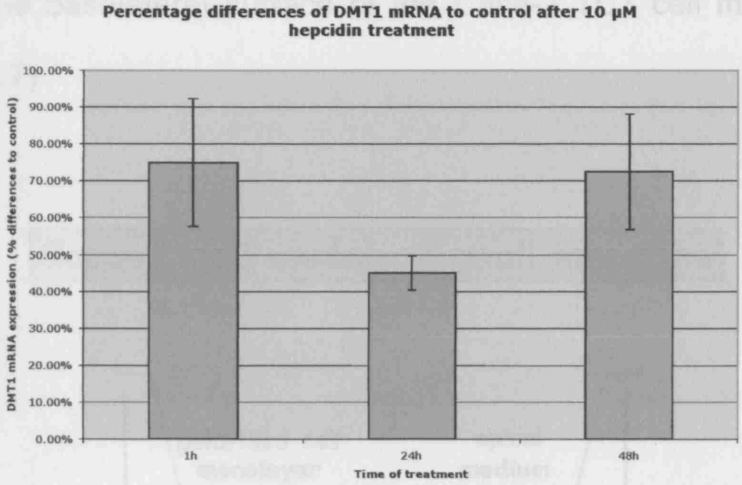

Fig. 5.4 Time course of 10 µM hepcidin treatment on DMT1 mRNA expression using Real-Time PCR in Caco-2 TC7 cells at 21 days. Cells were preincubated for indicated time at 37 °C with 10 µM of hepcidin prior to total RNA isolation. Gene expression was normalised to that of HPRT using RelQuant software (Roche) and presented in percentage difference to control. Data are presented as mean ±S.E.M. of three to five separate samples in each group.

5.3.2. Effects of hepcidin on iron transport across Caco-2 cell monolayers

In order to test the effect of hepcidin on iron absorption in intestine, synthetic human hepcidin was added to the basolateral chamber of the Transwell culture system 24 hours prior to experimentation (Fig. 5.5). The experiments were carried out as described in chapter 2.3. Uptake of iron across the apical membrane of Caco-2 TC7 cells was significantly decreased ($p<0.04$) following hepcidin treatment compared with untreated cells (Figure 5.6). In contrast there was no effect of hepcidin on the rate of iron efflux

across the basolateral surface of the Caco-2 TC7 cell monolayer (Figure 5.7).

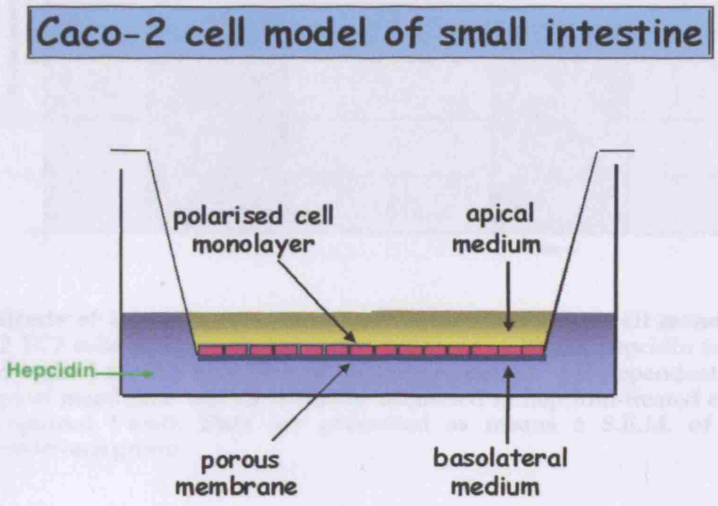

Fig. 5.5 Transwell culture system of Caco2-TC7 cells as a model of human intestine. Monolayer of Caco-2 TC7 cells were grown on porous membrane insert separating apical and basolateral mediums. Hepcidin was added to basolateral medium introducing the signal peptide from the body to the site of absorption.

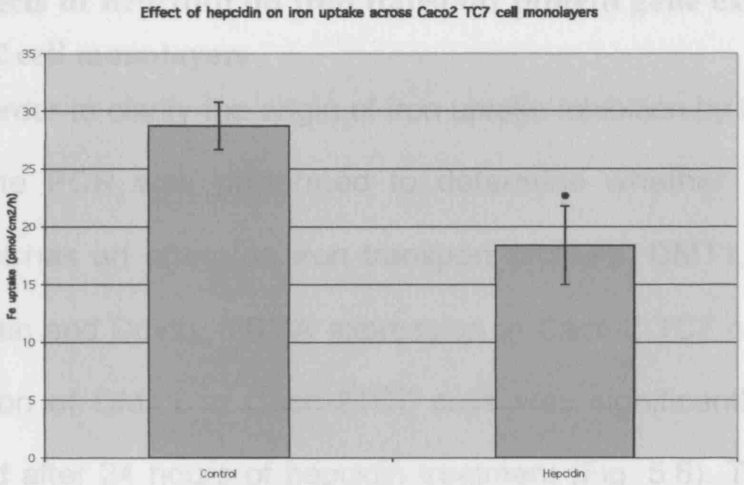

Figure 5.6 Effects of hepcidin on iron uptake across Caco-2 TC7 cell monolayers at 21 days. Caco-2 TC7 cells were incubated in the presence of 10 μM hepcidin (added to the basolateral chamber) for the final 24 h of the culture period. pH-dependent Fe^{2+} uptake across the apical membrane was significantly decreased in hepcidin-treated cells ($p<0.04$, Student's unpaired t-test). Data are presented as means ± S.E.M. of 5 separate determinations in each group.

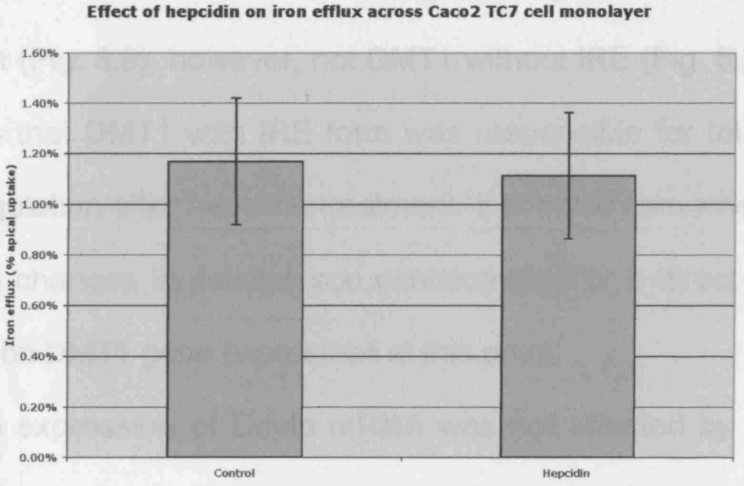

Figure 5.7 Effects of hepcidin on iron transport across Caco-2 TC7 cell monolayers at 21 days. Caco-2 TC7 cells were incubated in the presence of 10 μM hepcidin (added to the basolateral chamber) for the final 24 h of the culture period. Iron efflux across the basolateral membrane measured as a percentage of apical uptake was unaffected ($p>0.25$). Data are presented as means ± S.E.M. of 5 separate determinations in each group.

5.3.3 Effects of hepcidin on iron transport protein gene expression in Caco-2 cell monolayers

In order to clarify the origin of iron uptake inhibition by hepcidin, Real-Time PCR was performed to determine whether hepcidin treatment has an effect on iron transport proteins, DMT1, IREG1, hephaestin and Dcytb, mRNA expression in Caco-2 TC7 cells. The expression of DMT1 in Caco-2TC7 cells was significantly down-regulated after 24 hours of hepcidin treatment (Fig. 5.8). To further analyse which isoforms of DMT1 (with and without IRE at 3' UTR) is responsible for this down-regulation, gene expression of each DMT1 isoform was performed using IRE isoform specific primers. Gene expression of DMT1 with IRE was significantly decreased after the treatment (Fig. 5.9), however, not DMT1 without IRE (Fig. 5.10). This suggests that DMT1 with IRE form was responsible for total DMT1 down regulation after hepcidin treatment. It is not known whether this is due to changes in cellular iron concentration or a direct effect of hepcidin on DMT1 gene expression at this point.

The expression of Dcytb mRNA was not affected by hepcidin treatment (Fig. 5.11). Dcytb expression often coincides with changes in DMT1 expression, as they work together at the apical surface of the intestine, and are known to be regulated by internal iron levels (McKie *et al.* 2001).

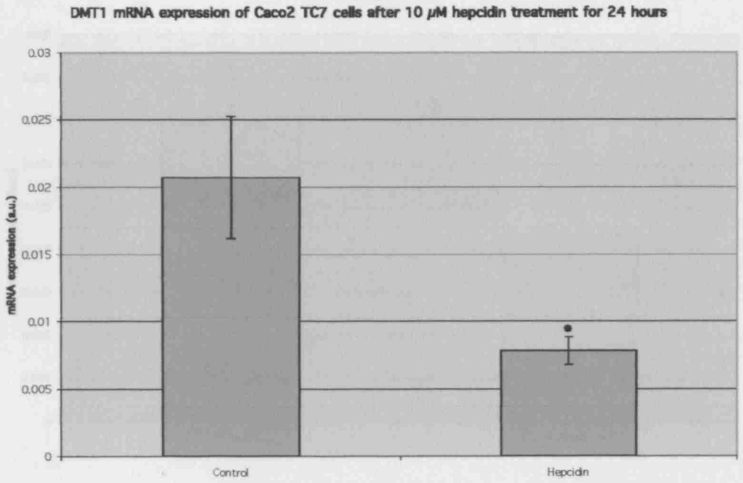

Fig. 5.8 Effect of hepcidin on DMT1 mRNA expression in Caco-2 TC7 cells at 21 days using Real-Time PCR. Cells were pre-incubated for 24 hours 37 °C with 10 μM of hepcidin prior to total RNA isolation. Gene expression was normalised to that of HPRT using RelQuant software (Roche) and presented in arbitrary units. Data are presented as mean ±S.E.M. of five separate samples in each group. •=$p<0.05$.

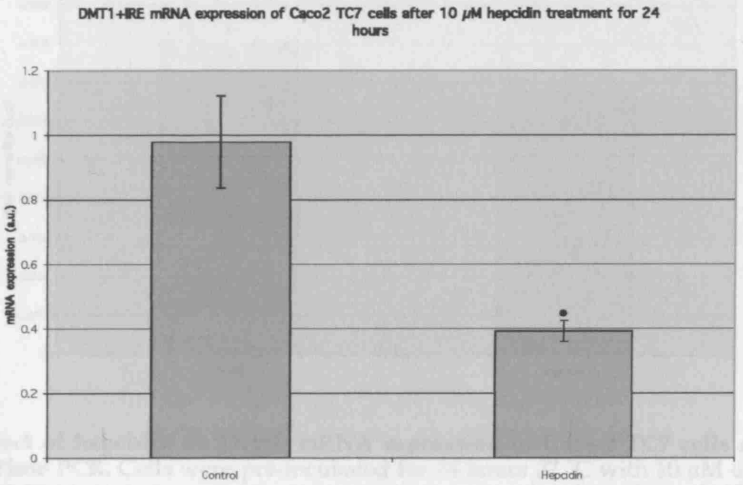

Fig. 5.9 Effect of hepcidin on DMT1 with IRE mRNA expression in Caco-2 TC7 cells at 21 days using Real-Time PCR. Cells were pre-incubated for 24 hours 37 °C with 10 μM of hepcidin prior to total RNA isolation. Gene expression was normalised to that of HPRT using RelQuant software (Roche) and presented in arbitrary units. Data are presented as mean ±S.E.M. of five separate samples in each group. •=$p<0.05$.

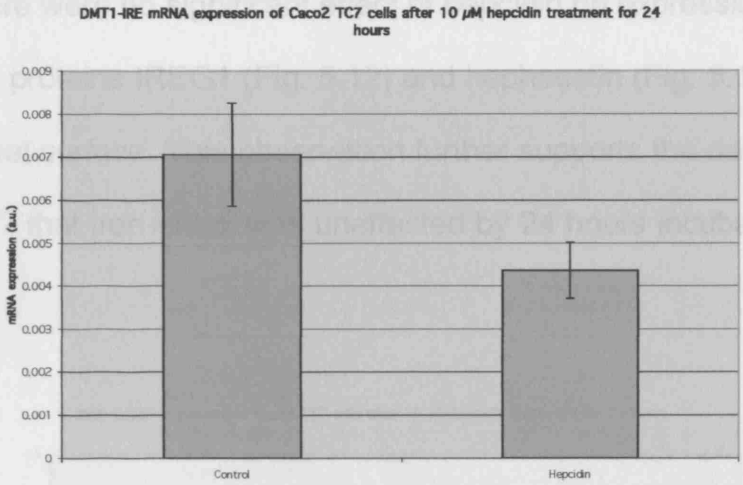

Fig. 5.10 Effect of hepcidin on DMT1 without IRE mRNA expression in Caco-2 TC7 cells at 21 days using Real-Time PCR. Cells were pre-incubated for 24 hours 37 °C with 10 μM of hepcidin prior to total RNA isolation. Gene expression was normalised to that of HPRT using RelQuant software (Roche) and presented in arbitrary units. Data are presented as mean ±S.E.M. of five separate samples in each group.

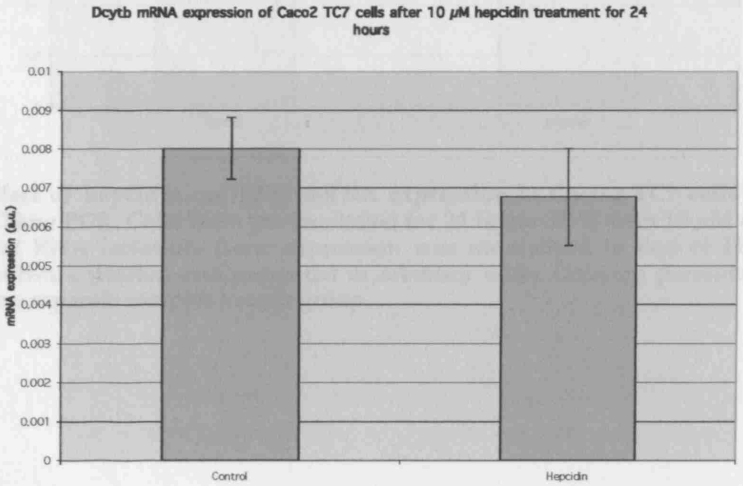

Fig. 5.11 Effect of hepcidin on Dcytb mRNA expression in Caco-2 TC7 cells at 21 days using Real-Time PCR. Cells were pre-incubated for 24 hours 37 °C with 10 μM of hepcidin prior to total RNA isolation. Gene expression was normalised to that of HPRT using RelQuant software (Roche) and presented in arbitrary units. Data are presented as mean ±S.E.M. of five separate samples in each group.

There were no significant effect of hepcidin on expression of iron transport proteins IREG1 (Fig. 5.12) and hephaestin (Fig. 5.13) at the basolateral surface. This observation further supports the data shown in Fig. 5.7 that iron efflux was unaffected by 24 hours incubation with hepcidin.

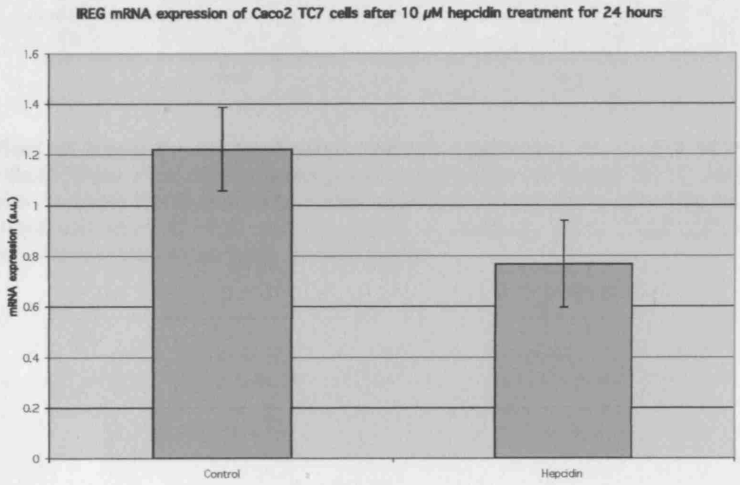

Fig. 5.12 Effect of hepcidin on IREG mRNA expression in Caco-2 TC7 cells at 21 days using Real-Time PCR. Cells were pre-incubated for 24 hours 37 °C with 10 μM of hepcidin prior to total RNA isolation. Gene expression was normalised to that of HPRT using RelQuant software (Roche) and presented in arbitrary units. Data are presented as mean ±S.E.M. of five separate samples in each group.

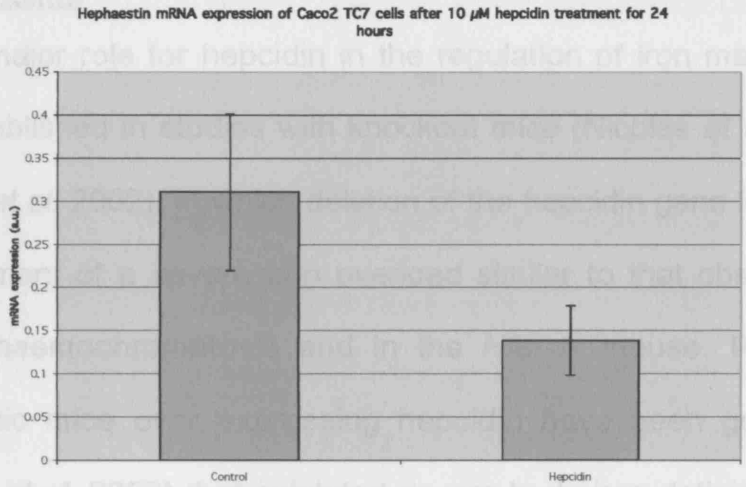

Fig. 5.13 Effect of hepcidin on hephaestin mRNA expression in Caco-2 TC7 cells at 21 days using Real-Time PCR. Cells were pre-incubated for 24 hours 37 °C with 10 μM of hepcidin prior to total RNA isolation. Gene expression was normalised to that of HPRT using RelQuant software (Roche) and presented in arbitrary units. Data are presented as mean ±S.E.M. of five separate samples in each group.

5.4 Discussion

A major role for hepcidin in the regulation of iron metabolism was established in studies with knockout mice (Nicolas *et al.* 2001; Nicolas *et al.* 2002), in which deletion of the hepcidin gene led to the development of a severe iron overload similar to that observed in human haemochromatosis and in the *Hfe -/-* mouse. Recently, transgenic mice over expressing hepcidin have been generated (Nicolas *et al.* 2002) that exhibited severe body iron deficiency and microcytic hypochromic anemia suggesting a reciprocal relationship exists between hepcidin expression and iron accumulation. Hepcidin expression has been shown to be elevated in inflammation and in chronic disease (Nicolas *et al.* 2002; Weinstein *et al.* 2002). In these pathological disorders, the ensuing anaemia is thought to occur as a consequence of both iron retention within the reticuloendothelial cells and inappropriately low intestinal iron absorption. Recent studies by Frazer *et al* (Frazer *et al.* 2002), demonstrated that liver hepcidin expression was decreased in response to dietary iron deficiency. Furthermore, the reduced liver hepcidin mRNA levels correlated with increased intestinal iron absorption and elevated expression of the intestinal DMT1+IRE transporter. In our laboratory, direct injection of hepcidin into mice decreased specifically the apical uptake step of duodenal iron absorption (Laftah *et al.* 2004).

In light of these findings, the aim of the study described in this chapter was to determine whether hepcidin produced its effects by interacting directly with intestinal epithelial cells. The serum hepcidin concentration is unclear. Extrapolations from urinary measurements suggested that circulating hepcidin was within the nanomolar range (Park *et al.* 2001) and was positively correlated with serum ferritin levels (Nemeth et al. 2003). However, a recent study indicated that serum levels could be much higher, in the mid to high micromolar range (Dallalio *et al.* 2003). The concentration of human synthetic hepcidin used in our study (10μM) sits between these two extremes. The data presented here demonstrate that hepcidin specifically decreases iron uptake across the apical surface of the Caco-2 epithelial layer, which is consistent with our previous findings (Laftah *et al.* 2004). At the molecular level these changes in iron transport are explained by a reduction in DMT1+IRE transporter expression following hepcidin treatment. Interestingly, Frazer *et al* (Frazer *et al.* 2002) also showed a correlation between decreased hepcidin and elevated IREG1 expression. Study in this chapter did not show any effect of hepcidin on IREG1 expression or function and this is supported by our previous work in which injection of hepcidin into mice had no effect on mucosal iron transfer (Laftah *et al.* 2004). Thus

it is possible that other humoral mediators in addition to hepcidin are required to regulate IREG1 expression.

As noted previously, our synthetic hepcidin contains a mixture of species including one or more active forms (Laftah *et al.* 2004). At present the nature of the circulating active form of hepcidin remains unclear. The effects of hepcidin observed in the present study are unlikely to be due to toxicity since there was no effect of peptide incubation on monolayer transepithelial resistance (data not shown).

In conclusion, our data provide the first direct evidence that hepcidin can regulate intestinal iron absorption by interacting with a intestinal epithelial cell line model. The primary effect of hepcidin is to modulate the apical membrane uptake via DMT1 with IRE protein thereby controlling the amount of iron absorbed from the diet.

Chapter 6 : Molecular mechanism of iron transport proteins regulation in macrophages

6.1 Introduction

Tissue macrophages either circulating in blood, dispersed in connective tissue or attached to capillary endothelium are known as the reticulo-endothelial system (RES). The reticuloendothelial system (RES) is composed of monocytes, macrophages, and their precursor cells. Monocytes arise from progenitor cells in the bone marrow and are released into the blood. After migration to different tissues, they differentiate into macrophages with characteristic morphology and functions. They attack foreign or tumour cells either by ingesting them or by lysis after adherence to them. They are abundant in liver sinusoids (Kupffer cells), large intestine, small intestine, bone marrow, spleen and kidney in descending order (Lee et al. 1985). In addition to being a storage pack for iron, macrophages of the reticuloendothelial system play an important role in iron metabolism by recycling more than 80 % of body iron from senescent erythrocytes (Andrews 1999).

Although macrophages can obtain iron by erythrophagocytosis, receptor-mediated uptake of haemoglobin, and receptor-mediated uptake of transferrin, erythrophagocytosis is the main system which macrophages utilise to acquire iron. One macrophage phagocytoses

one red cell per day on average (Kondo et al. 1988), and acquires approximately one billion iron atoms with each red cell ingested (Knutson and Wessling-Resnick 2003). The RES is able to acquire haem via the haemoglobin scavenger receptor, CD163, in intravascular erythrocyte destruction, but the amount taken up is probably not significant under normal circumstances as reviewed in Knutson and Wessling-Resnick (2003). Although macrophages express transferrin receptors, and are able to take up iron from transferrin, the extent to which this occurs *in vivo* is unknown. In human monocytic THP-1 cells, blocking of transferrin receptor-mediated uptake by addition of α1-AT did not cause iron deprivation (Weiss et al. 1996).

The normal human erythrocyte has a life span of about 120 days (Stryer 1995). In erythrophagocytosis, the senescent red blood cell (RBC) is first taken up into the phagosome by a 'membrane-zip' process in which adhesion between engulfing cell and senescent RBC occurs progressively until RBC is completely surrounded by the cell's pseudopodia (1) (Fig 6.1). Lysosomal enzymes are synthesised at ribosomes on endoplasmic reticulum (ER) and collected in the tubes of golgi apparatus (2).

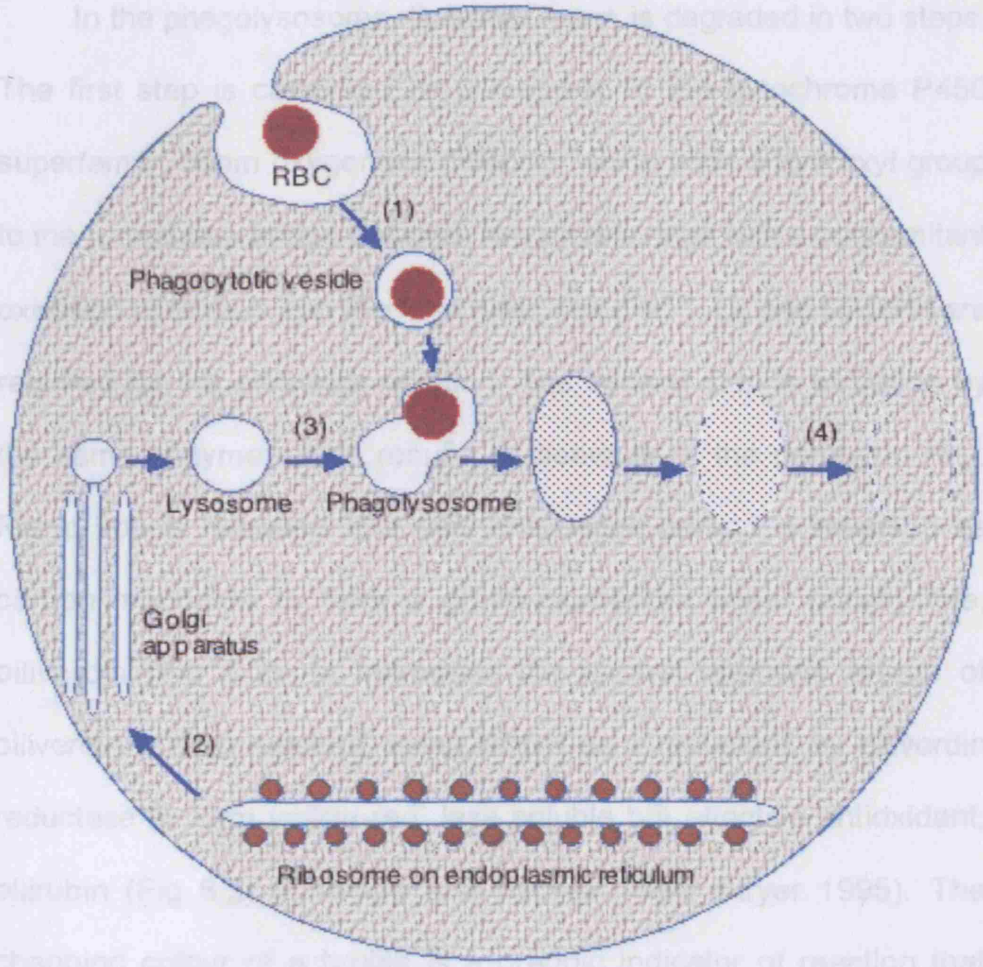

Figure 6.1 Illustration of senescent red blood cell phagocytosis by macrophage. Macrophages ingesting senescent red blood cell (RBC).

Lysosomes are formed by a budding process from the golgi apparatus and fuse with phagosomes to form single vesicles called phagolysosomes (3). The hydrolytic enzymes present in the lysosome degrade RBC, and digestion of haemoglobin liberates haem.

In the phagolysosome, liberated haem is degraded in two steps. The first step is catalysed by a member of the cytochrome P450 superfamily, haem oxygenase (HMOX), which adds a hydroxyl group to the α-methene bridge between two pyrrole rings with a concomitant oxidation of ferrous iron (Fe^{2+}) to ferric iron (Fe^{3+}). O_2 and NADPH are required for the cleavage reaction. The second step is oxidation by the same enzyme which results in cleavage of the porphyrin ring. Ferric iron is released and methene-bridge carbon is released as carbon monoxide to form a green-pigmented linear tetrapyrrole, biliverdin (Fig 6.2). In mammals the central methene bridge of biliverdin is then reduced, using NADH as a reductant, by biliverdin reductase to form yellow-red, less soluble but effective antioxidant, bilirubin (Fig 6.2) (Champe and Harvey 1994; Stryer 1995). The changing colour of a bruise is a graphic indicator of reaction that occurs during haem degradation.

Finally, the phagolysosome vesicle breaks down to release the products of digestion and (presumably) inactive enzymes to the cytoplasm (4). Bilirubin leaves the macrophage, covalently binds to albumin in blood to form a bilirubin-albumin complex, and is transported to the liver, where it is taken up and conjugated with glucuronic acid (Champe and Harvey 1994; Stryer 1995).

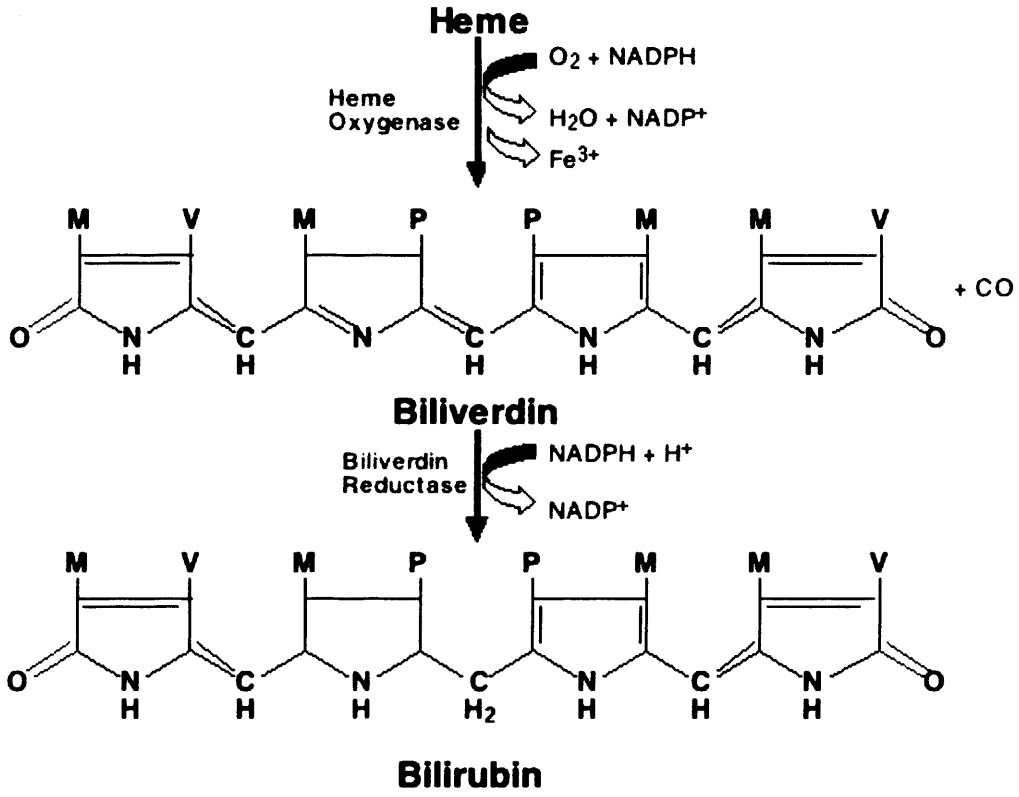

Figure 6.2 Degradation of haem to bilirubin. Modified from Stryer 1995 (Stryer 1995).

Although the RES plays an important role in storage and recycling iron, the precise mechanisms remained elusive. Figure 6.3 summarises the current understanding of the intracellular iron metabolism in reticuloendothelial cells.

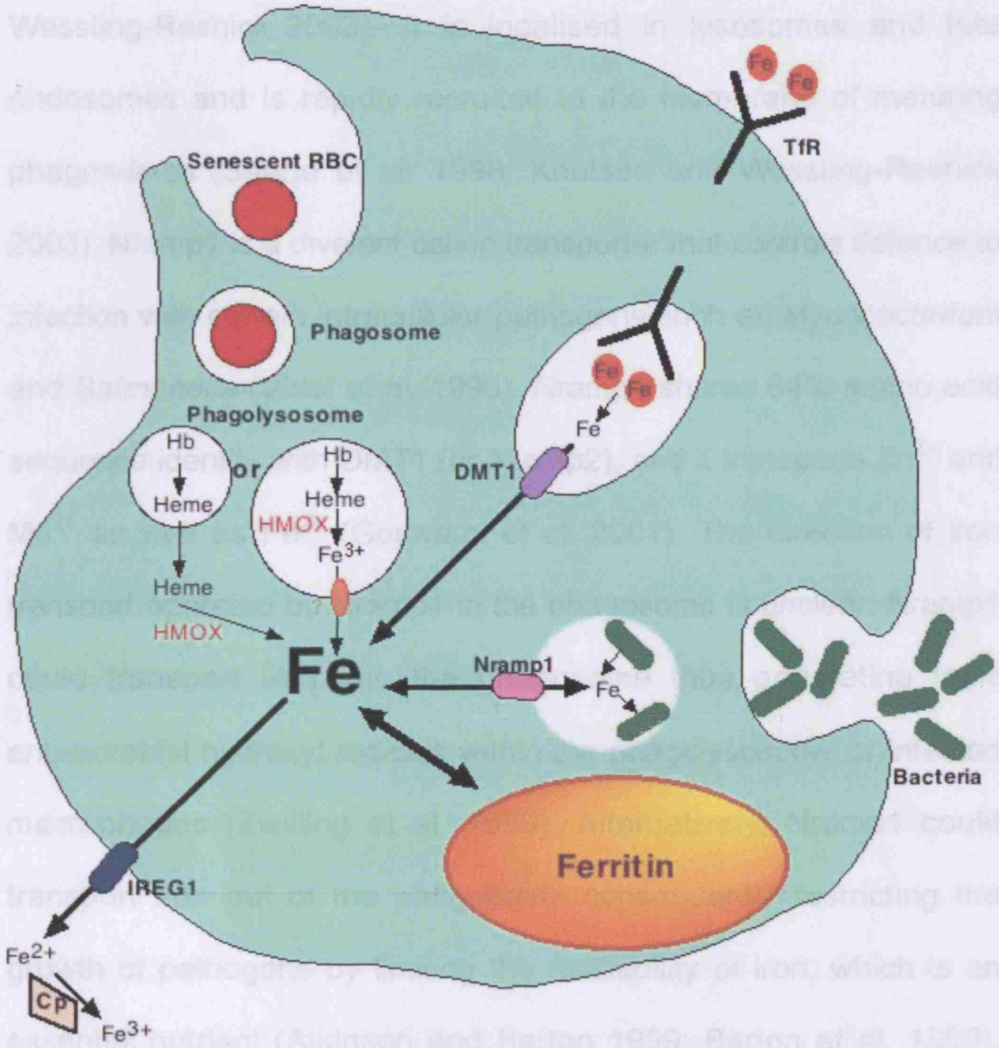

Figure 6.3 Hypothetical illustration of intracellular iron metabolism in macrophage. Macrophages obtain haemoglobin from ingested senescent red blood cell (RBC).

Natural resistance associated macrophage protein 1 (Nramp1) is a highly hydrophobic 56-KDa protein with 12 predicted transmembrane regions and expressed exclusively within monocytes and macrophages of the reticuloendothelial system (Knutson and

Wessling-Resnick 2003). It is localised in lysosomes and late endosomes and is rapidly recruited to the membrane of maturing phagosomes (Searle et al. 1998; Knutson and Wessling-Resnick 2003). Nramp1 is a divalent cation transporter that controls defence to infection with certain intracellular pathogens such as *Mycocacterium* and *Salmonella* (Vidal et al. 1996). Nramp1 shares 64% amino acid sequence identity with DMT1 (or Nramp2), and it transports Zn^{2+} and Mn^{2+} as well as Fe^{2+} (Goswami et al. 2001). The direction of iron transport operated by Nramp1 in the phagosome is unclear. Nramp1 could transport iron into the phagosome thus generating toxic antimicrobial hydroxyl radicals within the phagolysosome of infected macrophages (Zwilling et al. 1999). Alternatively, Nramp1 could transport iron out of the phagosome consequently restricting the growth of pathogens by limiting the availability of iron, which is an essential nutrient (Atkinson and Barton 1999; Barton et al. 1999). Recently, Nramp1 has been demonstrated to transport zinc bidirectionally in *Xenopus* oocytes, efflux at pH 5.5 and uptake at pH 9.0 (Goswami *et al.* 2001). It is possible that bidirectional transport also takes place across the plasma membrane depending on the pH gradient.

Degradation of haem catabolised by HMOX1 is essential to mammalian iron reutilization, HMOX1-deficient mice develop an anemia associated with abnormally low serum iron levels, and hepatic and renal iron accumulation (Poss and Tonegawa 1997). The intracellular location of iron liberation from haem is unclear. Because haem oxygenase functions in the endoplasmic reticulum, iron could be liberated from haem at the ER. Iron could also be liberated within the phagolysosome and transported out into the cytosol by an unknown transporter. Although Nramp1 is recruited in the phagolysosome, it is unlikely to be the transporter, because Nramp1 mutant mice have a normal haematological profile (Leboeuf et al. 1995). Another iron transporter DMT1 is expressed in RE cells. It is localised in the endosomes involved in transferrin-mediated endocytosis that transports iron from transferrin into the cytosol (Tabuchi *et al.* 2000). DMT1 co-localised with transferrin in a macrophage cell line (Gruenheid et al. 1999), and is likely to function in similar ways in macrophages. Furthermore, DMT1 is also associated with the phagolysosome in a macrophage cell line and could transport iron liberated from haem into the cytosol.

In RE cells, acquired iron is either utilised, stored in ferritin, or released as low molecular weight species that readily bind to

transferrin (Kondo *et al.* 1988). Although intracellular localisation was indicated by immunofluorescence in Kupffer cells (Abboud and Haile 2000), accumulated evidence suggest that release of iron from RE cells occurs via IREG1, like other cells in the body. IREG1 is strongly expressed in RE cells (Abboud and Haile 2000; Donovan *et al.* 2000; Yang *et al.* 2002) and mutation of IREG1 is associated with an autosomal dominant hemochromatosis in which iron is retained in Kupffer cells (Montosi *et al.* 2001; Njajou *et al.* 2001; Devalia *et al.* 2002; Roetto *et al.* 2002). Release of iron from RE cells is hypothesised to be regulated by hepcidin (Nicolas *et al.* 2001), however the exact mechanism of this proposed regulation is unknown.

As illustrated in Figure 6.3, the current knowledge of intracellular iron metabolism in RE cells is obscure. The aim of the work described in chapter was to gain better understanding of the site where iron is liberated from haem, and the mechanism and regulation of iron release from RE cells, by molecular techniques.

6.2 Methods

6.2.1 Cell culture

6.2.1.1 Cell culture of THP-1 Cells

THP-1 is a human monocytic cell line derived from the peripheral blood of a 1year old male with acute monocytic leukaemia. THP-1 monocytes were maintained in 175 cm^3 flasks in 50 ml "THP complete" medium (See 6.2.1.3) at about 1 x 10^6 cells/ml medium for 6 well plates using 1.5 - 1.8 x 10^6 cells /ml. Medium was changed after 3 days by spinning cells down at 1000 rpm for 5 min at room temperature; old medium were removed and discarded. Cells were resuspended in 50 ml fresh medium. Cells were diluted 1 in 5 up to 1 in 10 with fresh medium after a further 3 days. Each flask yielded approximately 80 x 10^6 cells (approximately yield 6 x 6 well plates per flask).

6.2.1.2 Differentiation into THP-1 Macrophages

THP-1 monocytes were transferred to 6 well plates/175 cm^3 flasks and differentiated into THP-1 macrophages by addition of 100 ng/ml of phorbol 12-myristate 13-acetate (PMA, Sigma Chemical Company, Poole, U.K.). The THP-1 macrophages were then used within 5-7 days from initial differentiation.

6.2.1.3 THP Complete Medium

450 ml RPMI 1640 medium with glutamine (Invitrogen Life Technologies, Paisley, U.K. Cat No: 21875-034) were added with 50 ml foetal bovine serum to give 10% FBS (FBS heat inactivated Australian from Invitrogen Life Technologies Cat No: 10100-). To each 500 ml, 5 ml Penicillin Streptomycin solution was added to give 100 IU/ml penicllin and 100mg/ml streptomycin (Invitrogen Life Technologies Cat No: 15140-122).

6.2.1.4 Serum Free Experimental Medium:

To each 500 ml of RPMI 1640 medium with glutamine, 5 ml Penicillin Streptomycin was added as above. Cells were incubated with 100 ng/ml LPS, hemin (Fe^{3+} oxidation product of haem), LPS and hemin or 10 and 100 μM 25 amino acid hepcidin for final 24 h.

6.2.2 Primary culture

6.2.2.1 Collection of macrophages from liver perfusate fluid

Reagents required

- Hanks solution with 5 mM EDTA (pH. 8.0)
- Ficoll
- Dulbecco's modified Eagle's minimal essential medium (DMEM)

Liver perfusates were obtained by perfusing human liver with saline solution before transplantation in operating surgery. Perfusates

were collected in Falcon tubes, and were centrifuged at 1800 rpm for 15 min at 20 °C. Supernatant was discarded, and cell pellets retained. Cell pellets were resuspended and swirled gently in 10 ml Hanks. The cell suspension was transferred to a fresh Falcon tube and gently swirled until the cells were in solution. Once the cells were in solution, the final volume was brought up to 30 ml with Hanks. It was then layered onto 20 ml Ficoll in a Falcon tube. Cells were centrifuged at 1500 rpm for 30 min at 20 °C with the brake off.

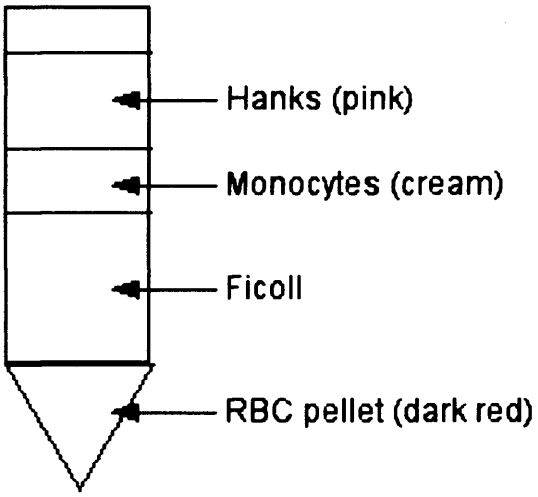

The macrophage layer was aspirated into new sterile Falcon and was brought up to 30 ml with Hanks. It was then layered onto 20 ml Ficoll again and centrifuged at 1800 rpm for 10 min at 20 °C with the brake off. Supernatants were discarded, and pellets were resuspended with Hanks to 30 ml and centrifuged at 1500 rpm for 10

min at 20 °C with the brake on. These procedures were repeated to wash the cells. the supernatant was discarded and retained cells were resuspended in 5 ml DMEM by gentle swirling. Cells were counted and resuspended at 1 x 10^6 cells/ml in DMEM with 10% heat-inactivated fetal bovine serum. Cells were cultured in a 95% air 5% CO_2 atmosphere at 37°C for 3-5 days. Cells were incubated with 100 ng/ml LPS, and/or 10 and 100 μM 25 amino acid hepcidin for the final 24 h. Blood macrophages were collected and cultured by the same procedure.

6.2.2 Gene expression using real time PCR

RT-PCR was carried out as described in chapter 2.2.3.

6.2.3 Data analysis

Data are presented as the mean ± S.E.M. and were analysed as described in chapter 2.4.

6.3 Results

6.3.1. Effects of LPS and hemin on iron transporter protein gene expression in human monocytic leukaemia cell line THP-1

These experiments were carried out to analyse the effect of haem on iron metabolism protein gene expression in macrophage cell lines. Because THP-1 cells were treated with hemin (Fe^{3+}), which is reduced to haem (Fe^{2+}) prior to oxidation by haem oxygenase, changes in the level of haem oxygenase mRNA was examined. Figure 6.4 shows real-time PCR HMOX1 gene expression in THP-1 cells treated with LPS, hemin, and LPS and hemin for 24 hours. HMOX1 mRNA was detected in control and LPS treated cells, and dramatically upregulated (130 fold) by treatment of hemin with or without LPS. This phenomenon of elevated HMOX1 mRNA is a clear indication that hemin was taken up by THP-1 cells and thus indicate increased cellular iron status within the hemin treated cells.

IRE-IRP binding activities in RE cells were demonstrated in THP-1 cells (Weiss *et al.* 1996), peripheral blood monocytes (Cairo et al. 1997) and the RAW 264.7 cell line (Kim and Ponka 1999; Kim and Ponka 2000; Wardrop and Richardson 2000). Increased cellular iron status decreases IRE-IRP binding activity by IRP1 inactivation via Fe-S cluster assembly or proteasomal degradation of IRP2. Transferrin receptor (TfR) and DMT1+IRE are post-transcriptionally regulated by

cellular iron status via the IRE-IRP system. IRP binding to multiple IREs of TfR or single IREs of DMT1+IRE in the 3' untranslated region (UTR) stabilises mRNA. Increased cellular iron inactivates IRP activity and increases mRNA degradation. As is evident from Figure 6.5, Transferrin receptor mRNA levels were significantly decreased by treatment with hemin but not by LPS compare to untreated control. This is in agreement with modulation of TfR mRNA by increased cellular iron level demonstrated by others previously using the same cell line (Weiss *et al.* 1996) and in J774 cells (Wardrop and Richardson 2000).

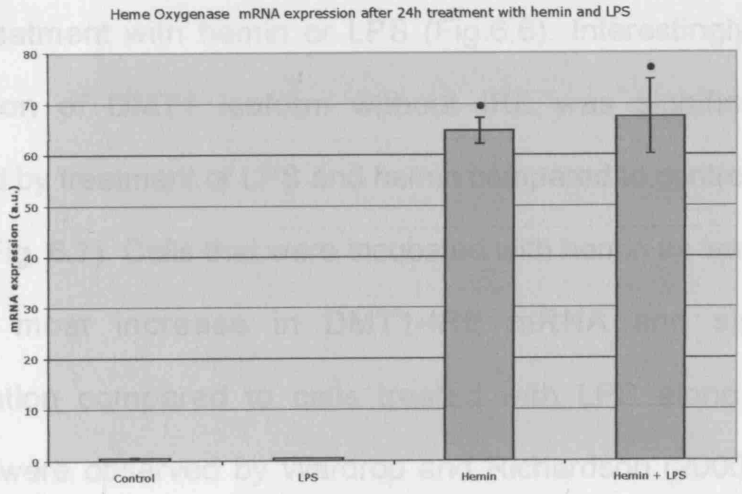

Fig. 6.4 The effect of hemin and LPS on the level of haem oxygenase mRNA in THP-1 cells. Cells were preincubated for 24h at 37°C with 100 ng/ml LPS or/and hemin prior to the isolation of total mRNA. Level of HMOX1 mRNA were normalised to HPRT and expressed in arbitrary units. Data are presented as mean±S.E.M. of 3 separate determinations in each group, •$p<0.05$.

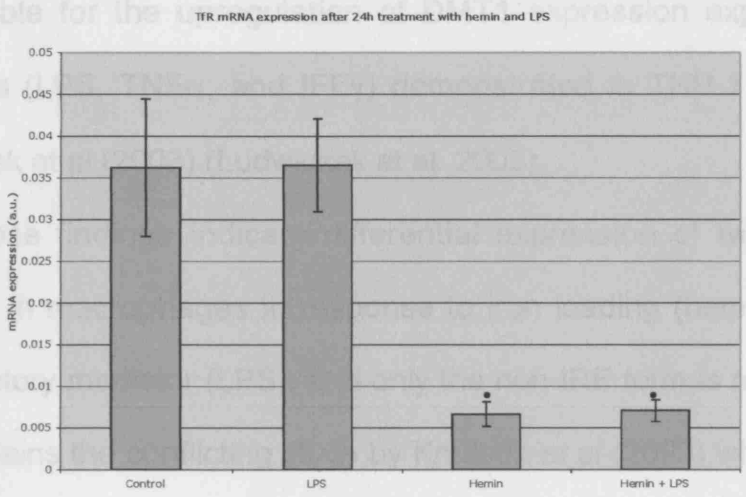

Fig. 6.5 The effect of hemin and LPS on the level of transferrin receptor mRNA in THP-1 cells. Cells were preincubated for 24h at 37°C with 100 ng/ml LPS or/and hemin prior to the isolation of total mRNA. Level of TfR mRNA were normalised to HPRT and expressed in arbitrary units. Data are presented as mean±S.E.M. of 3 separate determinations in each group, •$p<0.05$.

Incontrast, DMT1+IRE mRNA expression was not affected by 24 hours treatment with hemin or LPS (Fig.6.6). Interestingly, mRNA expression of DMT1 isoform without IRE was significantly up regulated by treatment of LPS and hemin compared to control in THP-1 cells (Fig. 6.7). Cells that were incubated with hemin as well as LPS showed most increase in DMT1-IRE mRNA and significant upregulation compared to cells treated with LPS alone. Similar findings were observed by Wardrop and Richardson (2000), where DMT1-IRE mRNA but not DMT1+IRE mRNA was elevated by LPS and FAC in J774 and RAW264.7 cells (Wardrop and Richardson 2000). Moreover, changes in DMT1 non IRE was probably

responsible for the upregulation of DMT1 expression exposed to cytokines (LPS, TNFα, and IFEγ) demonstrated in THP-1 cells by Ludwiczek et al (2003) (Ludwiczek et al. 2003).

These findings indicate differential expression of two DMT1 isoforms in macrophages in response to iron loading (hemin) or an inflammatory mediator (LPS), and only the non-IRE form is regulated. This explains the conflicting study by Knutson *et al* (2003) where they find no change in the level of DMT1 mRNA, measuring total DMT1, in J774 cells after erythrophagocytosis (Knutson et al. 2003). The post-transcriptional regulation of DMT1+IRE mRNA expression by IRE/IRP systems induced by cellular iron level was absent, and DMT1-IRE gene expression responds to both increased cellular iron level and inflammation by unknown regulatory mechanisms in macrophages.

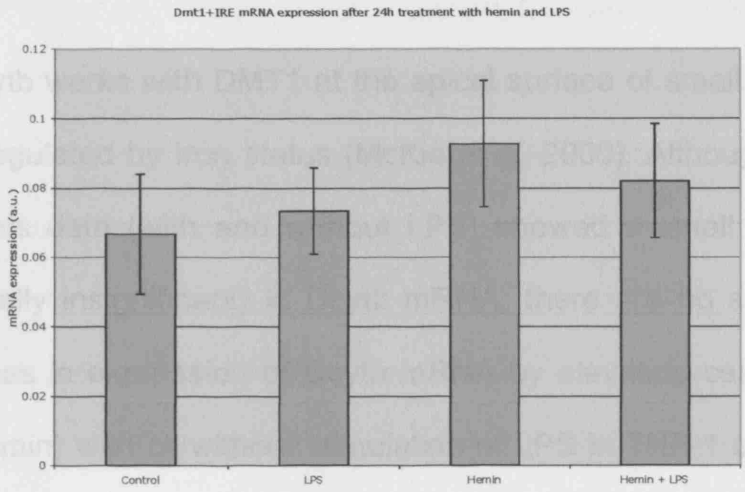

Fig. 6.6 The effect of hemin and LPS on the level of DMT1+IRE mRNA in THP-1 cells. Cells were preincubated for 24h at 37°C with 100 ng/ml LPS or/and hemin prior to the isolation of total mRNA. Level of DMT1+IRE mRNA were normalised to HPRT and expressed in arbitrary units. Data are presented as mean±S.E.M. of 3 separate determinations in each group, •$p<0.05$.

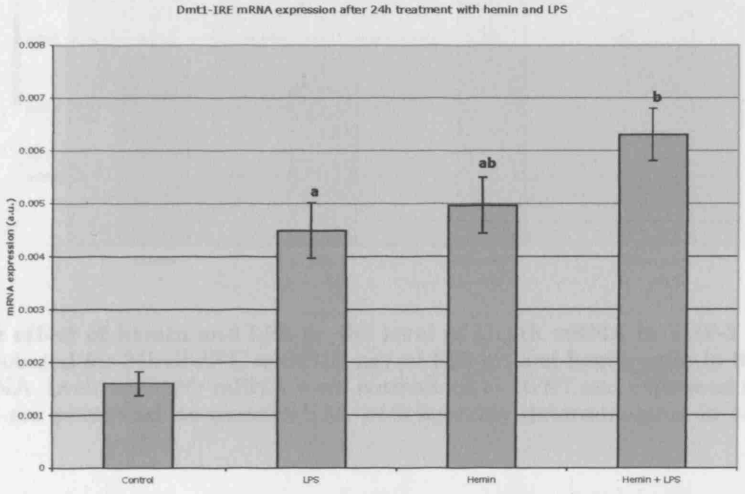

Fig. 6.7 The effect of hemin and LPS on the level of DMT1-IRE mRNA in THP-1 cells. Cells were preincubated for 24h at 37°C with 100 ng/ml LPS or/and hemin prior to the isolation of total mRNA. Level of DMT1-IRE mRNA were normalised to HPRT and expressed in arbitrary units. Data are presented as mean±S.E.M. of 3 separate determinations in each group. Different letters above data bars indicate that these groups are statistically different from each other ($p<0.05$).

Dcytb works with DMT1 at the apical surface of small intestine and is regulated by iron status (McKie *et al.* 2000). Although hemin treatments data (with and without LPS) showed a small increase (statistically insignificant) in Dcytb mRNA, there are no significant differences in expression of Dcytb mRNA by elevating cellular iron level (hemin) with or without stimulation of LPS in THP-1 cells (Fig. 6.8).

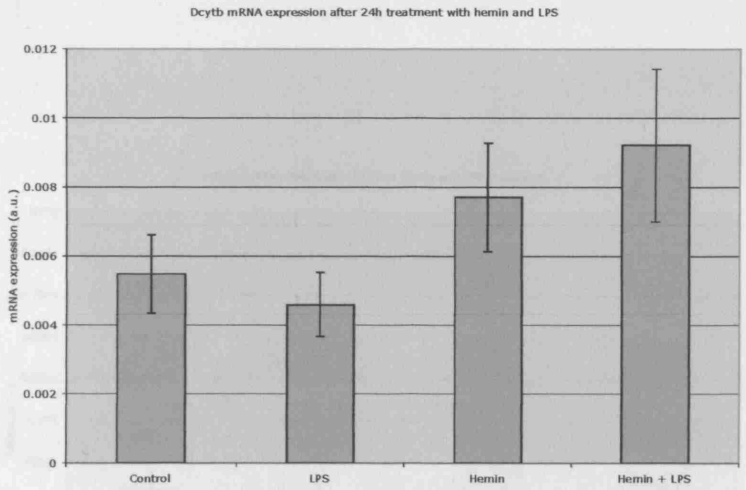

Fig. 6.8 The effect of hemin and LPS on the level of Dcytb mRNA in THP-1 cells. Cells were preincubated for 24h at 37°C with 100 ng/ml LPS or/and hemin prior to the isolation of total mRNA. Lvele of Dcytb mRNA were normalised to HPRT and expressed in arbitrary units. Data are presented as mean±S.E.M. of 3 separate determinations in each group, •$p<0.05$.

Iron export protein IREG1 is hypothesised to participate in iron recycling from senescent red blood cells in reticuloendothelial cells, most likely as the route of iron release. In THP-1 cells treated with

hemin for 24 hours, expression of IREG1 mRNA was significantly up-regulated compared to control (Fig. 6.9), consistent with another reports that IREG1 mRNA levels increased after erythrophagocytosis in J774 cells (Knutson *et al.* 2003). Surprisingly, treatment of LPS alone showed no significant change to the level of IREG mRNA in THP-1 cells, contradicting findings by others that LPS down regulates macrophage IREG1(Ludwiczek *et al.* 2003). Interestingly LPS also decreased IREG1 mRNA in mouse splenic macrophages (Yang *et al.* 2002).

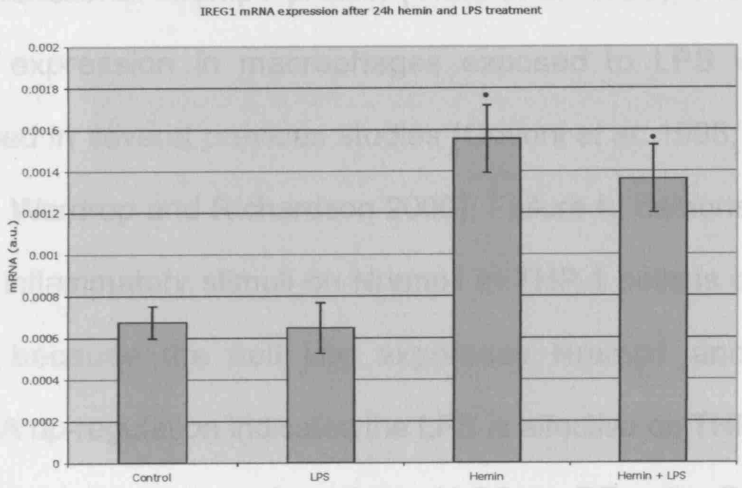

Fig. 6.9 The effect of hemin and LPS on the level of IREG1 mRNA in THP-1 cells. Cells were preincubated for 24h at 37°C with 100 ng/ml LPS or/and hemin prior to the isolation of total mRNA. Level of IREG1 mRNA were normalised to HPRT and expressed in arbitrary units. Data are presented as mean±S.E.M. of 3 separate determinations in each group, •$p<0.05$.

Nramp1 is another iron transporter expressed in macrophages. Treatment of THP-1 cells for 24 hours with hemin significantly decreased Nramp1 mRNA, but expression was unaffected by LPS (Fig. 6.10). Bone marrow-derived macrophages treated with hemin decreased in Nramp1 protein expression (Biggs et al. 2001) and increased mRNA and protein levels by ferric ammonium sulfate (Baker et al. 2000). Nramp1 may respond differently to distinct forms of iron, perhaps depending on whether the iron is phagocytosed or endocytosed. It is important to note that THP-1 cells express Nramp1 and mouse macrophage cell lines J774 and RAW264.7 do not express functional Nramp1 protein (Vidal *et al.* 1996). Induction of Nramp1 expression in macrophages exposed to LPS was well established in several previous studies (Govoni *et al.* 1995; Baker *et al.* 2000; Wardrop and Richardson 2000). Failure to demonstrate the effect of inflammatory stimuli on Nramp1 in THP-1 cells is difficult to explain, because the cell line expresses Nramp1 and DMT1-IREmRNA up-regulation indicates the LPS is effective on THP-1 cells.

In order to reassess the effect of LPS on RE cells, Real-Time PCR was performed to measure the changes in IREG1 mRNA level using human Kupffer cells. As expected, LPS treatment on human Kupffer cells dramatically decreased IREG1 mRNA (Fig. 6.11). This

confirms the direct down-regulation of macrophage IREG1 mRNA by LPS in human RE cells, consistent with other findings in mice (Yang *et al.* 2002) and THP-1 cells (Ludwiczek *et al.* 2003).

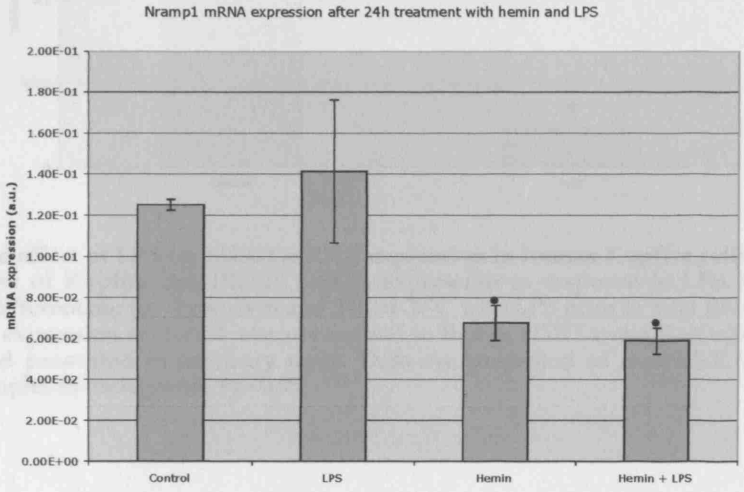

Fig. 6.10 The effect of hemin with or without LPS on the level of Nramp1 mRNA in the THP-1 macrophage cell line. Cells were preincubated for 24h at 37°C with the agent before isolation of total mRNA. DMT1-IRE mRNA was normalised to HPRT and expressed in arbitrary units. Data are presented as mean±S.E.M. of 3 separate determinations in each group, •$p<0.05$.

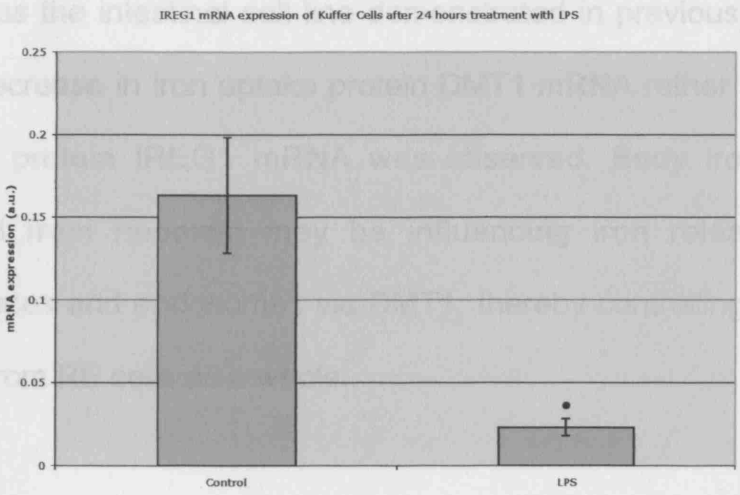

Fig. 6.11 The effect of LPS on IREG1 mRNA expression in human Kupffer cells. Real time PCR analysis of Kupffer cell IREG1 mRNA expression in response to LPS. Cells were allowed to differentiate for three days and 24h at 37°C with LPS prior to total RNA isolation. The mRNA expression of IREG1 was normalised to that of HTRT using RelQuant software (Roche), and presented in arbitrary units. Data are presented as mean±S.E.M. of three separate samples in each group, •$p<0.05$.

6.3.2 Effects of hepcidin on iron transporter protein gene expression in human Kupffer cells.

To investigate the possible regulation of iron metabolism in RE cells, the hepcidin experiment was repeated in human Kupffer cells. As in Caco-2 TC7 cells, DMT1 mRNA expression in Kupffer cells was significantly down regulated by the treatment of hepcidin (Fig. 6.12), whereas the level of IREG1 mRNA was unaffected (Fig. 6.13). Interestingly Dcytb mRNA expression was also significantly down regulated in Kupffer cells (Fig. 6.14). These data suggest that iron metabolism in macrophages is regulated by hepcidin in the same

manner as the intestinal cell line demonstrated in previous chapter, where decrease in iron uptake protein DMT1 mRNA rather than iron exporter protein IREG1 mRNA was observed. Body iron status signalled from hepcidin may be influencing iron release from phagosomes and endosomes via DMT1, thereby controlling the iron release from RE cells as a whole.

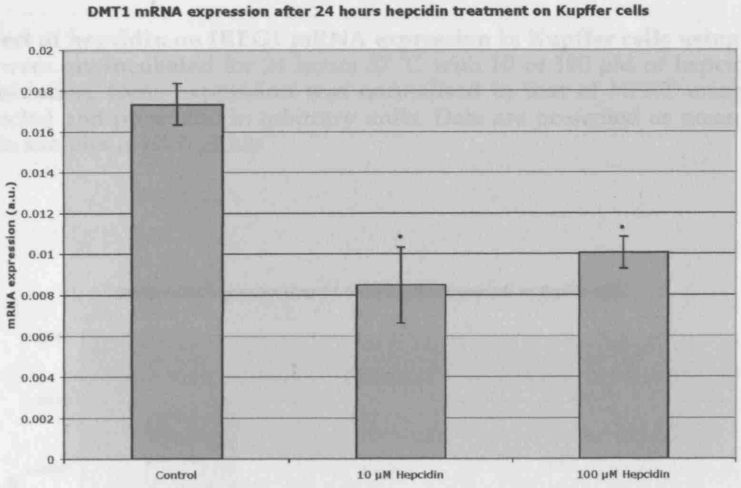

Fig. 6.12 Effect of hepcidin on DMT1 mRNA expression in Kupffer cells using Real-Time PCR. Cells were pre-incubated for 24 hours 37 °C with 10 or 100 μM of hepcidin prior to total RNA isolation. Gene expression was normalised to that of HPRT using RelQuant software (Roche) and presented in arbitrary units. Data are presented as mean ±S.E.M. of three separate samples in each group. •=$p<0.05$.

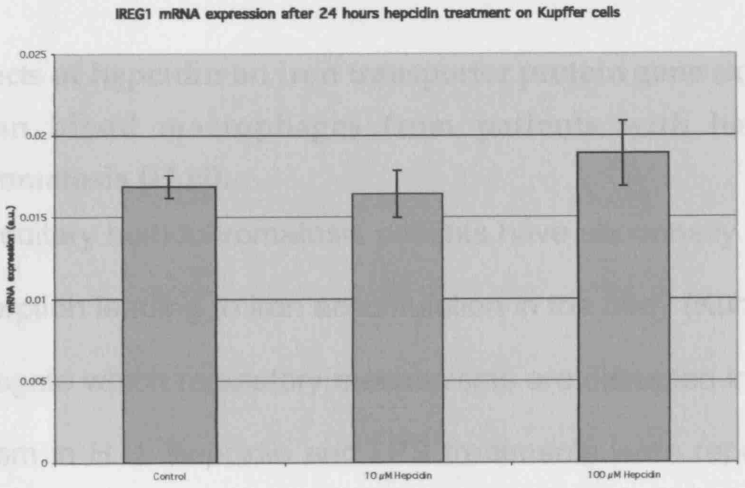

Fig. 6.13 Effect of hepcidin on IREG1 mRNA expression in Kupffer cells using Real-Time PCR. Cells were pre-incubated for 24 hours 37 °C with 10 or 100 μM of hepcidin prior to total RNA isolation. Gene expression was normalised to that of HPRT using RelQuant software (Roche) and presented in arbitrary units. Data are presented as mean ±S.E.M. of three separate samples in each group.

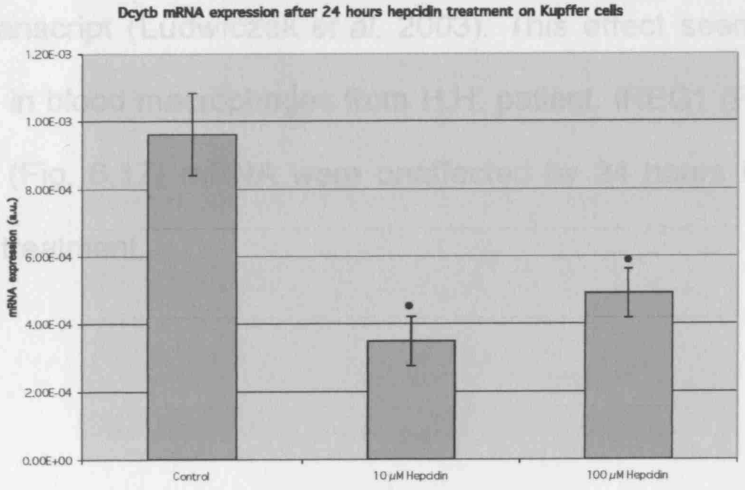

Fig. 6.14 Effect of hepcidin on Dcytb mRNA expression in Kupffer cells using Real-Time PCR. Cells were pre-incubated for 24 hours 37 °C with 10 or 100 μM of hepcidin prior to total RNA isolation. Gene expression was normalised to that of HPRT using RelQuant software (Roche) and presented in arbitrary units. Data are presented as mean ±S.E.M. of three separate samples in each group. •=$p<0.05$.

6.3.3 Effects of hepcidin on iron transporter protein gene expression in human blood macrophages from patients with hereditary hemochromatosis (H.H).

Hereditary hemochromatosis patients have abnormally elevated iron absorption leading to iron accumulation in the body (Kuhn 1999). To investigate which regulatory mechanisms are disrupted in RE iron metabolism in H.H, hepcidin and LPS treatments were repeated on blood macrophages from H.H. patients. Hepcidin mediated down regulation of DMT1 mRNA was not observed, and LPS alone decreased DMT1 mRNA but not when combined with hepcidin (Fig. 6.15). LPS and other cytokines were demonstrated to up regulate the DMT1 transcript (Ludwiczek *et al.* 2003). This effect seems to be reversed in blood macrophages from H.H. patient. IREG1 (Fig. 6.16) and TfR (Fig. 6.17) mRNA were unaffected by 24 hours LPS and hepcidin treatment.

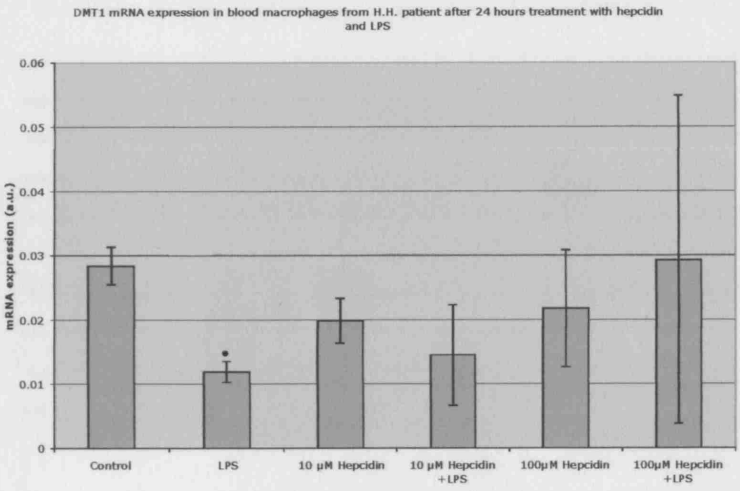

Fig. 6.15 Effect of hepcidin and LPS on DMT1 mRNA expression in blood macrophages from H.H patient using Real-Time PCR. Cells were pre-incubated for 24 hours 37 °C with LPS (100ng/ml) and hepcidin (10 or 100 μM) prior to total RNA isolation. Gene expression was normalised to that of HPRT using RelQuant software (Roche) and presented in arbitrary units. Data are presented as mean ±S.E.M. of two separate samples in each group. •=$p<0.05$

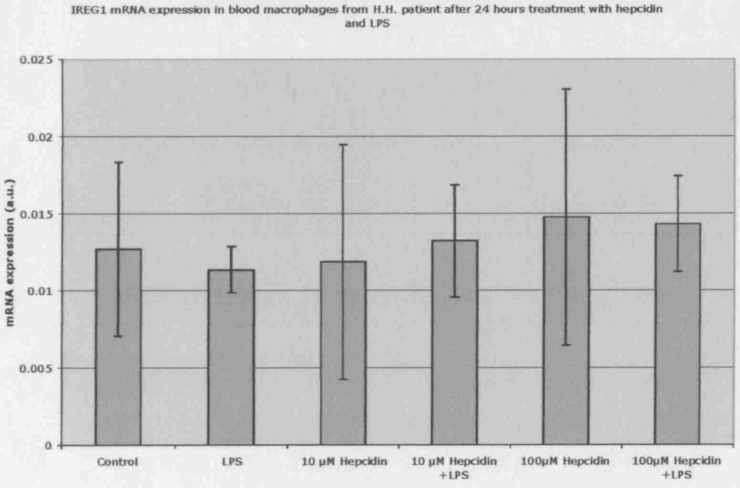

Fig. 6.16 Effect of hepcidin and LPS on IREG1 mRNA expression in blood macrophages from H.H patient using Real-Time PCR. Cells were pre-incubated for 24 hours 37 °C with LPS (100ng/ml) and hepcidin (10 or 100 μM) prior to total RNA isolation. Gene expression was normalised to that of HPRT using RelQuant software (Roche) and presented in arbitrary units. Data are presented as mean ±S.E.M. of two separate samples in each group. •=$p<0.05$

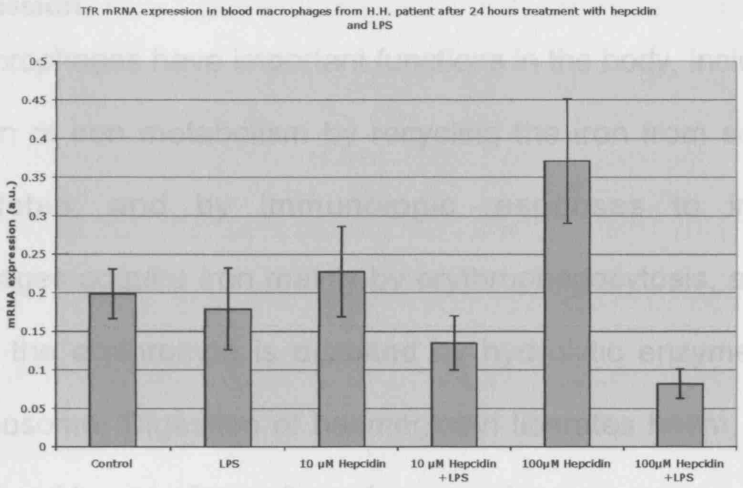

Fig. 6.17 Effect of hepcidin and LPS on TfR mRNA expression in blood macrophages from H.H patient using Real-Time PCR. Cells were pre-incubated for 24 hours 37 ˚C with LPS (100ng/ ml) and hepcidin (10 or 100 μM) prior to total RNA isolation. Gene expression was normalised to that of HPRT using RelQuant software (Roche) and presented in arbitrary units. Data are presented as mean ±S.E.M. of two separate samples in each group. •=$p<0.05$.

6.4 Discussion

Macrophages have important functions in the body, including the regulation of iron metabolism by recycling the iron from senescent haemoglobin, and by immunologic responses to infection. Macrophages acquire iron mainly by erythrophagocytosis, a process in which the erythrocyte is digested by hydrolytic enzymes in the phagolysosome. Digestion of haemoglobin liberates haem, which is then oxidised by membrane-bound enzyme haem oxygenase present in endoplasmic reticulum.

To investigate the molecular mechanism of iron metabolism in RE cells, THP-1 cells were exposed to hemin and LPS. Following the exposure to hemin, up-regulation of haem oxygenase 1 (HMOX1) mRNA indicates hemin was taken up by cells and iron was liberated from haem. In the IRE/IRP system of post-transcriptional regulation of iron metabolism, increased cellular iron decreases mRNA stability due to prevention of IRP binding to IREs in the 3' untranslated region of TfR and DMT1+IRE mRNA. Loss of mRNA protection from RNase degradation consequently reduces mRNA expression. However, parallel to changes in the HMOX1 transcript, the level of IREG1 and DMT1-IRE mRNA were elevated whereas transferrin receptor and Nramp1 mRNA were reduced when gene expression of the DMT1 isoform with IRE and Dcytb remain unaffected by the hemin treatment

in THP-1 cells. It is clear that IREG1, DMT1-IRE, TfR and Nramp1 mRNA are regulated by intracellular iron status, but the IRE/IRP system alone cannot explain these changes in mRNA levels. It has been demonstrated that stimulated IRE-binding of IRP function by α1-Antitrypsin failed to modulate post-transcriptional regulation of TfR mRNA (Weiss *et al.* 1996). The TfR transcript was regulated by cellular iron status but not via the IRE/IRP system as stimulated IRE-IRP binding was overridden by further iron addition. These findings and data from this chapter indicate that an alternative mechanism must be responsible for the regulation by intracellular iron level in RE cells.

Acute inflammation is a condition in which iron metabolism is altered, characterised by low serum iron concentration, decreased plasma iron turnover and reduced RE iron release (Knutson and Wessling-Resnick 2003). The molecular mechanisms responsible for the reduction in iron release from macrophages remain unidentified, although down-regulation of IREG1 has been suggested to plays a role (Yang *et al.* 2002; Ludwiczek *et al.* 2003). The data presented in this chapter fail to demonstrate down-regulation of IREG1 by LPS. Ludwiczek (2003) demonstrated the down-regulation of IREG1 mRNA by LPS parallel with a decrease in cellular iron release in THP-1 cells

(Ludwiczek *et al.* 2003). Both Yang *et al* (2002) and Ludwiczek *et al* (2003) used much higher concentrations of LPS, 5μg/ml in mice and 1-100 ng/ml in THP-1 cells respectively, compare to the LPS dose used here (100 ng/ml) for the same time period. The iron transporter Nramp1 contains a promoter region that is inducible by LPS and IFN-γ (Govoni et al. 1995), and mRNA expression was, not surprisingly, demonstrated to increase by LPS and other cytokines (Govoni *et al.* 1995; Govoni *et al.* 1997; Wardrop and Richardson 2000). The data presented in this chapter fail again to demonstrate down-regulation by LPS in Nramp1 mRNA. Because LPS-mediated regulation is dose dependent (Ludwiczek *et al.* 2003), the concentration used here was simply not adequate to change the transcript level of IREG1 and Nramp1 in THP-1 cells, even though the same dose up-regulated Nramp1 in mouse cell lines (Wardrop and Richardson 2000). The LPS-mediated up-regulation of DMT1-IRE was first demonstrated by Wardrop and Richardson (2000) using J774 and RAW 264.7 cells (Wardrop and Richardson 2000). In this chapter, the same dose (100 ng/ml) of LPS up-regulated DMT1-IRE mRNA, while DMT1+IRE mRNA was unaffected, indicating the differential regulation of two isoforms by LPS in macrophages. Interestingly DMT1 mRNA was decreased by exposure to LPS in blood macrophages from H.H.

patient. Ludwiczek (2003) demonstrated an increase in DMT1 mRNA parallel with an increase in non-transferrin bound iron (NTBI) uptake by LPS using THP-1 cell (Ludwiczek *et al.* 2003). Such an observation could possibly be due to up-regulation of the DMT1-IRE isoform and may be disrupted in patients with hereditary hemochromatosis.

The antimicrobial peptide hepcidin, predominantly synthesised by the liver, is a signalling molecule from the body iron store. Like the down-regulation of iron absorption by hepcidin in an intestinal cell line demonstrated in the previous chapter, hepcidin is proposed to down-regulate iron release from RE cells. Iron retention in RE cells is associated with IREG1 (Montosi *et al.* 2001; Njajou *et al.* 2001; Devalia *et al.* 2002; Roetto *et al.* 2002), however, data presented in this chapter showed no change in IREG1 mRNA level by hepcidin in Kupffer cells. Additionally, DMT1 and Dcytb mRNA was down-regulated by hepcidin, but not in blood macrophages from H.H. patients. These data suggests that hepcidin reduces NTBI uptake by modulating DMT1 and Dcytb expression, and modulation is disrupted in a Patient with H.H. It is consistent with data shown in the previous chapter using a intestinal cell line that DMT1 not IREG1 transcript was modulated by hepcidin. In Kupffer cells, immunofluorescence data

indicates a cytoplasmic/intracellular distribution of IREG1 (Abboud and Haile 2000). If iron is released from RE cells via IREG1, iron retention may be due to the cellular localisation, not expression level, of IREG1, and hepcidin decrease cellular iron accumulation by reduction in DMT1 and Dcytb expression in phagosome of RE cells.

In summary, this chapter analysed different pathways for iron transport and studied their regulation by cellular iron status, pro-inflammatory cytokine, and hepcidin in RE cells. Observation on the IRE/IRP independent post-transcriptional regulation of iron suggests alternative mechanisms exist in RE cells. Pro-inflammatory regulator LPS primarily stimulates DMT1-IRE expression thereby modulating the acquisition of NTBI by RE cells. Hepcidin on the other hand primarily lowers DMT1 expression thereby altering the intracellular iron traffic within RE cells. Figure 6.18 summarizes the intracellular pathway of iron and its regulation by iron, LPS and hepcidin discussed in this chapter.

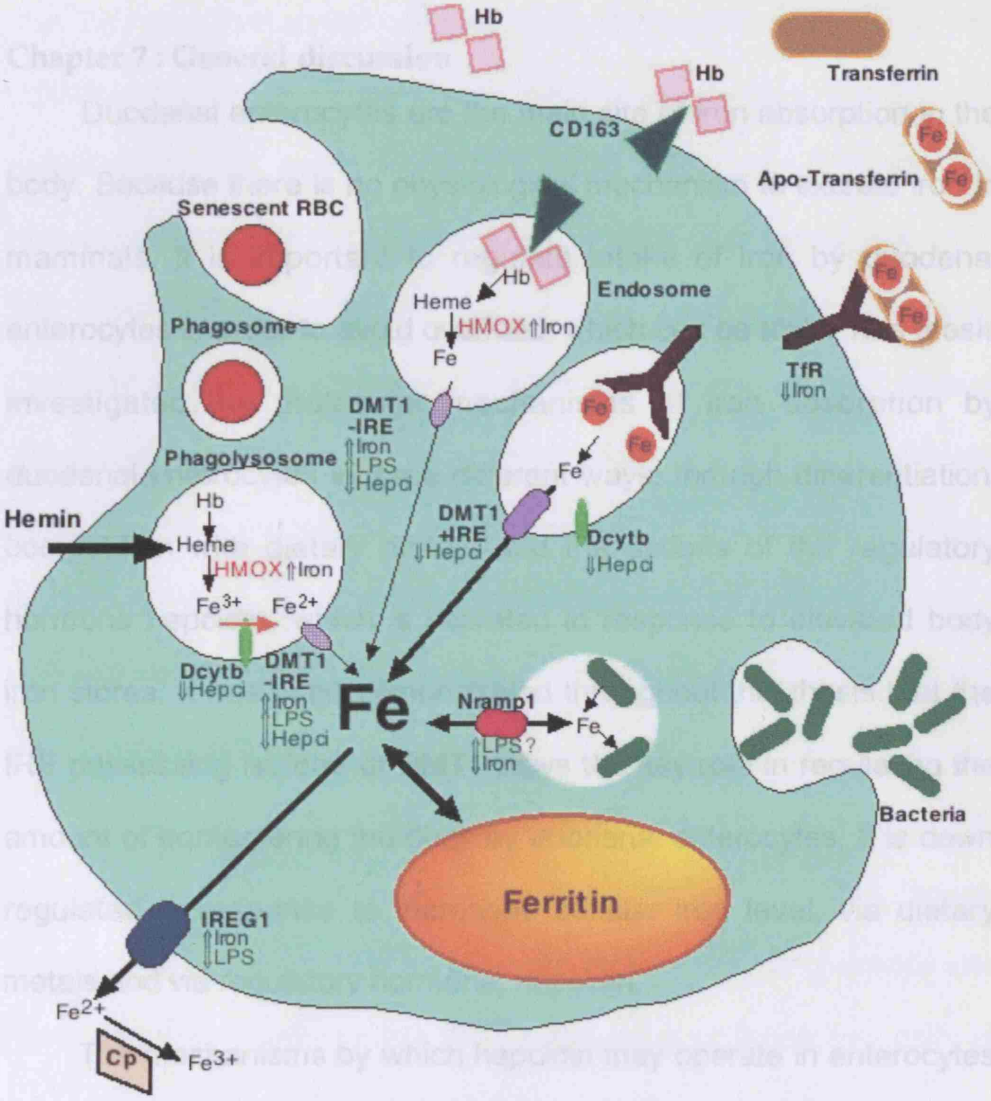

Fig. 6.18 Hypothetical intracellular pathway of iron and its regulation by iron, LPS and hepcidin in RE cell.

Chapter 7 : General discussion

Duodenal enterocytes are the main site of iron absorption in the body. Because there is no physiological mechanism to excrete iron in mammals, it is important to regulate intake of iron by duodenal enterocytes in order to avoid overload, which can be toxic. This thesis investigated the molecular mechanisms of iron absorption by duodenal enterocytes in three different ways, through differentiation, competition with dietary metals and the actions of the regulatory hormone hepcidin, which is secreted in response to elevated body iron stores. It has been demonstrated throughout this thesis that the IRE possessing isoform of DMT1 plays the key role in regulating the amount of iron entering the body by duodenal enterocytes. It is down regulated in response to increased cellular iron level, via dietary metals and via regulatory hormone, hepcidin.

The mechanisms by which hepcidin may operate in enterocytes were clarified in a study by Nemeth et al (2004), after this thesis was written. They demonstrated that hepcidin (the 25 amino acid form) binds directly to IREG1 and internalises it within 1 to 3 hours, depending on the hepcidin concentration. Internalised IREG1 is the degraded by lysosome leading to cellular retention of iron. This may explain more clearly the data shown in chapter 5, which demonstrates

that 24 hours incubation with hepcidin decreased DMT1 with IRE mRNA but not other genes of iron metabolism proteins. Cellular iron retention caused by hepcidin prevented IRP binding to IRE that increased degradation DMT1 with IRE mRNA, and genes that lacks IRE was unaffected. IREG1 mRNA was unaffected in intestinal (Chapter 5) and macrophage (Chapter 6) cell lines after incubation with hepcidin for 24 hours. This lack of response in IREG1 expression could be due to the longer incubation period compared with the study by Nemeth et al., who exposed cells to hepcidin for only 4 hours. It is possible over a prolonged incubation period that IREG1 expression may have recovered.

In addition to enterocytes, the molecular mechanisms of iron absorption by macrophages were also included in this thesis. Macrophages play a role in iron storage and the recycling of body iron from senescent erythrocytes. The behaviours of these two cells of opposing function in iron metabolism were interesting. In contrast to studies carried out in the Caco-2 cell enterocyte model, the DMT1 isoform without the IRE played a part in response to iron and LPS in macrophage cells. Increasing cellular iron levels with hemin led to gene regulation (most likely through IRE/IRP interaction) of transferrin receptor 1 and IREG1. However, DMT1 mRNA was clearly not

regulated this way in macrophage cells. Therefore there must be other mechanisms that regulate DMT1 gene expression, at least in macrophage cells, and this will be an interesting point to investigate further.

In conclusion, the strategy of duodenal enterocytes in response to high iron (in diet or in body) seems to be to withdraw the main entry pathway (DMT1) thereby restricting the intake of iron and avoiding toxic overload. Macrophages respond to iron in a more intricate manner, and this mechanism involves many genes. These differing roles in the regulation of body iron metabolism will be the subject of further investigation, and are likely to be important in relation to iron overload conditions such as in haemochromatosis.

References

"Discovery of the ceruloplasmin homologue hephaestin: new insight into the copper/iron connection." nutr rev **58**(1): 22-26.

Abboud, S. and D. J. Haile (2000). "A novel mammalian iron-regulated protein involved in intracellular iron metabolism." J Biol Chem **275**(26): 19906-12.

Aisen, P. (2004). "Transferrin receptor 1." Int J Biochem Cell Biol **36**(11): 2137-43.

Andrews, N. C. (1999). "Disorders of iron metabolism." N Engl J Med **341**(26): 1986-95.

Atkinson, P. G. and C. H. Barton (1999). "High level expression of Nramp1G169 in RAW264.7 cell transfectants: analysis of intracellular iron transport." Immunology **96**(4): 656-62.

Bacon, B. R., L. W. Powell, P. C. Adams, T. F. Kresina and J. H. Hoofnagle (1999). "Molecular medicine and hemochromatosis: at the crossroads." Gastroenterology **116**(1): 193-207.

Baker, S. T., C. H. Barton and T. E. Biggs (2000). "A negative autoregulatory link between Nramp1 function and expression." J Leukoc Biol **67**(4): 501-7.

Barone, A., R. G. Harper and R. A. Wapnir (1998). "Placental copper transport in the rat. III: Interaction between copper and iron in maternal protein deficiency." Placenta **19**(1): 113-8.

Barton, C. H., T. E. Biggs, S. T. Baker, H. Bowen and P. G. Atkinson (1999). "Nramp1: a link between intracellular iron transport and innate resistance to intracellular pathogens." J Leukoc Biol **66**(5): 757-62.

Beutler, E., V. F. Fairbanks and A. L. Fahey (1963). Clinical disorder of iron metabolism, Grune & Stratton.

Biggs, T. E., S. T. Baker, M. S. Botham, A. Dhital, C. H. Barton and V. H. Perry (2001). "Nramp1 modulates iron homoeostasis in vivo and in vitro: evidence for a role in cellular iron release involving de-acidification of intracellular vesicles." Eur J Immunol **31**(7): 2060-70.

Brittenham, G. M., G. Weiss, P. Brissot, F. Laine, A. Guillygomarc'h, D. Guyader, R. Moirand and Y. Deugnier (2000). "Clinical Consequences of New Insights in the Pathophysiology of Disorders of Iron and Heme Metabolism." Hematology (Am Soc Hematol Educ Program): 39-50.

Burdo, J. R., S. L. Menzies, I. A. Simpson, L. M. Garrick, M. D. Garrick, K. G. Dolan, D. J. Haile, J. L. Beard and J. R. Connor

(2001). "Distribution of divalent metal transporter 1 and metal transport protein 1 in the normal and Belgrade rat." J Neurosci Res **66**(6): 1198-207.

Cairo, G., S. Recalcati, G. Montosi, E. Castrusini, D. Conte and A. Pietrangelo (1997). "Inappropriately high iron regulatory protein activity in monocytes of patients with genetic hemochromatosis." Blood **89**(7): 2546-53.

Canonne-Hergaux, F., S. Gruenheid, P. Ponka and P. Gros (1999). "Cellular and subcellular localization of the Nramp2 iron transporter in the intestinal brush border and regulation by dietary iron." Blood **93**(12): 4406-17.

Canonne-Hergaux, F., J. E. Levy, M. D. Fleming, L. K. Montross, N. C. Andrews and P. Gros (2001). "Expression of the DMT1 (NRAMP2/DCT1) iron transporter in mice with genetic iron overload disorders." Blood **97**(4): 1138-40.

Champe, P. C. and R. A. Harvey (1994). Biochemistry, Lippincott-Raven.

Chen, H., Z. K. Attieh, T. Su, B. A. Syed, H. Gao, R. M. Alaeddine, T. C. Fox, J. Usta, C. E. Naylor, R. W. Evans, A. T. McKie, G. J. Anderson and C. D. Vulpe (2004). "Hephaestin is a ferroxidase that maintains partial activity in sex-linked anemia mice." Blood **103**(10): 3933-9.

Conrad, M. E. and J. N. Umbreit (2000). "Iron absorption and transport-an update." Am J Hematol **64**(4): 287-98.

Conrad, M. E., J. N. Umbreit, E. G. Moore, L. N. Hainsworth, M. Porubcin, M. J. Simovich, M. T. Nakada, K. Dolan and M. D. Garrick (2000). "Separate pathways for cellular uptake of ferric and ferrous iron." Am J Physiol Gastrointest Liver Physiol **279**(4): G767-74.

Costello, L. C. Liu, Y. Zou, J. and Franklin, R. B. (1999). " Evidence for a zinc uptake transporter in human prostate cancer cells which is regulated by prolactin and testosterone" J Biol Chem **274**(25): 17499-17504.

Dallalio, G., T. Fleury and R. T. Means (2003). "Serum hepcidin in clinical specimens." Br J Haematol **122**(6): 996-1000.

Devalia, V., K. Carter, A. P. Walker, S. J. Perkins, M. Worwood, A. May and J. S. Dooley (2002). "Autosomal dominant reticuloendothelial iron overload associated with a 3-base pair deletion in the ferroportin 1 gene (SLC11A3)." Blood **100**(2): 695-7.

Donovan, A., A. Brownlie, Y. Zhou, J. Shepard, S. J. Pratt, J. Moynihan, B. H. Paw, A. Drejer, B. Barut, A. Zapata, T. C. Law, C. Brugnara, S. E. Lux, G. S. Pinkus, J. L. Pinkus, P. D. Kingsley, J. Palis, M. D. Fleming, N. C. Andrews and L. I. Zon

(2000). "Positional cloning of zebrafish ferroportin1 identifies a conserved vertebrate iron exporter." Nature **403**(6771): 776-81.

EBI.

Enns, C. A. (2001). "Pumping iron: the strange partnership of the hemochromatosis protein, a class I MHC homolog, with the transferrin receptor." Traffic **2**(3): 167-74.

FAO/WHO (2002). Expert consultation on human vitamin and mineral requirements.

Ferguson, C. J., M. Wareing, D. T. Ward, R. Green, C. P. Smith and D. Riccardi (2001). "Cellular localization of divalent metal transporter DMT-1 in rat kidney." Am J Physiol Renal Physiol **280**(5): F803-14.

Fleming, M. D., C. C. Trenor, 3rd, M. A. Su, D. Foernzler, D. R. Beier, W. F. Dietrich and N. C. Andrews (1997). "Microcytic anaemia mice have a mutation in Nramp2, a candidate iron transporter gene." Nat Genet **16**(4): 383-6.

Fleming, M. D., M. A. Romano, M. A. Su, L. M. Garrick, M. D. Garrick and N. C. Andrews (1998). "Nramp2 is mutated in the anemic Belgrade (b) rat: evidence of a role for Nramp2 in endosomal iron transport." Proc Natl Acad Sci U S A **95**(3): 1148-53.

Fleming, R. E., M. C. Migas, X. Zhou, J. Jiang, R. S. Britton, E. M. Brunt, S. Tomatsu, A. Waheed, B. R. Bacon and W. S. Sly (1999). "Mechanism of increased iron absorption in murine model of hereditary hemochromatosis: increased duodenal expression of the iron transporter DMT1." Proc Natl Acad Sci U S A **96**(6): 3143-8.

Frazer, D. M., C. D. Vulpe, A. T. McKie, S. J. Wilkins, D. Trinder, G. J. Cleghorn and G. J. Anderson (2001). "Cloning and gastrointestinal expression of rat hephaestin: relationship to other iron transport proteins." Am J Physiol Gastrointest Liver Physiol **281**(4): G931-9.

Frazer, D. M., S. J. Wilkins, E. M. Becker, C. D. Vulpe, A. T. McKie, D. Trinder and G. J. Anderson (2002). "Hepcidin expression inversely correlates with the expression of duodenal iron transporters and iron absorption in rats." Gastroenterology **123**(3): 835-44.

Frazer, D. M. and G. J. Anderson (2003). "The orchestration of body iron intake: how and where do enterocytes receive their cues?" Blood Cells Mol Dis **30**(3): 288-97.

Gaither, L. A. (2001). "The human ZIP1 Transporter..." J Biol Chem **276**(25): 22258-22264.

Garrick, L. M., K. G. Dolan, M. A. Romano and M. D. Garrick (1999). "Non-transferrin-bound iron uptake in Belgrade and normal rat erythroid cells." J Cell Physiol **178**(3): 349-58.

Garrick, M. D., K. G. Dolan, C. Horbinski, A. J. Ghio, D. Higgins, M. Porubcin, E. G. Moore, L. N. Hainsworth, J. N. Umbreit, M. E. Conrad, L. Feng, A. Lis, J. A. Roth, S. Singleton and L. M. Garrick (2003). "DMT1: a mammalian transporter for multiple metals." Biometals **16**(1): 41-54.

Goswami, T., A. Bhattacharjee, P. Babal, S. Searle, E. Moore and M. Li (2001). "Natural-Resistance-associated macrophage protein1 is an H^+/ bivalent cation antiporter." Biochem J **354**: 511-519.

Govoni, G., S. Vidal, M. Cellier, P. Lepage, D. Malo and P. Gros (1995). "Structural organisation and cell specific expression of the mouse Nramp1 gene." Genomics **27**: 9-19.

Govoni, G., S. Vidal, M. Cellier, P. Lepage, D. Malo and P. Gros (1995). "Genomic structure, promoter sequence, and induction of expression of the mouse Nramp1 gene in macrophages." Genomics **27**(1): 9-19.

Govoni, G., S. Gauthier, F. Billia, N. N. Iscove and P. Gros (1997). "Cell-specific and inducible Nramp1 gene expression in mouse macrophages in vitro and in vivo." J Leukoc Biol **62**(2): 277-86.

Gray, N. K. and M. W. Hentze (1994). "Iron regulatory protein prevents binding of the 43S translation pre-initiation complex to ferritin and eALAS mRNAs." Embo J **13**(16): 3882-91.

Gruenheid, S., F. Canonne-Hergaux, S. Gauthier, D. J. Hackam, S. Grinstein and P. Gros (1999). "The iron transport protein NRAMP2 is an integral membrane glycoprotein that colocalizes with transferrin in recycling endosomes." J Exp Med **189**(5): 831-41.

Gunshin, H., B. Mackenzie, U. V. Berger, Y. Gunshin, M. F. Romero, W. F. Boron, S. Nussberger, J. L. Gollan and M. A. Hediger (1997). "Cloning and characterization of a mammalian proton-coupled metal-ion transporter." Nature **388**(6641): 482-8.

Haile, D. J., T. A. Rouault, C. K. Tang, J. Chin, J. B. Harford and R. D. Klausner (1992). "Reciprocal control of RNA-binding and aconitase activity in the regulation of the iron-responsive element binding protein: role of the iron-sulfur cluster." Proc Natl Acad Sci U S A **89**(16): 7536-40.

Hallberg, L., H. G. Harwerth and A. Vannotti (1970). Iron deficiency; Pathogenesis. Clinical aspect. Therapy, Academic Press.

Han, O., J. C. Fleet and R. J. Wood (1999). "Reciprocal regulation of HFE and Nramp2 gene expression by iron in human intestinal cells." J Nutr **129**(1): 98-104.

Hentze, M. W., M. U. Muckenthaler and N. C. Andrews (2004). "Balancing acts: molecular control of mammalian iron metabolism." Cell **117**(3): 285-97.

Hubert, N. and M. W. Hentze (2002). "Previously uncharacterized isoforms of divalent metal transporter (DMT)-1: implications for regulation and cellular function." Proc Natl Acad Sci U S A **99**(19): 12345-50.

Hunter, H. N., D. B. Fulton, T. Ganz and H. J. Vogel (2002). "The solution structure of human hepcidin, a peptide hormone with antimicrobial activity that is involved in iron uptake and hereditary hemochromatosis." J Biol Chem **277**(40): 37597-603.

Iwai, K., S. K. Drake, N. B. Wehr, A. M. Weissman, T. LaVaute, N. Minato, R. D. Klausner, R. L. Levine and T. A. Rouault (1998). "Iron-dependent oxidation, ubiquitination, and degradation of iron regulatory protein 2: implications for degradation of oxidized proteins." Proc Natl Acad Sci U S A **95**(9): 4924-8.

Kim, S. and P. Ponka (1999). "Control of transferrin receptor expression via nitric oxide-mediated modulation of iron-regulatory protein 2." J Biol Chem **274**(46): 33035-42.

Kim, S. and P. Ponka (2000). "Effects of interferon-gamma and lipopolysaccharide on macrophage iron metabolism are mediated by nitric oxide-induced degradation of iron regulatory protein 2." J Biol Chem **275**(9): 6220-6.

Knutson, M. and M. Wessling-Resnick (2003). "Iron metabolism in the reticuloendothelial system." Crit Rev Biochem Mol Biol **38**(1): 61-88.

Knutson, M. D., M. R. Vafa, D. J. Haile and M. Wessling-Resnick (2003). "Iron loading and erythrophagocytosis increase ferroportin 1 (FPN1) expression in J774 macrophages." Blood **102**(12): 4191-7.

Kondo, H., K. Saito, J. P. Grasso and P. Aisen (1988). "Iron metabolism in the erythrophagocytosing Kupffer cell." Hepatology **8**(1): 32-8.

Krause, A., S. Neitz, H. J. Magert, A. Schulz, W. G. Forssmann, P. Schulz-Knappe and K. Adermann (2000). "LEAP-1, a novel highly disulfide-bonded human peptide, exhibits antimicrobial activity." FEBS Lett **480**(2-3): 147-50.

Kuhn, L. C. (1999). "Iron overload: molecular clues to its cause." Trends Biochem Sci **24**(5): 164-6.

Kuo, Y. M., T. Su, H. Chen, Z. Attieh, B. A. Syed, A. T. McKie, G. J. Anderson, J. Gitschier and C. D. Vulpe (2004). "Mislocalisation of hephaestin, a multicopper ferroxidase involved in basolateral intestinal iron transport, in the sex linked anaemia mouse." Gut **53**(2): 201-6.

Laftah, A. H., B. Ramesh, R. J. Simpson, N. Solanky, S. Bahram, K. Schumann, E. S. Debnam and S. K. Srai (2004). "Effect of

hepcidin on intestinal iron absorption in mice." Blood **103**(10): 3940-4.

Latunde-Dada, G. O., J. Van der Westhuizen, C. D. Vulpe, G. J. Anderson, R. J. Simpson and A. T. McKie (2002). "Molecular and functional roles of duodenal cytochrome B (Dcytb) in iron metabolism." Blood Cells Mol Dis **29**(3): 356-60.

Leboeuf, R., C., D. Tolson and J. W. Heinecke (1995). "Dissociation between tissue iron concentrations and transferrin saturation among inbred mouse strains." J Lab Clin Med **126**: 128-136.

Lee, P. L., T. Gelbart, C. West, C. Halloran and E. Beutler (1998). "The human Nramp2 gene: characterization of the gene structure, alternative splicing, promoter region and polymorphisms." Blood Cells Mol Dis **24**(2): 199-215.

Lee, S. H., P. M. Starkey and S. Gordon (1985). "Quantitative analysis of total macrophage content in adult mouse tissue. Immunochemical studies with monoclonal antibody F4/80." J Exp Med **161**: 475-489.

Lioumi, M., C. A. Ferguson, P. T. Sharpe, T. Freeman, I. Marenholz, D. Mischke, C. Heizmann and J. Ragoussis (1999). "Isolation and characterization of human and mouse ZIRTL, a member of the IRT1 family of transporters, mapping within the epidermal differentiation complex." Genomics **62**(2): 272-80.

Ludwiczek, S., E. Aigner, I. Theurl and G. Weiss (2003). "Cytokine-mediated regulation of iron transport in human monocytic cells." Blood **101**(10): 4148-54.

McKie, A. T., P. Marciani, A. Rolfs, K. Brennan, K. Wehr, D. Barrow, S. Miret, A. Bomford, T. J. Peters, F. Farzaneh, M. A. Hediger, M. W. Hentze and R. J. Simpson (2000). "A novel duodenal iron-regulated transporter, IREG1, implicated in the basolateral transfer of iron to the circulation." Mol Cell **5**(2): 299-309.

McKie, A. T., D. Barrow, G. O. Latunde-Dada, A. Rolfs, G. Sager, E. Mudaly, M. Mudaly, C. Richardson, D. Barlow, A. Bomford, T. J. Peters, K. B. Raja, S. Shirali, M. A. Hediger, F. Farzaneh and R. J. Simpson (2001). "An iron-regulated ferric reductase associated with the absorption of dietary iron." Science **291**(5509): 1755-9.

McKie, A. T., D. Barrow, G. O. Latunde-Dada, A. Rolfs, G. Sager, E. Mudaly, M. Mudaly, C. Richardson, D. Barlow, A. Bomford, T. J. Peters, K. B. Raja, S. Shirali, M. A. Hediger, F. Farzaneh and R. J. Simpson (2001). "An iron-regulated ferric reductase associated with the absorption of dietary iron." Science **291**(5509): 1755-9.

Montosi, G., A. Donovan, A. Totaro, C. Garuti, E. Pignatti, S. Cassanelli, C. C. Trenor, P. Gasparini, N. C. Andrews and A.

Pietrangelo (2001). "Autosomal-dominant hemochromatosis is associated with a mutation in the ferroportin (SLC11A3) gene." J Clin Invest **108**(4): 619-23.

Muckenthaler, M., N. K. Gray and M. W. Hentze (1998). "IRP-1 binding to ferritin mRNA prevents the recruitment of the small ribosomal subunit by the cap-binding complex eIF4F." Mol Cell **2**(3): 383-8.

Nemeth, E., E. V. Valore, M. Territo, G. Schiller, A. Lichtenstein and T. Ganz (2003). "Hepcidin, a putative mediator of anemia of inflammation, is a type II acute-phase protein." Blood **101**(7): 2461-3.

Nemeth, E., Tuttle, M. S., Powelson, J., Vaughn, M. B., Donovan, A., Ward, D. M., Ganz, T. and Kaplan, J (2004). " Hepcidin regulates cellular iron efflux by binding to ferroportin and inducing its internalization" Science **306**(5704): 2090-3

Nicolas, G., M. Bennoun, I. Devaux, C. Beaumont, B. Grandchamp, A. Kahn and S. Vaulont (2001). "Lack of hepcidin gene expression and severe tissue iron overload in upstream stimulatory factor 2 (USF2) knockout mice." Proc Natl Acad Sci U S A **98**(15): 8780-5.

Nicolas, G., M. Bennoun, A. Porteu, S. Mativet, C. Beaumont, B. Grandchamp, M. Sirito, M. Sawadogo, A. Kahn and S. Vaulont (2002a). "Severe iron deficiency anemia in transgenic mice expressing liver hepcidin." Proc Natl Acad Sci U S A **99**(7): 4596-601.

Nicolas, G., C. Chauvet, L. Viatte, J. L. Danan, X. Bigard, I. Devaux, C. Beaumont, A. Kahn and S. Vaulont (2002b). "The gene encoding the iron regulatory peptide hepcidin is regulated by anemia, hypoxia, and inflammation." J Clin Invest **110**(7): 1037-44.

Njajou, O. T., N. Vaessen, M. Joosse, B. Berghuis, J. W. van Dongen, M. H. Breuning, P. J. Snijders, W. P. Rutten, L. A. Sandkuijl, B. A. Oostra, C. M. van Duijn and P. Heutink (2001). "A mutation in SLC11A3 is associated with autosomal dominant hemochromatosis." Nat Genet **28**(3): 213-4.

Oshiro, S., K. Nozawa, M. Hori, C. Zhang, Y. Hashimoto, S. Kitajima and K. Kawamura (2002). "Modulation of iron regulatory protein-1 by various metals." Biochem Biophys Res Commun **290**(1): 213-8.

Paraskeva, E., N. K. Gray, B. Schlager, K. Wehr and M. W. Hentze (1999). "Ribosomal pausing and scanning arrest as mechanisms of translational regulation from cap-distal iron-responsive elements." Mol Cell Biol **19**(1): 807-16.

Park, C. H., E. V. Valore, A. J. Waring and T. Ganz (2001). "Hepcidin, a urinary antimicrobial peptide synthesized in the liver." J Biol Chem **276**(11): 7806-10.

Pigeon, C., G. Ilyin, B. Courselaud, P. Leroyer, B. Turlin, P. Brissot and O. Loreal (2001). "A new mouse liver-specific gene, encoding a protein homologous to human antimicrobial peptide hepcidin, is overexpressed during iron overload." J Biol Chem **276**(11): 7811-9.

Ponka, P., C. Beaumont and D. R. Richardson (1998). "Function and regulation of transferrin and ferritin." Semin Hematol **35**(1): 35-54.

Poss, K. D. and S. Tonegawa (1997). "Heme oxygenase 1 is required for mammalian iron reutilization." Proc Natl Acad Sci U S A **94**(20): 10919-24.

Robinson, N. J., C. M. Procter, E. L. Connolly and M. L. Guerinot (1999). "A ferric-chelate reductase for iron uptake from soils." Nature **397**: 694-697.

Roetto, A., A. T. Merryweather-Clarke, F. Daraio, K. Livesey, J. J. Pointon, G. Barbabietola, A. Piga, P. H. Mackie, K. J. Robson and C. Camaschella (2002). "A valine deletion of ferroportin 1: a common mutation in hemochromastosis type 4." Blood **100**(2): 733-4.

Roth, J. A., C. Horbinski, L. Feng, K. G. Dolan, D. Higgins and M. D. Garrick (2000). "Differential localization of divalent metal transporter 1 with and without iron response element in rat PC12 and sympathetic neuronal cells." J Neurosci **20**(20): 7595-601.

Roy, C. N. and C. A. Enns (2000). "Iron homeostasis: new tales from the crypt." Blood **96**(13): 4020-7.

Sacher, A., A. Cohen and N. Nelson (2001). "Properties of the mammalian and yeast metal-ion transporters DCT1 and Smf1p expressed in Xenopus laevis oocytes." J Exp Biol **204**(Pt 6): 1053-61.

Samaniego, F., J. Chin, K. Iwai, T. A. Rouault and R. D. Klausner (1994). "Molecular characterization of a second iron-responsive element binding protein, iron regulatory protein 2. Structure, function, and post-translational regulation." J Biol Chem **269**(49): 30904-10.

Sandstrom, B. (2001). "Micronutrient interactions: effects on absorption and bioavailability." Br J Nutr **85 Suppl 2**: S181-5.

Schalinske, K. L., K. P. Blemings, D. W. Steffen, O. S. Chen and R. S. Eisenstein (1997). "Iron regulatory protein 1 is not required for the modulation of ferritin and transferrin receptor expression

by iron in a murine pro-B lymphocyte cell line." Proc Natl Acad Sci U S A **94**(20): 10681-6.

Searle, S., N. A. Bright, T. I. Roach, P. G. Atkinson, C. H. Barton, R. H. Meloen and J. M. Blackwell (1998). "Localisation of Nramp1 in macrophages: modulation with activation and infection." J Cell Sci **111 (Pt 19)**: 2855-66.

Sharp, P., S. Tandy, S. Yamaji, J. Tennant, M. Williams and S. K. Singh Srai (2002). "Rapid regulation of divalent metal transporter (DMT1) protein but not mRNA expression by non-haem iron in human intestinal Caco-2 cells." FEBS Lett **510**(1-2): 71-6.

Stryer, L. (1995). "Biochemistry." Fourth edition. W.H. Freeman & Company

Su, M. A., C. C. Trenor, J. C. Fleming, M. D. Fleming and N. C. Andrews (1998). "The G185R mutation disrupts function of the iron transporter Nramp2." Blood **92**(6): 2157-63.

Syed, B. A., N. J. Beaumont, A. Patel, C. E. Naylor, H. K. Bayele, C. L. Joannou, P. S. Rowe, R. W. Evans and S. K. Srai (2002). "Analysis of the human hephaestin gene and protein: comparative modelling of the N-terminus ecto-domain based upon ceruloplasmin." Protein Eng **15**(3): 205-14.

Tabuchi, M., T. Yoshimori, K. Yamaguchi, T. Yoshida and F. Kishi (2000). "Human NRAMP2/DMT1, which mediates iron transport across endosomal membranes, is localized to late endosomes and lysosomes in HEp-2 cells." J Biol Chem **275**(29): 22220-8.

Tabuchi, M., N. Tanaka, J. Nishida-Kitayama, H. Ohno and F. Kishi (2002). "Alternative splicing regulates the subcellular localization of divalent metal transporter 1 isoforms." Mol Biol Cell **13**(12): 4371-87.

Tallkvist, J., C. L. Bowlus and B. Lonnerdal (2001). "DMT1 gene expression and cadmium absorption in human absorptive enterocytes." Toxicol Lett **122**(2): 171-7.

Tandy, S., M. Williams, A. Leggett, M. Lopez-Jimenez, M. Dedes, B. Ramesh, S. K. Srai and P. Sharp (2000). "Nramp2 expression is associated with pH-dependent iron uptake across the apical membrane of human intestinal Caco-2 cells." J Biol Chem **275**(2): 1023-9.

Tennant, J., M. Stansfield, S. Yamaji, S. K. Srai and P. Sharp (2002). "Effects of copper on the expression of metal transporters in human intestinal Caco-2 cells." FEBS Lett **527**(1-3): 239-44.

Touret, N., W. Furuya, J. Forbes, P. Gros and S. Grinstein (2003). "Dynamic traffic through the recycling compartment couples the metal transporter Nramp2 (DMT1) with the transferrin receptor." J Biol Chem **278**(28): 25548-57.

Trinder, D., P. S. Oates, C. Thomas, J. Sadleir and E. H. Morgan (2000). "Localisation of divalent metal transporter 1 (DMT1) to the microvillus membrane of rat duodenal enterocytes in iron deficiency, but to hepatocytes in iron overload." Gut **46**(2): 270-6.

Vidal, S., E. Pinner, P. Lepage, S. Gauthier and P. Gros (1996). "Natural Resistance to Intracellular Infections." J Immunol **157**: 3559-3568.

Vulpe, C. D., Y. M. Kuo, T. L. Murphy, L. Cowley, C. Askwith, N. Libina, J. Gitschier and G. J. Anderson (1999). "Hephaestin, a ceruloplasmin homologue implicated in intestinal iron transport, is defective in the sla mouse." Nat Genet **21**(2): 195-9.

Vulpe, C. D., Y. M. Kuo, T. L. Murphy, L. Cowley, C. Askwith, N. Libina, J. Gitschier and G. J. Anderson (1999). "Hephaestin, a ceruloplasmin homologue implicated in intestinal iron transport, is defective in the sla mouse." Nat Genet **21**(2): 195-9.

Wapnir, R. A. (1998). "Copper absorption and bioavailability." Am J Clin Nutr **67**(suppl): 1054S-60S.

Wardrop, S. L. and D. R. Richardson (2000). "Interferon-gamma and lipopolysaccharide regulate the expression of Nramp2 and increase the uptake of iron from low relative molecular mass complexes by macrophages." Eur J Biochem **267**(22): 6586-93.

Weinstein, D. A., C. N. Roy, M. D. Fleming, M. F. Loda, J. I. Wolfsdorf and N. C. Andrews (2002). "Inappropriate expression of hepcidin is associated with iron refractory anemia: implications for the anemia of chronic disease." Blood **100**(10): 3776-81.

Weiss, G., I. Graziadei, M. Urbanek, K. Grunewald and W. Vogel (1996). "Divergent effects of α1-antitrypsin on the regulation of iron metabolism in human erythroleukaemic (K562) and myelomonocytic (THP-1) cells." Biochem J **319**: 897-902.

Worwood, M. (1999). "Inborn errors of metabolism: iron." Br Med Bull **55**(3): 556-67.

Yamaji, S., J. Tennant, S. Tandy, M. Williams, S. K. Singh Srai and P. Sharp (2001). "Zinc regulates the function and expression of the iron transporters DMT1 and IREG1 in human intestinal Caco-2 cells." FEBS Lett **507**(2): 137-41.

Yang, F., X. B. Liu, M. Quinones, P. C. Melby, A. Ghio and D. J. Haile (2002). "Regulation of reticuloendothelial iron transporter MTP1 (Slc11a3) by inflammation." J Biol Chem **277**(42): 39786-91.

Zwilling, B. S., D. E. Kuhn, L. Wikoff, D. Brown and W. Lafuse (1999). "Role of iron in Nramp1-mediated inhibition of mycobacterial growth." Infect Immun **67**(3): 1386-92.

Appendix

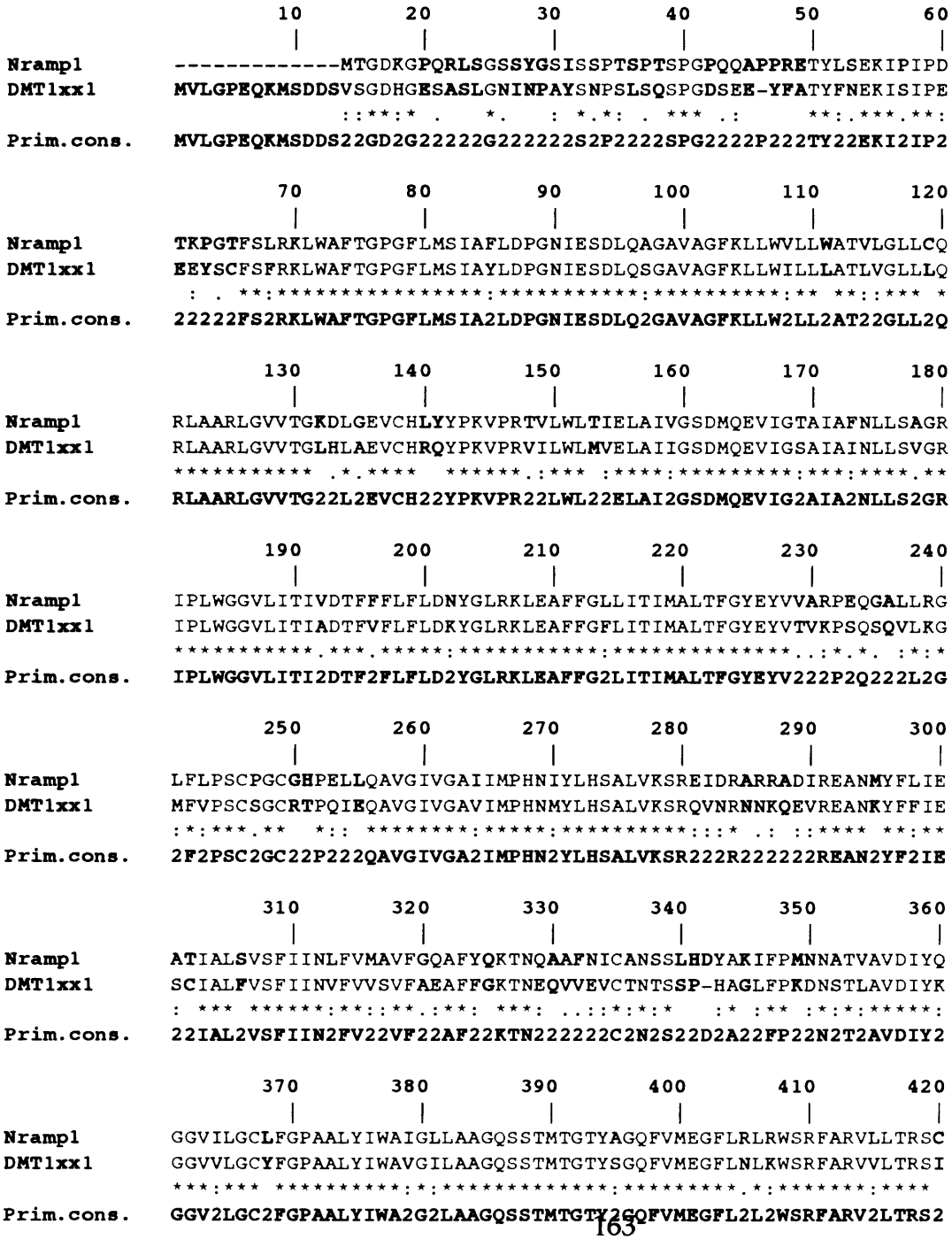
10 20 30 40 50 60
Nramp1 ----------MTGDKGPQRLSGSSYGSISSPTSPTSPGPQQAPPRETYLSEKIPIPD
DMT1xx1 MVLGPEQKMSDDSVSGDHGESASLGNINPAYSNPSLSQSPGDSEE-YFATYFNEKISIPE
Prim.cons. MVLGPEQKMSDDS22GD2G22222G222222S2P2222SPG2222P222TY22EKI2IP2
70 80 90 100 110 120
Nramp1 TKPGTFSLRKLWAFTGPGFLMSIAFLDPGNIESDLQAGAVAGFKLLWVLLWATVLGLLCQ
DMT1xx1 EEYSCFSFRKLWAFTGPGFLMSIAYLDPGNIESDLQSGAVAGFKLLWILLLATLVGLLLQ
Prim.cons. 22222FS2RKLWAFTGPGFLMSIA2LDPGNIESDLQ2GAVAGFKLLW2LL2AT22GLL2Q
130 140 150 160 170 180
Nramp1 RLAARLGVVTGKDLGEVCHLYYPKVPRTVLWLTIELAIVGSDMQEVIGTAIAFNLLSAGR
DMT1xx1 RLAARLGVVTGLHLAEVCHRQYPKVPRVILWLMVELAIIGSDMQEVIGSAIAINLLSVGR
Prim.cons. RLAARLGVVTG22L2EVCH22YPKVPR22LWL22ELAI2GSDMQEVIG2AIA2NLLS2GR
190 200 210 220 230 240
Nramp1 IPLWGGVLITIVDTFFFLFLDNYGLRKLEAFFGLLITIMALTFGYEYVVARPEQGALLRG
DMT1xx1 IPLWGGVLITIADTFVFLFLDKYGLRKLEAFFGFLITIMALTFGYEYVTVKPSQSQVLKG
Prim.cons. IPLWGGVLITI2DTF2FLFLD2YGLRKLEAFFG2LITIMALTFGYEYV222P2Q222L2G
250 260 270 280 290 300
Nramp1 LFLPSCPGCGHPELLQAVGIVGAIIMPHNIYLHSALVKSREIDRARRADIREANMYFLIE
DMT1xx1 MFVPSCSGCRTPQIEQAVGIVGAVIMPHNMYLHSALVKSRQVNRNNKQEVREANKYFFIE
Prim.cons. 2F2PSC2GC22P222QAVGIVGA2IMPHN2YLHSALVKSR222R222222REAN2YF2IE
310 320 330 340 350 360
Nramp1 ATIALSVSFIINLFVMAVFGQAFYQKTNQAAFNICANSSLHDYAKIFPMNNATVAVDIYQ
DMT1xx1 SCIALFVSFIINVFVVSVFAEAFFGKTNEQVVEVCTNTSSP-HAGLFPKDNSTLAVDIYK
Prim.cons. 22IAL2VSFIIN2FV22VF22AF22KTN222222C2N2S22D2A22FP22N2T2AVDIY2
370 380 390 400 410 420
Nramp1 GGVILGCLFGPAALYIWAIGLLAAGQSSTMTGTYAGQFVMEGFLRLRWSRFARVLLTRSC
DMT1xx1 GGVVLGCYFGPAALYIWAVGILAAGQSSTMTGTYSGQFVMEGFLNLKWSRFARVVLTRSI
Prim.cons. GGV2LGC2FGPAALYIWA2G2LAAGQSSTMTGTY2GQFVMEGFL2L2WSRFARV2LTRS2

```
                  430       440       450       460       470       480
                    |         |         |         |         |         |
Nramp1       AILPTVLVAVFRDLRDLSGLNDLLNVLQSLLLPFAVLPILTFTSMPTLMQEFANGLLNKV
DMT1xx1      AIIPTLLVAVFQDVEHLTGMNDFLNVLQSLQLPFALIPILTFTSLRPVMSDFANGLGWRI
             **:**:*****:*:..*:*:**:******* ****::*******: .:*.:*****  ::
Prim.cons.   AI2PT2LVAVF2D222L2G2ND2LNVLQSL2LPFA22PILTFTS2222M22FANGL2222

                  490       500       510       520       530       540
                    |         |         |         |         |         |
Nramp1       VTSSIMVLVCAINLYFVVSYLPSLPHPAYFGLAALLAAAYLGLSTYLVWTCCLAHGATFL
DMT1xx1      AGGILVLIICSINMYFVVVYVRDLGHVALYVVAAVVSVAYLGFVFYLGWQCLIALGMSFL
             . . :::::*:**:**** *: .* * * : :**::::.****:  ** * * :* * :**
Prim.cons.   222222222C2IN2YFVV2Y222L2H2A2222AA2222AYLG222YL2W2C22A2G22FL

                  550       560
                    |         |
Nramp1       AHSSHHHFLYGLLEEDQKGETSG
DMT1xx1      DCGHTVSISKGLLTEEATRGYVK
               .     :  *** *: .
Prim.cons.   2222222222GLL2E22222222
```

Alignment data :

Alignment length : 563
Identity (*) : 346 is 61.46 %
Strongly similar (:) : 93 is 16.52 %
Weakly similar (.) : 34 is 6.04 %
Different : 90 is 15.99 %
Sequence 0001 : Nramp1 (550 residues).
Sequence 0002 : DMT1xx1 (561 residues).

CLUSTALW options used :

endgaps=1
gapdist=8
gapext=0.2
gapopen=10.0
hgapresidues=GPSNDQERK
ktuple=1
matrix=gonnet
maxdiv=30
outorder=aligned
pairgap=3
score=percent
topdiags=5
type=PROTEIN
window=5